Understanding Membrane Dynamics in The Intestinal Pathogen *Entamoeba invadens*.

Submitted by **Shatha Abdul Wahab Raof** to the University of Exeter

as a thesis for the degree of

Masters by Research in Biological Sciences

In July 2021

I certify that all material in this thesis which is not my own work has been identified and that no material has previously been submitted and approved for the award of a degree by this or any other University.

Signature: ……Shatha……..

Abstract

Amoebiasis, is a parasitic disease caused by *Entamoeba histolytica*, causing a wide range of clinical manifestations, from asymptomatic infection to amoebic dysentery and liver abscess, and encystation is a key process enabling this parasite to cause disease. Because encystation of *E. histolytica* has not been successfully reproduced under laboratory conditions, it is often conducted in surrogate model species. The cyst wall of *E. invadens*, a model for *E. histolytica*, is mainly composed of chitin fibrils, two chitin-binding lectins, Jacob that cross-link chitin fibrils and Jessie that self-aggregates on the cyst wall and an enzyme, chitinase, which remodels chitin. Current research aims to identify new biological drugs that can target the cyst formation process but that does not affect human cells. In this study I aimed to study the membrane dynamics of *E. invadens* during encystation using Langmuir trough apparatus and cell fluctuation analysis. The effect of cyst wall components; chitin and its deacetylated form chitosan on *E. invadens* plasma membrane lipids (PML) and red blood cells (RBCs) membrane have been studied. I demonstrated that the addition of chitin and chitosan to *E. invadens* PML has increased the stiffness of plasma membrane lipids and increased the rigidity of RBCs membrane. Furthermore, I aimed to study the effect of Jacob and Jessie lectin on PML and RBCs membrane. Jacob and Jessie were successfully amplified and cloned into an expression vector, however, several experiments to purify these proteins were unsuccessful. This may be due to the protein being unstable and/or toxic to *E. coli* host, or caused by inefficient transcription, translation and/or posttranslational modifications. In order to resolve these issues, it may be

necessary to use different host cells such as mammalian or insect cells. Together, the data presented in this thesis provides evidence that chitin and chitosan contribute to increased rigidity of the lipid monolayer/bilayer. This knowledge in the future may contribute to research aimed at the development of treatments to combat amoebiasis.

Acknowledgements

Firstly, I would like to thank my supervisors Dr Eduarda Santos, Prof Mark Van der Giezen, Prof Peter Winlove and Dr Peter Petrov for the opportunity to do this project and for their thoughtful advice and support throughout this project.

Particularly I would like to thank Dr Eduarda Santos for her devoted support and guidance. Eduarda constantly provided encouragement and was ready and keen to assist in any way she could.

I am also thankful to the Biosciences and Biophysics / University of Exeter and everyone in the Biocatalysis building and Mezzanine floor in the Geoffrey Pope Building.

Further, I would like to express my gratitude and appreciation for Laura Yeves Gonzalez (PGR Support Officer) and Dr Magdalena Katomeri (Student Support Welfare Caseworker) for their support and encouragement.

Special thanks: To My husband Maulood Turfah for all the unconditional support, I simply couldn’t have done this without you. To my parents, who set me off on the road to learning and studying a long time ago with all support that I needed. To my angels Masarra, Yousif and Sami for your being in my life, one look on your smiling faces relieves me of the trouble of a whole day.

List of Contents

List of Figures

Chapter 1

Chapter 2

Chapter 3

Chapter 4

List of Tables

Chapter 2

Chapter 3

Chapter 4

Abbreviations

ABS	Adult Bovine Serum
ATP	Adenine Triphosphate
bp	base pair
BSA	Bovine Serum Albumin
CBDs	Chitin-Binding Domains
Chs	Chitin synthases
CTAB	Cetyl-Trimethyl-Ammonium Bromide
Cys	Cysteine
DNA	Deoxyribonucleic Acid
dNTPs	Deoxyribose Nucleotides
DPPC	Dipalmitoylphosphatidylcholine
DPPG	Dipalmitoylphosphatidylglycerol
E. coli	*Escherichia coli*
E. histolytica	*Entamoeba histolytica*
E. invadens	*Entamoeba invadens*
EDTA	Ethylenediaminetetraacetic Acid
ER	Endoplasmic Reticulum
Gal/GalNAc	Galactose/N-acetylgalactosamine
GTP	Guanosine Triphosphate
GTPase	Guanosine Triphosphatase
His tag	Polyhistidine-tag

IPTG	Isopropyl-beta-D-thiogalactopyranoside
kD	Kilodalton
LB	Luria-Bertani
LYI-S medium	Liver digest, Yeast extract, Iron and Serum
mRNA	Messenger Ribonucleic Acid
OD	Optical Density
PAGE	Polyacrylamide Gel Electrophoresis
PAH	Poly Allylamine Hydrochloride
PBS	Phosphate Buffer Solution
PCR	Polymerase Chain Reaction
PML	Plasma Membrane Lipids
PTFE	Polytetrafluoroethylene
RBC	Red Blood Cell
RNA	Ribonucleic Acid
SDS	Sodium Dodecyl Sulfate
SREHP	Serine-rich *E. histolytica* Protein
TAE buffer	Tris base, Acetic acid and EDTA buffer
TMK	Transmembrane Kinase
Tris	2-Amino-2-hydroxymethyl-propane-1,3-diol
UDP-GlcNAc	Uridine Diphosphate *N*-acetylglucosamine
v/v	Volume by olume
w/v	Weight over volume
WCL	Whole Cell Lipids

Chapter 1 - Introduction

1.1 *Entamoeba histolytica*

The protozoan parasite *Entamoeba histolytica* is the causative agent of amoebiasis, a serious and potentially fatal disease in humans. Infection occurs after the ingestion of cyst-contaminated food and water. *E. histolytica* is the third parasitic disease-causing deaths worldwide, after malaria and schistosomiasis. Approximately 90% of cases are asymptomatic and only 10% exhibit clinical symptoms resulting in 50 million infections and 100,000 deaths annually (Cornick and Chadee, 2017; Kantor *et al.*, 2018; Shahi *et al*., 2019). In 2013 there were 11,300 deaths from amoebiasis, ranking it the fourth leading cause of parasitic diseases (Naghavi *et al*., 2015). Despite the fact that amoebiasis is worldwide distributed, the parasite infects primarily people living in the developing countries. Infection arises due to the lack of basic hygienic standards, mostly in the Indian subcontinent, the sub-Saharan and tropical regions of Africa, Central and South America, and Mexico. However, the disease was recorded in some developed countries including the United States and Canada, in which it was attributed to the emigration from Mexico and Central America (Ximénez *et al*., 2009; Zermeño *et al*., 2013). Whilst, *E. histolytica* is the main cause of amoebiasis, other closely related species such as *Entamoeba dispar* and *Entamoeba coli* were considered non-pathogenic (Weinke *et al*., 1990). The tissue invasion and non-stop multiplication of trophozoites can cause amoebic dysentery (Lozano *et al*., 2012). The parasite has the ability to kill the host cells due to the potent cytotoxic activity of some membrane proteins such as amoebapore, cysteine protease and Gal

(galactose)/GalNAc (*N*-acetylgalactosamine) lectin-mediated adherence, that target cell calcium influx, tyrosine dephosphorylation and activation of caspase 3 which is important for apoptosis and cell death (Ralston *et al* 2011). Moreover, *E. histolytica* can kill the killer immune cells via the production of pore-forming proteins such amoebapore that punch holes in the membrane of the cell being attacked (Pritt and Clark 2011). Generally, trophozoites invade the intestine and colonize the epithelial mucosa resulting in flask-shaped ulcers. In some cases, the parasite penetrates the intestine epithelia, reaching the blood vessels and the portal veins, and spreading via the blood stream to other organs causing liver, pulmonary, and even brain abscess and peritonitis (invasive extra-intestinal amoebiasis) (Espinosa-Cantellano and Martínez-Palomo, 2000).

The cell division machinery in *Entamoeba* trophozoites is dissimilar to other protists and eukaryotes. Due to the absence of conserved checkpoint proteins, chromosome segregation happens in various microtubular assemblies such as radial, bipolar, or fan-shaped structures (Mukherjee *et al*., 2009). The knockout of checkpoint proteins in eukaryotes, initiates defective DNA synthesis, asymmetrical chromosome segregation and abnormal cell division. Although studies have proven the presence of microtubules in *Entamoeba*, the metaphase and chromosomes segregation is still poorly understood (Das & Lohia, 2002), but the anaphase and telophase can be simply discriminated depending on the nuclear shape. Usually, *E. histolytica* shows different mechanisms of cell division. Firstly, the intracellular bridge is formed at random sites followed by extension, and rupture leads to formation of two daughter

cells. Secondly, the rupture of the intercellular bridge is assisted by helper cells. Thirdly, the two cells are separated by a long intracellular bridge, which fails to rupture, resulting in multiple rounds of cytokinesis failure with multiple nuclei (Mukherjee *et al*., 2009).

Generally, *Entamoeba* trophozoites have nucleus, cytoplasm, plasma membrane, endoplasmic reticulum (ER), and Golgi complex (Vaithilingam *et al*., 2008), but lack the mitochondria and instead, they possess mitochondria-related organelle (reduced mitochondria) called mitosomes. Mitosomes are homogeneous double membrane-bound organelles that lack cristae but contain the mitochondrial-type chaperone (Cnp60) (Tovar *et al*., 1999; Makiuchi *et al*., 2017). Moreover, mitosomes play a key role in sulfate activation that leads to the formation of cholesteryl sulfate which is vital for trophozoites growth and cyst formation (Santos *et al*., 2019). Inhibition of cholesteryl sulfate pathway by chlorate, halts cyst formation in a dose dependent mode. Chlorate is a selective inhibitor of ATP sulfurylase, the main enzyme in the sulfate-activation pathway. This feature could assist to develop anti parasitic drugs. Mitosomal membranes have numerous divergent components, including transport systems for proteins and metabolites (Mi-ichi *et al*., 2015). Analyses of the genomes *Entamoeba* suggested few mitosomal membrane proteins that are different from the ancestry mitochondrial proteins, suggesting that they might have been replaced by lateral gene transfer (Siegesmund *et al*. 2011). The study of these proteins could help to understand the role of mitosomes in *Entamoeba* pathogenesis and transmission.

Different cellular events are involved in the growth and pathogenesis of *E. histolytica* such as phagocytosis, and motility. Phagocytosis is vital in food engulfing and virulence by destroying host cells and escaping the immune system (Avalos-Padilla *et al*., 2015). It involves signal transduction, receptor-mediated recognition of the particle, rearrangement of the cytoskeleton and remodelling of the membrane and contents (Hanadate *et al*., 2016). Cytoskeletal proteins such as actin and myosin are required for phagocytosis, and they are controlled by a combination of signalling proteins. These signalling proteins are transmembrane kinases (TMKs), calcium (Ca^{2+}) binding proteins, GTP binding proteins and surface proteins. Previous studies referred to some surface proteins involved in target recognition such as Gal/GalNAc lectin (a heterotrimer of GPI-anchored transmembrane peptide), and other transmembrane proteins such as TMK96, TMK39 and SREHP (serine-rich *E. histolytica* protein) (Mansuri *et al*., 2014). In addition to Gal/GalNAc lectin, there are several molecules associated with *Entamoeba* virulence such as cysteine proteases and amoebapores. Cysteine proteases are proteolytic enzymes that targets the first line of host immune system, while amoebapores, are cytolytic peptides, with potent cytolytic and destructive activity toward human epithelial cells and bacteria. These proteins are expressed by trophozoites during invasive and extra-intestinal amoebiasis (Cruz *et al*., 2016).

1.1.1 Life cycle

E. histolytica has a simple life cycle that interchanges between trophozoite and cyst stages. The trophozoites (the invasive stage) is the actively metabolizing,

mobile form, 20-40 µm in diameter, whereas the cyst (the infective stage) is dormant and environmentally resistant, with a diameter of 10-16 µm and has four nuclei in the fully mature cysts (Farthing *et al*., 2009; Pritt and Clark, 2011; Debnath *et al*., 2019). The main route of transmission is fecal-oral, which usually involves contaminated food or water, and to a lesser extent ano-genital transmission or oro-anal sexual contact (Alvarado-Esquivel *et al*., 2017; Billet *et al*., 2019; Kantor *et al*., 2018). Ingested cysts excyst in the lower portion of the small intestine, releasing trophozoites, which in turn aggregate in the lumen of the large intestine to initiate replication and feeding on living host cells and bacteria (see Figure 1.1 for details of the *E. histolytica* life cycle) (Nakada-Tsukui *et al*., 2019; Pritt and Clark, 2011).

Colonization of the intestinal mucosa occurs following *E. histolytica* infection in 10% of the cases. Factors contributing to colonisation include the inoculum size, intestinal motility, the presence or absence of intestinal bacteria, the host's diet and the ability of the amoebae to adhere to the colonic mucosal cells. This colonization is mediated by the galactose and *N*-Acetyl-D-Galactosamine (Gal/GalNAc)–specific lectin (Haque *et al*., 2003; Cornick and Chadee, 2017;). However, due to unknown causes, some trophozoites stop feeding, and become rounded and non-motile, followed by the cyst formation. At this stage, the cysts will require another susceptible host in order to complete their development (Espinosa-Cantellano and Martínez-Palomo, 2000). The cysts released in the environment are highly resistant to adverse environmental conditions and this resistance is conferred by their walls, allowing them to persist in the external environment for up to two weeks (Aguilar-Díaz *et al*.,

2011). Invasive intestinal disease may occur days to years after initial infection, causing most of the fatalities (Bernet Sánchez *et al.*, 2019; Chandnani *et al.*, 2019). However the presence of mucin, which is a glycoprotein secreted by the submucosal layer, acts as an intestinal protective layer and defence mechanism (Mukherjee *et al*., 2008). The trophozoites have an ability to overcome this innate immunity in two ways: Firstly, Trophozoites secrete cell surface Gal/GalNAc lectin to adhere to the galactose (Gal) and N-acetylgalactosamine (GalNAc) ligands of the mucin layers. Gal/GalNAc lectin has a mucolytic effect with high affinity to bind sugar ligands that abundantly found in the intestinal mucin (Eichinger, 2001). Secondly, trophozoites secrete the proteolytic enzyme, cysteine protease, which degrades mucin and destroys colon epithelial cells which in turn facilitates trophozoites migration and invasion (Cruz *et al*., 2016). Understanding the cellular events that happens during life cycle, might provide us with clue about and stage conversion which could be exploited to stop the disease.

1.2 *Entamoeba invadens* as a model species

E. invadens, a reptilian parasite that is related to *E. histolytica*, is widely studied as a model for *E. histolytica* encystation given that successful methodologies for inducing differentiation of *E. histolytica* from trophozoite to cyst in the laboratory conditions have not been developed yet. The strain IP-1 of *E. invadens* was used as a model due to its ability to form cysts in the laboratory (Segovia-Gamboa *et al*., 2010; Wang *et al*., 2003; Eichinger, 2001). *E. invadens* can readily be induced to undergo encystation *in vitro* by glucose starvation and can

live in up to a 100-fold-diluted medium; *E. histolytica* is not able to survive in these conditions (Eichinger, 1997; Rengpien and Bailey, 1975; Vazquezdelara-Cisneros and Arroyo-Begovich, 1984). *E. invadens* has very similar life cycle and morphology of *E. histolytica*. Additionally, all of the cyst wall components of proteins in *E. invadens* are present in *E. histolytica* (Chatterjee, Sudip K. Ghosh, *et al*., 2009; Marta Frisardi *et al*., 2000; Van Dellen *et al*., 2002).Together, these characteristics render *E. invadens* a good surrogate species to investigate the fundamental biology of the related *E. histolytica* and allow for progress in disease treatment and prevention.

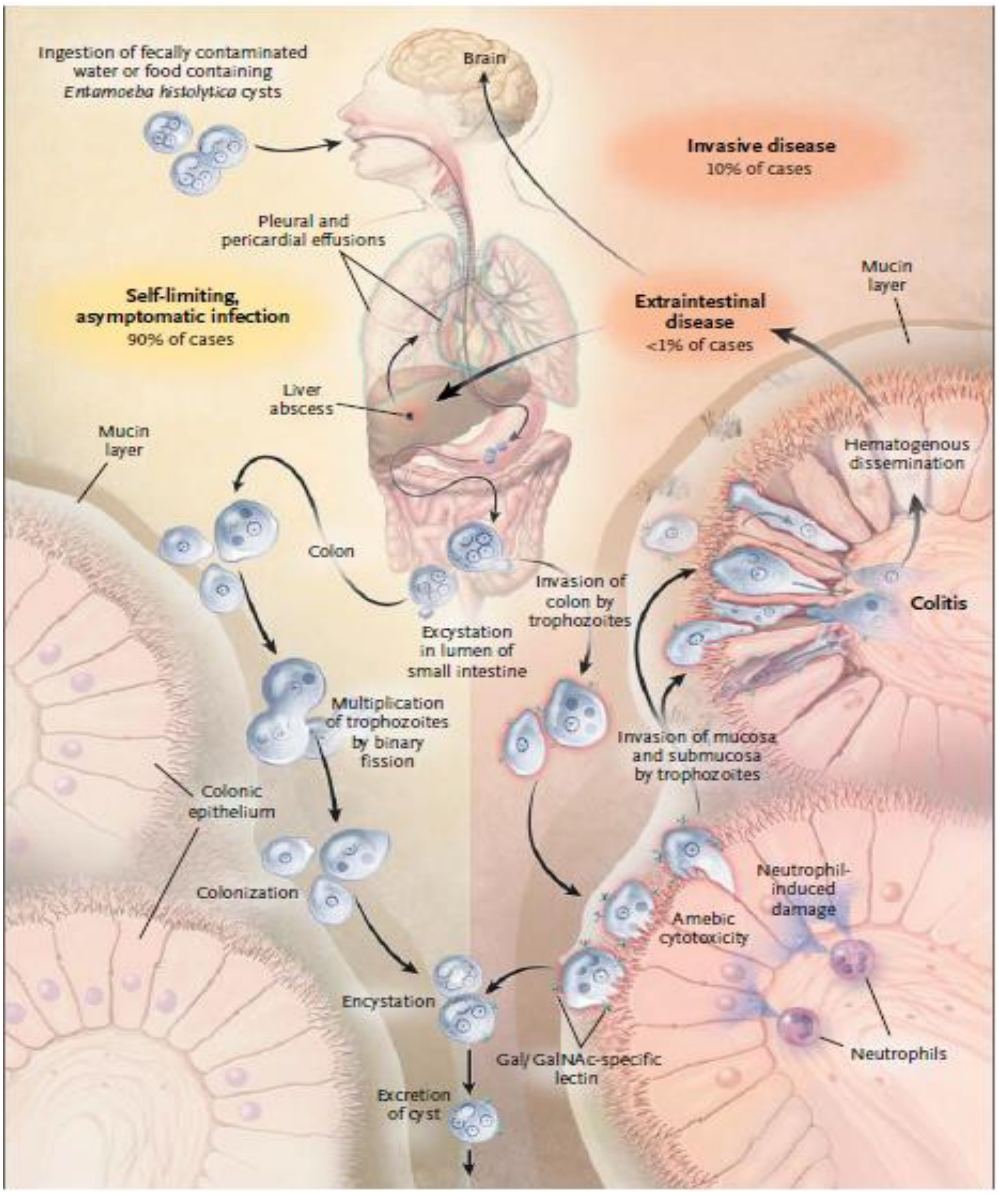

Figure1. 1 Life cycle of *E. histolytica*. Infection occurs by the ingestion of faecal contaminated water or food by *E. histolytica* cysts. Excystation occurs in the small intestine, and 4 trophozoites are released, multiply and migrate to the colon. In most infections the trophozoites continue to multiply, forming new cysts and then are excreted. In some cases, an invasion of colon epithelium by the trophozoites occurs, causing ulcers. Invasion of the colon epithelium may be followed by an extra-intestinal spread via portal circulation to the liver, lung and sometimes the brain resulting in abscess within those tissues (Haque *et al.*, 2003).

1.3 Encystation process

The mechanism of stage differentiation from the invasive motile trophozoite to the infective dormant cyst is called encystation. Encystation is vital for pathogenesis and transmission of *Entamoeba* and the life cycle of numerous other intestinal protozoa, including *Giardia* (Gaechter *et al.*, 2008)*, Toxoplasma* (van Dooren *et al.*, 2009) and *Cryptosporidium* (Samuelson *et al*., 2013). It involves the formation of cyst walls to protect the parasite from harsh environmental conditions (Mi-Ichi *et al.*, 2016). In protozoa, there are different intestinal factors that might direct stage transition. In *Giardia intestinalis*, and during the parasite journey to the lower part of small intestines, the high pH and lipid starvation are the most likely encystation triggers, whereas in *Cryptosporidium*, encystation is mainly triggered by low pH and high temperature. However, the factors that trigger encystation in *E. histolytica* are still unknown. *E. invadens,* the reptilian parasite, is widely used as a laboratory model to study *Entamoeba* encystation. *E. invadens* is distantly related to *E. histolytica* and they share a similar life cycle, morphology, the number of nuclei and cyst wall components (Sanchez *et al.*, 1994; Eichinger, 1997). Hypo-osmotic shock and glucose starvation of axenic medium periods are the most widely *in vitro* standard methods used for encystation induction in *E. invadens* (Aguilar-Díaz *et al.*, 2011).

The molecular factors that trigger encystation in *Entamoeba* are still unknown (De Cádiz *et al.*, 2013; Eichinger, 1997). However, in the intestinal parasite, *Giardia intestinalis*, the single large GTPase dynamin related protein was reported to play a role in the regulation of encystation specific vesicles. Mutant *Giardia* dynamin, has

been found to block stage conversion (Gaechter *et al*., 2008). In *Entamoeba*, numerous researchers have attempted to study the molecular and cellular changes associated with stage conversion. The surface protein Gal/GalNAc lectin has been proposed as a trigger for the signal transduction leading to encystation (Mi-Ichi *et al*., 2016). This protein is thought to regulate cell to cell interaction via the Gal-terminated legened (galactose terminal) that lead to trophozites aggregation prior to encystation (García *et al.*, 2015). Coppi *et al* (2002) studied the effect of the autocrine catecholamine during *Entamoeba* encystation, using quantitative and qualitative biochemical analysis. They reported that *Entamoeba* express adrenergic-like molecules that release catecholamines into the medium to enhance cyst formation. Catecholamines are vertebrate hormones synthesized from tyrosine and plays important roles through adrenergic receptor-mediated signal transduction. The addition of this hormone to a serum-free medium increases the encystation efficiency to more than 90% (Coppi, *et al*., 2002). Cholesteryl sulfate, the final metabolite of sulfate activation, was revealed to increase encystation efficiency when added in a specific concentration (0–500 μM)(Mi-Ichi *et al.*, 2015.). Chlorate, an inhibitor of ATP sulfurylase and the first enzyme in the sulfate-activation pathway, was found to inhibit cyst formation. A study, by Singh *et al.*, (2015), proved the negative role of heat shock protein 90 (Hsp90) on *Entamoeba* encystation. The inhibition of Hsp90 stimulates encystation in both *Entamoeba* (Singh *et al*., 2015) and *G. intestinalis* (Nageshan *et al*., 2014). One of the possible promising drug targets is chitin, which is a significant cyst wall component. As aforementioned, during encystation glucose is diverted into chitin production (Samanta and Ghosh, 2012), and chitin is synthesised during the early phase of stage transition (Chatterjee *et al*., 2009).

The cyst wall of *E. invadens* primarily consists of chitin, chitosan (deacetylated form of chitin), chitinase, and two lectins, Jacob and Jessie, with chitin-binding domains (CBDs) (Arroyo-Begovich *et al*., 1980; Das, Van Dellen, *et al*., 2006; Samuelson and Robbins, 2011). The process of cyst formation is based on the hypothesis that encystation goes through three phases called the "wattle-and-daub" model (Chatterjee *et al*., 2009). According to this hypothesis, the early encystation phase (the foundation phase) includes constitutive expression of the plasma membrane Gal/GalNAc lectins followed by the binding of Jacob lectins (glycoprotein containing Gal) to the surface of the encysting amebae. Successively, in the mid-encystation (wattle phase), the Jacob lectins cross-link with chitin fibrils deposited on the surface of encysting amebae. Finally, in the aggregation induced by the addition of the Jessie3 lectin, that binds the chitin at the late encystation (daub phase), the cyst wall becomes solid as a result of self- C-terminal domain, making them impenetrable to small molecules (Figure 1.2) (Marta Frisardi *et al*., 2000; Wang *et al*., 2003). During encystation, amino acids are utilized as an alternative source of energy instead of glucose as a result of the redirection of glucose from glycolysis to chitin metabolism (Samanta and Ghosh, 2012; Spindler *et al*., 1990).

In *E. invadens*, the encystation process finishes after nearly 72 hours post induction, and it is associated with many cellular and molecular events. Early encystation is accompanied by the synthesis and deposition of the cyst wall components Jacob lectins and chitin to the cell membrane, whereas the synthesis of Jessie proteins happens in late encystation along with the assembly of the cyst wall *(Aguilar-Díaz et al*., 2010; Chatterjee, Sudip K. Ghosh, *et al*., 2009). It is well known that D-fructose-

6P is the key metabolite in glycolysis, converting glucose to ethanol, the fuel required for trophozoite motility.

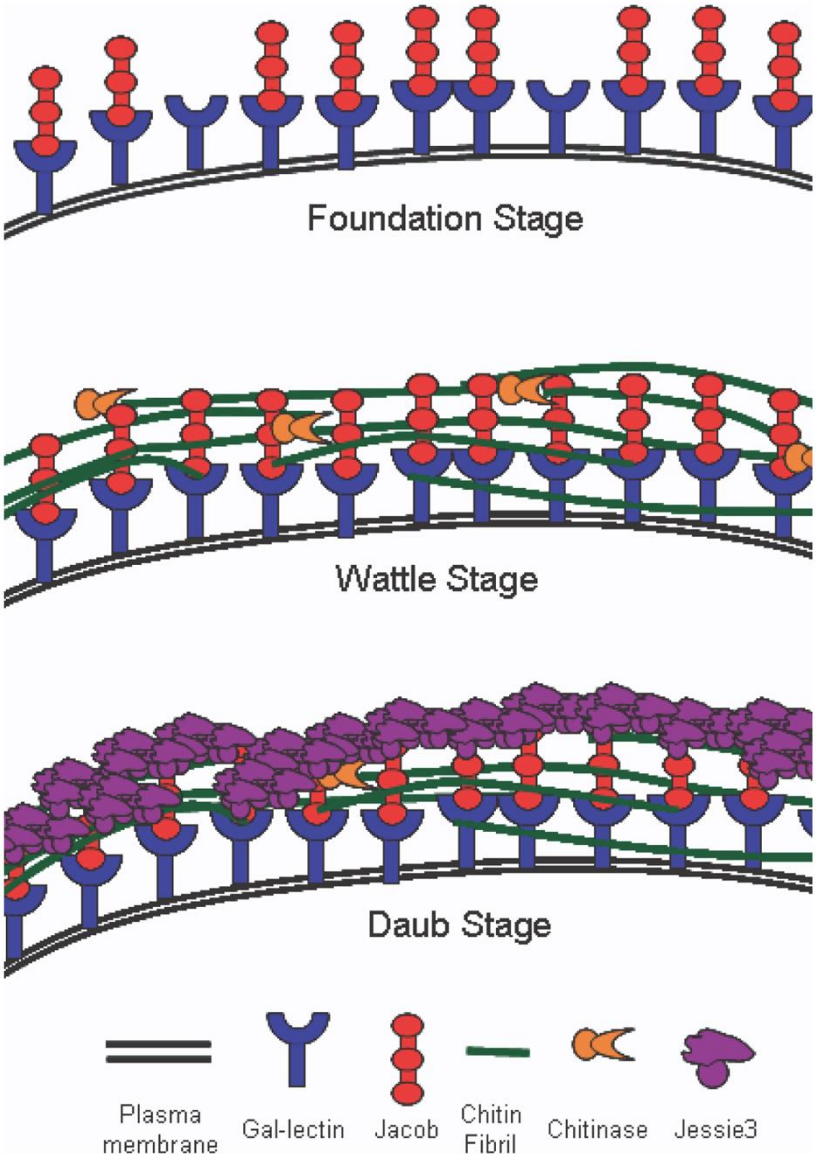

Figure1. 2 Predicted scheme of encystation in *Entamoeba*. In the foundation stage of encystation, Jacob lectins are bound to the surface of an encysting amoebae plasma membrane. In the wattle stage, chitin fibrils appear to cross-link with Jacob lectins, and chitinase remodels the chitin. In the daub stage, Jessie lectins appear to solidify the cyst wall and make it impermeable to small molecules. This figure is taken from Chatterjee *et al* (2009).

However, glycolysis interruption occurs during encystation in which glucose redirected toward chitin synthesis, where *Entamoeba* transforms D-fructose-6-phosphate into chitin synthase (Samanta and Ghosh, 2012). Moreover, the amino acids aspartate and asparagine are used as a substitute source of energy (Zuo and Coombs, 1995). Encystation is essential for the existence of *Entamoeba* and several protozoan parasites. Unlike *Giardia*, the factors that trigger encystation in *Entamoeba* are still unknown and this is a priority for study, given the importance of this process in the life cycle of these organisms.

1.3.1Chitin and Chitosan

Chitin is a single sugar polymer of N-acetylglucosamine, GlcNAC, abundantly found in the exoskeleton of arachnids and crustaceans. It has been shown to be a major component of some structures in various Metazoa such as Protostomia that synthesize chitin and some of Deuterostomia that possesses microfibrils containing chitin. Chitin has been identified in some of Protozoa, Nematodes, Pentastomatida and arthropods (Spindler, *et al.,* 1990). Chitin and chitosan (deacetylated form of chitin) play an important role in the pathogenesis and life cycle of several protists. For example, the cyst walls of *Entamoeba* and *Acanthamoeba* and the cell wall of fungi are composed of chitin and chitosan (Fanelli *et al*., 2005; Geoghegan and Gurr, 2017; Spindler *et a*l., 1990; Samuelson *et al.*, 2013).

In *Entamoeba*, chitin and chitosan are responsible for the rigidity of *Entamoeba* cyst wall. The synthesis of chitin occurs only during encystation to protect the parasites from undesirable environmental conditions. Analysis of mRNA expression of the chitin biosynthesis pathway showed that chitin is highly expressed during early encystation (9-12 hour post induction) and at the lowest level or absent in trophozoites (Samanta and Ghosh, 2012). Before encystation, *Entamoeba* starts to deacetylate chitin to chitosan by removing the acetyl groups (CH_3CO) from chitin by the action of chitin deacetylase (deacetylation). When N-acetylation is less than 50% (defined as the average number of N-acetyl-D-glucosamine units per 100 monomers expressed as a percentage), chitin becomes soluble in aqueous acidic solution, and it is then called chitosan (Figure 1.3). Chitin deacetylation makes the polymer more elastic to protect it from the adverse effect of chitinase (Casadidio *et al*., 2019; Narayanasamy *et al*., 2018; Rinaudo, 2006; Kumirska *et al*., 2010; Das, Van Dellen, *et al*., 2006).

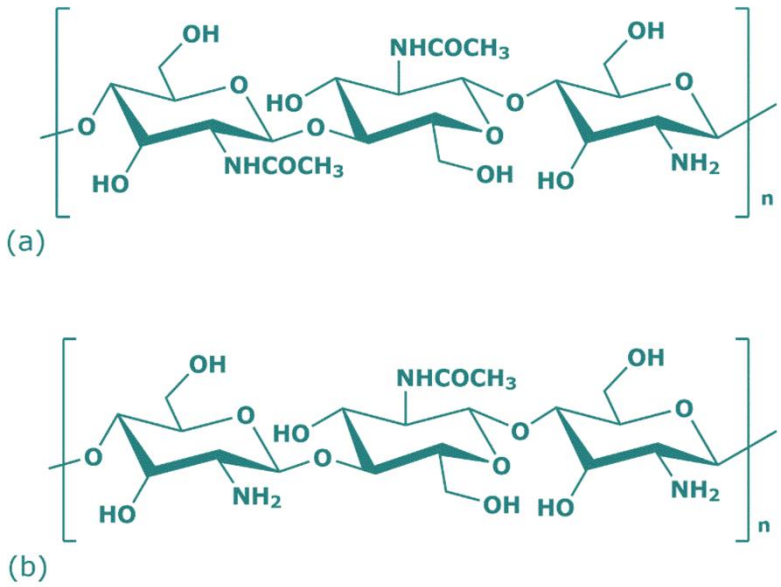

Figure1. 3 Chemical structure of chitin (a) and its deacylated form chitosan (b). Image taken from Casadidio *et al* 2019.

1.3.1.1 Chitin synthases

Chitin is synthesised by chitin synthases (Chs) that shares similar ancestry with cellulose synthases and hyaluronan synthase (Merzendorfer and Zimoch, 2003). Chs are variable transmembrane proteins possess conserved catalytic domains end with C-terminus transmembrane helices. Chitin synthesis pathway starts with glucose ending with UDP-GlcNAc (Uridine diphosphate *N*-acetylglucosamine), in which UDP-GlcNAc is converted into a chitin homopolymer and then looped via the transmembrane helices into the extra-cellular space. Phylogenetic studies showed that chitin synthase was found in many eukaryotes including amoebozoa and mycota, few bacteria and viruses (Figure 1.4) (Gonçalves *et al*., 2016). Chs are widely studied in fungi, and it has been reported that most fungi have several genes

encoding for Chs in their genome. In *S. cerevisiae*, four proteins, encoded by the Chs4–7 genes were identified (Trilla *et al*., 1999). The *E. histolytica* genome possesses two Chs (EhChs-1 and EhChs-2). EhChS-1 is 642 amino acids long with 7 predicted transmembrane helices, and EhCHS-2, is 980 amino acids long with 17 predicted transmembrane helices. The *E. histolytica* EhCHS-2 complements a *S. cerevisiae* chs1/chs3 mutant and the function of EhChs2 is independent of the four accessory peptides (Van Dellen *et al*., 2006). This suggests the possibility that chimaeras of *E. histolytica* and *S. cerevisiae* Chs may be used to map domains in the *S. cerevisiae* Chs that interact with the accessory peptides.

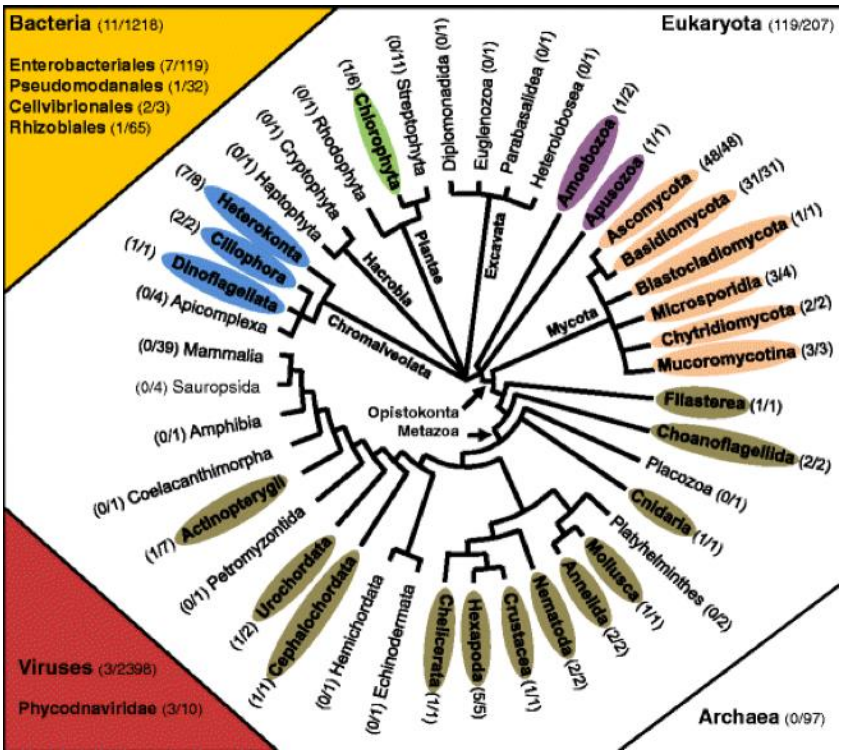

Figure1. 4 Phylogenetic analysis of the distribution of chitin synthases among eukaryotes, bacteria, viruses and archaea. Chitin synthase containing clades were written in bold and shaded. The number of species carrying chitin synthase to the number of species analysed were included between brackets.

Chitin synthase was identified in about 119 of eukaryotes, 3 viruses, 11 bacteria and not detected in archaea. Image taken from Gonçalves, *et al* (2016).

Moreover, the metabolism of chitin in encysted *Entamoeba* is similar to that of β-1,3 GalNAc homopolymer in *Giardia intestinalis*, where the synthesis of UDP-N-acetylglucosamine from glucose ends by the formation of chitin in *Entamoeba* and β-1,3 GalNAc homopolymer in *Giardia* (Loftus *et al*., 2005; Samanta and Ghosh, 2012). Chitin metabolism might be exploited as a possible drug target against *Entamoeba* as it doesn't exist in mammalian cells. All genes encoding for enzymes involved in chitin synthesis pathway are highly upregulated during encystation and no expression was recorded in trophozoites (Mi-Ichi *et al*., 2016). These enzymes include, glycogen phosphorylase, glucose-6-phosphate-Isomerase, D-glucosamine-6-phosphate, glucosamine 6-phosphate N-acetyltransferase, UDP-N-acetylglucosamine pyro-phosphorylase and chitin synthase (Samanta and Ghosh, 2012). The addition of double strand RNA encoding for glucosamine-6-phosphate isomerase, decreases its mRNA levels in encysted cells, resulting into a significant reduction in chitin synthesis. Moreover, the addition of glycogen phosphorylase inhibitor, to the *in vitro* newly encysted cells, reduces chitin level in the cyst wall. Glycogen phosphorylase supplies glucose to chitin synthesis by the break- down of glycogen (Mi-Ichi *et al*., 2016). Protein kinase C, a post translational modification protein, also plays a key role during encystation, through its regulatory effect on glycogen phosphorylase and other chitin synthesis pathway genes (Samanta *et al*., 2018). Chitin synthase synthesizes chitin at the vesicular membrane system that

involves the endoplasmic reticulum and Golgi network. On the other hand, UDP-GlcNAc transporter, a cytosolic nucleotide sugar transporter based at the vesicular membrane system, indirectly regulates chitin synthesis. The inhibition of UDP-GlcNAc may affect the ER or Golgi glycosyltransferase, which in turns disturbs the cyst wall formation and chitin deposition (Nayak and Ghosh, 2019). Chitin could be a potential therapeutic target in the control amoebiasis, therefore building a detailed understanding of the chitin synthesis pathway is an important research priority.

1.3.2 Chitinase

Although chitin is a ubiquitous polysaccharide, it does not accumulate to large amounts in nature due to the action of chitinolytic bacteria (Oyeleye and Normi, 2018). In eukaryotes, chitin deposition is balanced between the biosynthesis by chitin synthase and the degradation by chitinase (Schmitz *et al*., 2019). Chitinase, endo-β-1,4-N-acetylglucosamidase, is the degrading enzyme of chitin. Chitinases are abundantly produced by host cells as a defence mechanism against infestation with chitin-containing pathogens (Lee *et al*., 2011). The process of degrading pathogen chitin is part of the innate immune response. Chitinases plays a key role in the life cycle of chitin-containing fungi such as *Saccharomyces cerevisiae* and parasites such as *Entamoeba* (Shahabuddin and Vinetz, 1999). Approximately, 20% of the cyst wall is composed of chitinase, which has a single N-terminal CBD containing 8-Cys residues. *Entamoeba* chitinases shows 4-18 hydrophilic heptapeptide repeats between an N-terminal signal sequence and a C-terminal glycohydrolase domain that have an amino acid composition similar to that of the

spacers between CBDs of the Jacob and Jessie lectins. The single 8-Cys CBD lies close to the N terminus of the *E. histolytica* and *E. invadens* chitinases. Although chitinase is present in *E. invadens* trophozoites, the protein is only expressed during cyst formation and chitinase was seen in the secretory vesicle early during encystation in *E. invadens* (Herman *et al*., 2017).

Three chitinases might be involved in the remodeling of the walls during encystation or in the degrading of the walls during excystation (Van Dellen *et al*., 2002). Thus, understanding the role of these chitinases could be used as a drug target to stop encystation.

1.3.3 Lectins

1.3.3.1 Jacob

Jacob lectins are a cyst wall protein, an acidic 45 kD glycoprotein, which forms around 30% of the cyst wall components. The *Entamoeba* genome shows seven genes duplication encoding for Jacob lectins, three of which (Jacob1, Jacob2 and Jacob3) are the most abundant in the cyst wall of *E. invadens*. Each Jacob has three to seven tandemly arranged CBDs, each containing six conserved cysteine (Cys) residues and some aromatic amino acids. Some Jacob lectins can be cleaved between CBDs at conserved sites resembling to (TPSVDK), that lies before the lysine in the serine and threonine-rich spacers by site-specific cysteine proteases and O-phosphodiester-linked glycans. Jacob1 and Jacob3 are cleaved between the first and the second CBDs, while Jacob2 is cleaved between the third and the fourth

CBDs. The serine and threonine-rich spacers of *Ei*Jacob1 to *Ei*Jacob3 undergo post-translational modifications whereas, *Ei*Jacob6 and *Ei*Jacob7 contain long, low-complexity, sequences between CBDs. It is thought that the CBDs allow for the cross linking between Jacob lectin and chitin (Das, Van Dellen, *et al*., 2006; Marta Frisardi *et al*., 2000). It has been suggested that Jacob proteins make cross-links between chitin and the cell membrane, whereas chitinase remodels the chitin (Figure 1.2), (Spadafora *et al*., 2016; Chatterjee, Sudip K. Ghosh, *et al*., 2009; Marta Frisardi *et al*., 2000). According to Chatterjee *et al*. (2009) Jacob and chitinase are expressed early during encystation inside secretory vesicles (Herman *et al*., 2017; Chatterjee *et al.*, 2009). Studying the interaction of Jacob with other cyst components would help us to understand cyst formation.

1.3.3.2 Jessie

Jessie lectin is the most abundant glycoprotein in the *Entamoeba* cyst wall and forms about 70% of cyst wall proteins. *E. invadens* genome has five predicted Jessie lectins, *Ei*Jessie1a-*Ei*Jessie1c, *Ei*Jessie3a and *Ei*Jessie3b, whereas *E. histolytica* contains three genes representing *Eh*Jessie1-*Eh*Jessie3. *Ei*Jessie1a-*Ei*Jessie1c, *Eh*Jessie1 and *Eh*Jessie2 lectins have an N-terminal eight-cysteine lectin domain signal peptide and unknown domain, while *Ei*Jessie3a, *Ei*Jessie3b and *Eh*Jessie3 show N-terminal eight-cysteine CBD, serine and threonine-rich spacer, and conserved C-terminal domain. The unknown domain involved in chitin modification might play a role in self aggregation that allows Jessie to form the mortar or daub between chitin fibrils and Jacob lectins. This protein is expressed late during

encystation and acts as a daub or mortar to solidify the cyst wall and reduce its permeability (Chatterjee, Sudip K. Ghosh, *et al*., 2009; Das, Van Dellen, *et al*., 2006; Marta Frisardi *et al*., 2000). Jessie protein is an important part of cyst components, therefore, understanding its interaction with other components and role during encystation could be used to stop this process.

1.4 Aim of this study

Amoebiasis is one of the most death causing diseases due to parasites, responsible for thousands of deaths worldwide. Amoebiasis is primarily treated with metronidazole which is an antibiotic working directly on inhibition of DNA synthesis in anaerobic microorganisms (Duchêne, 2015). Moreover, auranofin and nitazoxanide, newly emerged drugs of choice, are widely used as a potent treatment for amoebiasis (Ralston, 2015). Recently, researchers are attempting to find new drugs that can target the parasite but that do not affect human cells. The study of the cyst wall components of *Entamoeba* might provide us with a better understanding about the process of encystation and offer opportunities to identify targets for new and effective treatments for amoebiasis.

The aim of this thesis was to understand membrane dynamics and study the interactions between cyst wall components to identify crucial points that control the encystation process, and which could be used to disrupt the parasite's life cycle

In chapter three, I hypothesize that the addition of chitin, chitosan and cyst wall lectins (Jacobs and Jessies) to the plasma membrane lipids of *E. invadens* would increase the stiffness of the monolayer of these lipids. To achieve that, the lipids was

extracted from the plasma membrane lipids (PML) of *E. invadens*, followed by, using Langmuir trough to study the interaction between the PML and the cyst wall components. The Langmuir trough experiments carried out with monolayer of lipids, while the plasma membrane consist of bilayer, therefore, to confirm the trough experiments results, thermal fluctuation analysis has been used, when red blood cells used as a membrane model. In these experiments I assume that the addition of chitin, chitosan and lectins would increase the rigidity of RBCs membrane. In chapter four, I hypothesize that the addition of cyst wall components (Jacob, Jessie and chitin) to the plasma membrane would change the membrane dynamic and increase the rigidity. In order to study that I need to get the protein expressed and purified. Jacob and Jessie were amplified from *E. invadens* genomic DNA and cloned into an expression vector for protein purification. Several attempts were done to purify Jacobs and Jessies, however, due to technical issues and time limitation, I couldn't purify them.

Chapter 2 - General Materials and Methods

2.1 Micro-organisms

In this study two kinds of microorganisms were used: a parasite, *Entamoeba invadens* and bacteria *Escherichia coli*.

2.1.1 *Entamoeba invades*

Trophozoites of *E. invadens* strain IP-1 were grown at room temperature, in borosilicate tubes containing 13 ml LYI-S medium (Liver digest, Yeast extract, Iron and Serum), 15% adult bovine serum and 2% Diamond vitamin mix. Cultures were maintained by sub-culturing every two weeks. Parent cultures were placed on ice for 5-10 minutes and tubes were gently inverted several times to ensure detachment of trophozoites. Thirteen ml of new culture medium was pre-warmed to room temperature, seeded with 100 µl of parent culture and incubated at room temperature at a slight angle for two weeks (Diamond, 1987). For lipid extraction and plasma membrane isolation, *E. invadens* trophozoites were transferred into a 250 ml LYI-S medium.

The medium and solutions of cultivation are as follow:

2.1.1.1 LYI-S Medium, pH 6.8 for culturing of *E. invadens*

Components for 880 ml stock (Diamond and Cunnick, 1991):

- 0.6 g KH_2PO_4
- 2 g NaCl
- 25 g yeast extract

- 5 g liver digest neutralized
- 10 g glucose
- 1 g cysteine
- 0.2 g ascorbic acid
- 2 ml ferric ammonium citrate (22.8 mg/ml)
- 1 M sodium hydroxide to adjust pH to 6.8
- H_2O up to 880 ml
- The medium base was aliquoted into 10 x 88 ml, autoclaved at 121 °C for 15 min and stored at -20 °C.

2.1.1.2 Vitamin mixture (Diamond and Cunnick, 1991)

❖ Solution 1

- 45 mg niacinamide
- 4 mg pyridoxal hydrochloride
- 23 mg pantothenic acid
- 5 mg thiamine hydrochloride
- 1.2 mg vitamin B12
- H_2O up to 25 ml

❖ Solution 2

- 7 mg riboflavin dissolved in a minimum amount of 0.1 M NaOH.
- H_2O added to a final volume of 45 ml.

❖ Solution 3

- 5.5 mg folic acid dissolved in a minimum amount of 0.1 M NaOH.

- H_2O added to a final volume of 45 ml.

❖ Solution 4

- 2 mg D-biotin dissolved in 45 ml of H_2O.

Solutions 1 – 4 were combined.

❖ Solution 5

- 1 mg DL-6-8-thioctic acid (oxidized form)
- 5 ml 95% ethanol
- 500 mg Tween-80
- H_2O up to 30 ml

Solution 5 was added to the combined solutions 1 – 4.

The final volume was adjusted to 200 ml with distilled H_2O, filter-sterilized and stored at -20.

2.1.2 Bacterial strains and the media

Three strains of *E. coli* were used in this study; they are as following:

1. ***E. coli* DH5α (New England BioLabs Inc.):** This strain has a high transformation efficiency and used in all cloning experiments.
2. **BL21 (DE3) *E. coli* (New England BioLabs Inc.):** These cells are chemically competent, derived from *E. coli* B strain and carrying the Lambda DE3 lysogen. The expression of heterologous genes is highly expressed in these cells than other types of *E. coli*.

3. **Rosetta (Novagen, UK; prepared in house):** These cells are derived from BL21 (DE3), used for gene expression and designed to enhance the expression of eukaryotic proteins that contain codons rarely used in *E. coli*.

Media for the bacterial culture:

1. Luria Bertani (LB) broth and agar (Green and Sambrook, 2012) was used to grow *E. coli* cells in different stages in this study, and to prepare one litter of broth, 10 g/L tryptone, 10 g/L NaCl, 5 g/L yeast extract were added to distilled water and autoclaved for 20 minutes at 120 ºC, and to prepare LB agar, 10 g agar were added to 1000 ml of LB broth.

2. ZYM-5052 (Studier, 2005)

This medium was used for autoinduction in protein expression experiments. To make 400 ml, the following chemicals were added to 380 ml of demineralised water and autoclaved:

- 1% N-Z-amine (tryptone or other casein digest)

- 0.5% yeast extract

The following sterile stocks were added to the above autoclaved mixture:

- 8 ml 50 X M solution

- 8 ml 50 X 5052 solution

- 800 µl 1 M $MgSO_4$ (400 µl 2M $MgSO_4$)

- 80 µl 1000 X metals

Then ampicillin (100 mg/ml) was added.

50 X M Solution

- 25 mM Na_2HPO_4

- 25 mM KH_2PO_4

-50 mM NH_4Cl

- 5 mM Na_2SO

50 X 5052 Solution

-0.5 % glycerol = 54 mM

-0.05 % glucose = 2.8 mM

-0.2 % α-lactose = 5.6 mM 68

1000 X metals, in 100 ml

- 36 ml sterile H_2O

- 50 ml 0.1 M $FeCl_2$ in 0.12 M HCl

- 2 ml 1 M $CaCl_2$

- 1 ml 1 M $MnCl_2$-$4H_2O$

- 1 ml 1 M $ZnSO_4$-$7H_2O$

- 1 ml 0.2 M $CoCl_2$-6H2O

- 2 ml 0.1 M CuCl2-$2H_2O$

- 1 ml 0.2 M $NiCl_2$-$6H_2O$

- 2 ml 0.1 M Na2MoO_4-$2H_2O$

- 2 ml 0.1 M Na_2SeO_3-$5H_2O$

- 2 ml 0.1 M H_3BO_3

- 1 ml 0.2 M $CoCl_2$-$6H_2O$

- 2 ml 0.1 M $CuCl_2$-$2H_2O$

2.2 *Entamoeba invadens* plasma membrane isolation

Isolation of *E. invadens* plasma membrane was carried out according to van Vliet *et al* (van Vliet *et al.*, 1976). *E. invadens* cells cultured in 250 ml flasks were harvested after 8 – 10 days and washed two times with phosphate buffer solution (PBS, one tablet dissolved in 500 mL of distilled water, containing 0.01 M phosphate buffer, 0.0027 M KCl, and 0.137 M NaCl, pH 7.4, Fisher scientific) by centrifugation at 500 *g* for 5 min. Cells were re-suspended in cold sucrose solution containing 1 mM EDTA, 10 mM $NaHCO_3$ and 10% sucrose, adjusted at pH 7.0 and subsequently homogenized using a loose fitting Dounce homogenizer (10-15 strokes). Afterward, samples were centrifuged at 500 *g* for 10 min to separate the nuclei and cell debris (pellet) from the other parts of the cell. The supernatant was transferred into a new tube and centrifuged at 4500 *g* for 20 min. The floated layer on the supernatant was carefully taken and disposed (contains phagolysosomes). Then the supernatant was centrifuged at 1500 *g* for 10 min, and subsequently the supernatant which contains the microsomes was discharged. The pellet was washed twice using 10 % sucrose solution (2 mg of sucrose dissolved in 20 ml of distilled water) at 1500 *g* for 10 min, then the pellet which contains the crude plasma membrane was re-suspended in 10 % sucrose solution. Meanwhile, five of sucrose solutions (30%-50% sucrose) were prepared, and 2 ml of each concentration were added carefully into 14 ml ultracentrifuge tube (Ultra-Clear tubes, Beckman), by placing a long syringe needle to the tube bottom and loaded the gradients in which the lightest gradient concentration is loaded first to make a continuous sucrose gradient layer. The final

pellet with 10 % sucrose solution was laid down on the continuous sucrose gradients and centrifuged at 25200 rpm for 150 min using ultracentrifuge (Beckman SW 40 Ti rotor, USA). The major part of the plasma membranes that banded at 47 % sucrose was collected and stored at -20 °C.

2.3 Lipid extraction

Lipids from whole cell and plasma membrane (isolated as described in section 2.2) were extracted according to Folch *et al* (Folch *et al*., 1957). To avoid contamination with plastic material, for the extraction process, only glassware was used as one of the extraction solutions contained chloroform. Harvested cells or plasma membranes were homogenized in chloroform/methanol (2:1 ratio) to a total volume 20 times the sample volume. The mixture was shaken for 15 – 20 min at room temperature (Infors-HT Shaker incubator, multitron, Switzerland). The homogenate was filtered using Whatman quantitative filter paper. The filtrate was washed with 0.9 % NaCl solution (4 ml for 20 ml), vortexed and centrifuged at 600 *g* for 10 min to separate the two phases (chloroform and methanol). The upper, methanol, phase was removed, and the interface was washed two times with methanol/water (1:1). The lower, chloroform, phase (containing the lipids) was evaporated under a nitrogen stream. Lipids dried on the wall of the tube were collected by rinsing the tube with 1 ml of chloroform. The mixture (chloroform/lipids) was aliquoted in small glass vials and stored at -80 °C.

2.4 Langmuir trough

A Langmuir trough technique was used to investigate the behaviour of monolayers of lipids spread on air-water interfaces and their interaction with molecules added to the subphase. A commercially produced trough was used (Kibron Inc, Micro Trough S, Filmware version 2.41, Finland). The trough and two barriers are made from polytetrafluoroethylene (PTFE). The barriers are moved by a stepper motor and a wire probe used to measure the surface pressure. A computer controls barrier movement and records position and surface pressure with specific software to record the data (Figure 2.1).

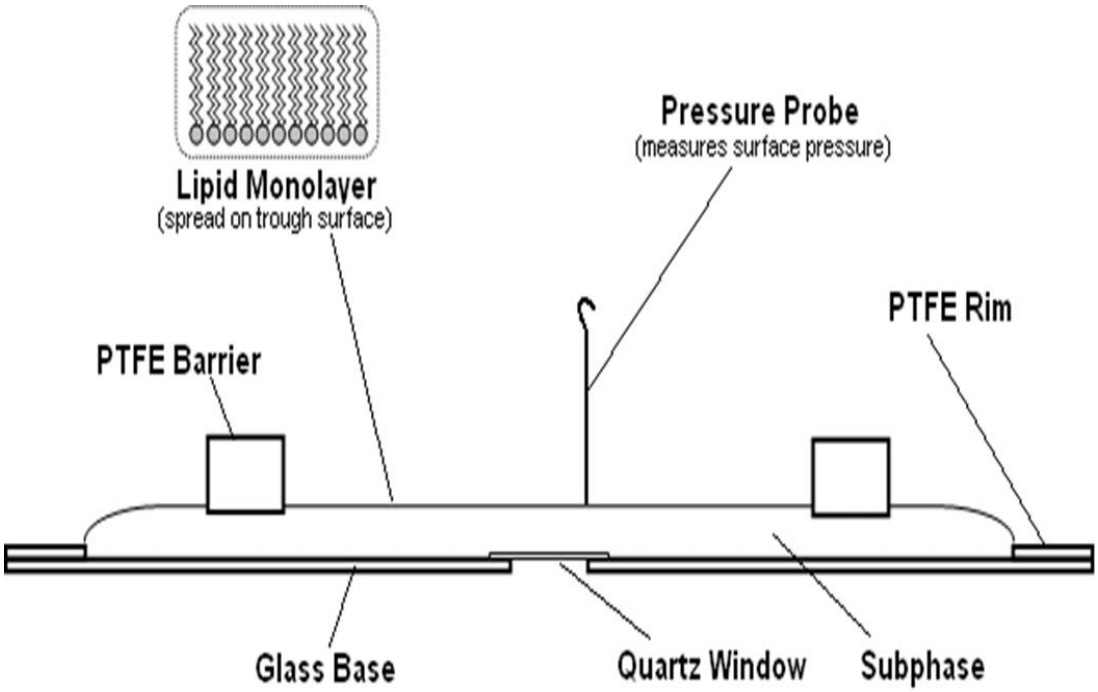

Figure 2. 1 Schematic of a Langmuir trough, showing the trough, two moving barriers, the aqueous subphase and a pressure probe (Abdul Rahman, 2008).

60 ml of purified water was used as a subphase, and to ensure that its surface was clean and there was no contamination, the water surface was swept repeatedly with the barriers and the surface was aspirated using a suction pump. When the surface pressure displays between (0 ± 1) mN/m, the surface was considered free from contamination, several drops of the lipid chloroform solution were placed regularly on the water surface and the organic solvent was allowed to evaporate for one hour. The pressure-area isotherms were recorded during compression and expansion of the lipid monolayer by movement of the barriers. During monolayer compression, the average molecular area decreases, and the pressure increases, and the lipid molecules rearrange and orientate in a specific way depending on the interactions between them. Usually, distinct phases are observed (*e.g.* gas, liquid expanded, liquid condensed, solid), which correspond to specific molecular arrangements that have different physical properties (Figure 2.2). The dilatational modulus (which characterises the monolayer elasticity) can then be calculated from the gradient of the isotherms to obtain information about the elasticity of the lipid monolayer using the following formula:

$$\varepsilon = -A\frac{d\pi}{dA}$$

where ε is the dilatational modulus, A is the area and π is the surface pressure.

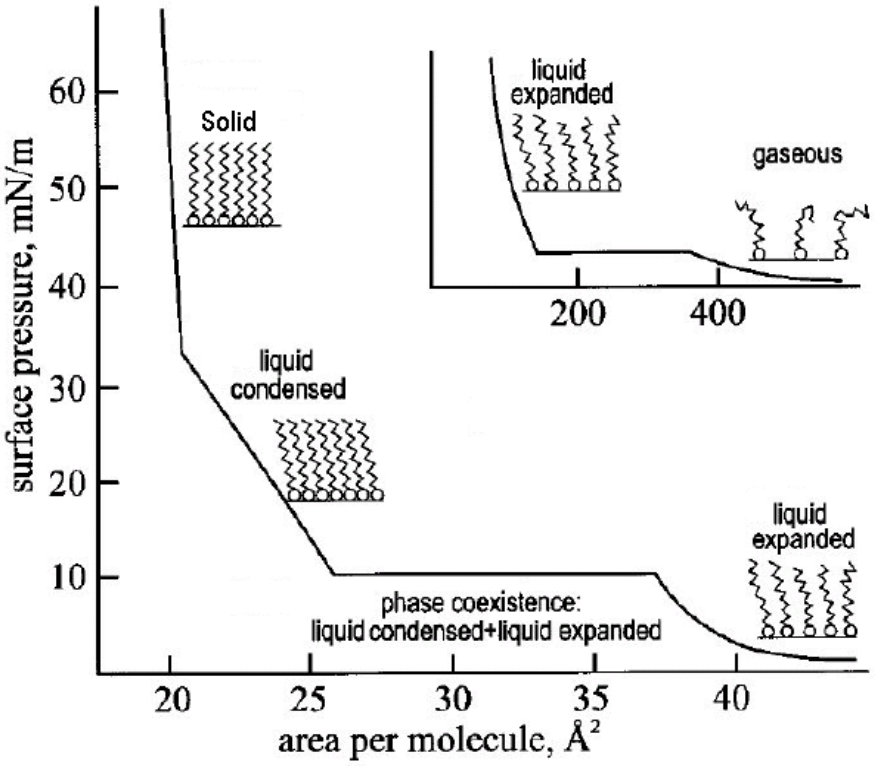

Figure 2. 2 Distinct phase regions during the monolayer compression (Kaganer *et al*., 1999). The different phases are indicated on the figure.

2.5 Thermal fluctuation analysis

Thermal fluctuation analysis was used to study the interaction between *E. invadens* cyst wall components (chitin, and chitosan) and the erythrocyte plasma membrane by monitoring their effects on the red blood cells RBCs membrane bending elastic modulus. RBCs were used as a model for lipid bilayers since its composition is similar to that of the *E. invadens'* plasma membrane. RBC membrane consists of two layers, the outer one is a fluid lipid bilayer, and the inner layer is called membrane skeleton which is an elastic protein network composed mainly of spectrin. Both are associated with cell flexibility and mechanical stability (Sackmann, 1995): the lipid

bilayer endows bending stiffness to the membrane, whereas the protein membrane skeleton provides the membrane with shear resistance Approximately half the RBC membrane mass is composed of proteins, with 40% being lipids and 8% being carbohydrates (Mohandas and Evans, 1994). This methodology was used to clarify any effects of cyst wall components on the lipid membrane as this project aims to investigate the dynamics of the encystation which includes interactions between cyst wall components and the plasma membrane of *E. invadens*.

Five microliters of fresh human blood obtained by finger prick from a volunteer were suspended in 1 ml of PBS (same preparation in section 2.2.) mixed with 1 mg/ml bovine serum albumin (Sigma-Aldrich, UK). Fifty µl from the suspension were then mounted onto a clean microscope slide and covered by a coverslip which was fixed to the slide by two strips of Parafilm on the long slide edges to construct an open sided observation chamber (Hale *et al*., 2011). After RBCs stabilized at the bottom of the slide chamber, one RBC was selected, and first video was recorded for the cell in the PBS before the addition of chitin/chitosan, and this was done to have the fluctuation spectrum and elastic modulus for the normal, untreated cell. Then the buffer was exchanged with 1000 µl of buffer containing 100 µg / ml of either chitin or chitosan. Then, videos of RBCs were recorded at different time points: 0, 5, 10 and 20 minutes after buffer exchange. These videos were recorded using fast-video phase contrast microscopy (Leica DMLFS upright microscope equipped with a 63x PL Phase-contrast objective) and Moticam 2000 2 MP progressive scan digital video camera (Motic, Hong Kong) at a typical frame rate of 60 fps. The videos were then analysed using a plugin for ImageJ (Schneider *et al*., 2012), a special software

developed in the Biophysics at the University of Exeter to extract 2D contour of the cell perimeter with sub-pixel resolution. The coordinates of the points for each contour are stored as a text file, which were used to obtain the thermal fluctuation spectrum of the cell and it's bending elastic modulus. A series of contours of tested RBCs was obtained (between 1500 and 2500), then analysed for membrane fluctuations quantification. All contours were represented with a Fourier series according to the following equation (Hale *et al.*, 2011).

$$r(\theta) = R\left\{1 + \sum_{n}[a_n\ \cos(n\theta) + \ b_n\ \sin(n\theta)]\right\}$$

In which *r* and θ represent the polar coordinates, *R* is the mean contour radius and a_n and b_n are the Fourier amplitudes. Followed by calculating the mean-squared amplitudes from a_n and b_n for the entire set of contours, according to below equation (Hale *et al.*, 2011):

$$\langle\delta_n^2\rangle = \ [\langle a_n^2\rangle - \langle a_n\rangle^2] + \ [\langle b_n^2\rangle - \langle b_n\rangle^2]$$

After that the fluctuation spectrum was plotted as $\langle\delta_n^2\rangle$ as a function of the mode number, n.

The following equation was used to obtain the value of the bending modulus, and to fit this equation to the experimentally obtained fluctuation spectrum, a non-linear fitting procedure was used (Hale *et al.*, 2011):

$$\langle\delta_n^2\rangle = \frac{1}{2\pi}\frac{k_BT}{k}\frac{\left[\left(\tilde{\sigma} + n^2 - \sqrt{\tilde{\sigma} - \tilde{\gamma}}\right)^{-1/2} - \left(\tilde{\sigma} + n^2 + \sqrt{\tilde{\sigma} - \tilde{\gamma}}\right)^{-1/2}\right]}{(\tilde{\sigma}^2 - \tilde{\gamma})^{1/2}}$$

where K is representing the bending modulus, $\tilde{\sigma}$ is the dimensionless membrane tension, $\tilde{\gamma}$ is the dimensionless strength of the confinement potential, k_B is the Boltzmann constant and T is the temperature. The mean-squared amplitudes and the bending modulus equations were performed by special software developed in the Biophysics at the University of Exeter.

2.6 Molecular biology

2.6.1 DNA extraction

E. invadens IP-1 was sub-cultured in 50 ml flasks for 72 hours. Cells were harvested by centrifugation at 4000 *g* for 5 minutes and washed twice with PBS. DNA was extracted according to Ali *et al* (Ali *et al*., 2005). The pelleted trophozoites (50 µl) were re-suspended in 250 µl lysis buffer (0.25% SDS in 0.1 M EDTA, pH 8.0) 100 µg/ml of proteinase K (3 µl from a 10 mg/ml stock) (Sigma – Aldrich). Afterward cells were dispersed and incubated at 55 °C for 15 minutes. At room temperature, 75 µl of 3.5 M NaCl were added and mixed, followed by the addition of 42 µl of 10% CTAB/0.7 M NaCl (heated to 55 °C), mixed and incubated at 65 °C for 10 minutes. Around 400 µl of chloroform was added (inside a fume hood), mixed well by inversion and centrifuged at full speed in a micro-centrifuge for 5 minutes. The supernatant was removed and transferred into a new tube (inside a fume hood) and 400 µl of phenol: chloroform: isoamyl alcohol were added, mixed well by inversion and centrifuged at full speed in a micro-centrifuge for 5 minutes. The supernatant was then transferred to a new tube. Followed by, the subsequent addition of two volumes of 100% ethanol, mixed gently by inversion, incubated at room temperature

for 5 minutes and centrifuging for 10 minutes at full speed. The supernatant was discarded carefully from the pellet. The pellet was then washed in 200 µl of 70% ethanol by centrifuging for 5 minutes as above. The pellet was air dried and re-suspended in 50 µl of sterile water (overnight at 4 °C is best). The DNA was quantified using a NanoDrop 2000c (Thermo-scientific) and visualized using agarose gel electrophoresis.

Solutions:

- CTAB lysis buffer, 100 ml:
    - 3.72 g EDTA
    - 0.25 g SDS
    - Dissolve in distilled water to a final volume of 1,000 ml (pH 8.0)

- 10 % CTAB in 0.7 M NaCl, 100 ml:
    - 10 g CTAB Up to 100 ml.
    - 0.7 M NaCl.
- Proteinase K, 2 mg/ml:
    - Dissolve proteinase K powder in distilled water then filter-sterilize through a 2 µm filter.
    - The final concentration used is 0.1 mg/ml.

2.6.2 PCR amplification of the targeted genes

The genes encoding *E. invadens* cyst wall proteins were amplified from genomic DNA. *Ei*Jacob2 (GenBank accession number DQ324634.2) was amplified from *E. invadens* genomic DNA using the forward primer (5'-ATG ATA CTA CTG TTT TTG G) and reverse primer (5'-TTA ATT CTT CTT TGC CCA G). Primers were designed by Dr Mark van der Giezen. Genes were amplified using GoTaq G2 Hot Start Green Master Mix (Promega) which adds an adenine overhang to the PCR product which is utilised for cloning into a TA cloning vector containing a complementary thymine overhang. The thermal cycler was programmed using the recommended parameters for GoTaq G2 Hot Start Green Master Mix (Table 2.1). The *Ei*Jacob1 (AF175527), *Ei*Jacob3 (DQ324635.2), *Ei*Jessie3a (DQ324645.1) and *Ei*Jessie3b (DQ324646.2) genes were amplified from the *E. invadens* genomic DNA using primers with restriction sites for the cloning into the expression vector pET14b. Primers are described in Table 2.2. A high fidelity KOD DNA polymerase (Merck-Millipore) was used to amplify these genes to reduce the possibility of mutation, using a gradient PCR machine (Bio-Rad T100 Thermal Cycler, USA) to reveal the optimal annealing temperature (Table 2.3).

Table 2. 1 Thermal cycler conditions using GoTaq DNA polymerase.

Segment	No of cycles	Temperature °C	Duration
Initial denaturation	1	95	5 minutes
Denaturation	35	95	45 seconds
Annealing temperature		46	45 seconds
Extension		72	1 min / 1 kb
Final extension	1	72	5 minutes
Final temperature	1	4	∞

Table 2. 2 Primers for Jacob and Jessie genes with restriction sites. Underlined letters represent the restriction sites, uppercase indicate homologous sequence and lowercase indicate nonsense sequence.

Protein	Primers
*Ei*_Jacob1-*Xho*I-F	aga aga CTC GAG ATG TTA TCT TTT ATA TTG TTC
*Ei*_Jacob1-*Bam*HI-R	tct tct gga tcc TTA GAT CTT CTT CCC CCA AG
*Ei*_Jacob2-*Xho*I-F	aga aga CTC GAG ATG ATA CTA CTG TTT TTG G
*Ei*_Jacob2-*Bam*HI-R	tct tct GGA TCC TTA ATT CTT CTT TGC CCA GG
*Ei*_Jacob3-*Xho*I-F	aga aga CTC GAG ATG TTG ATA CTA CTG TTA CTG G
*Ei*_Jacob3-*Bam*HI-R	tct tct gga tcc TTA CCA CTC TGT TTG GTC C
*Ei*_Jessie3a-*Xho*I-F	aga aga CTC GAG ATG AAA ATC ACT TTC ATT GTA C
*Ei*_Jessie3a-*Bam*HI-R	tct tct GGA TCC TCA CTT ATT TAT TGT GTA ATT C
*Ei*_Jessie3b-*Nde*I-F	aga aga CAT ATG ATG AAC AGA GCG ATT ATA AC
*Ei*_Jessie3b-*Nde*I-R	tct tct CAT ATG TCA TTT GCA TAA GTT CTT TC

Table 2. 3 Thermal cycler conditions using KOD Hot Start DNA Polymerase.

Segment	No of cycles	Temperature °C	Duration
Initial denaturation	1	95	2 minutes
Denaturation	30	95	20 seconds
Annealing temperature		59 - 65	10 seconds
Extension		70	20 sec / 1 kb
Final extension	1	70	5 minutes
Final temperature	1	4	∞

2.6.3 Agarose gel electrophoresis

One percent agarose gel was usually used for gel electrophoresis. However, when analysing small DNA fragments a 2% gel was used. The agarose was dissolved in 1x Tris-acetate-EDTA (TAE) buffer, heated until fully dissolved and Midori green (Nucleic acid stain, Nippon Genetics) was added as a working concentration of 0.5 µg/ml. To set the gel, 1x TAE buffer was poured onto the gel tray until it was covered and left for 20 minutes to solidify. DNA samples mixed with 6x DNA loading dye buffer (New England Biolabs) were loaded into the wells with DNA ladder 1 kb (New England Biolabs). DNA fragments were separated by gel electrophoresis at 100-120 volts for 30-60 minutes. The DNA was visualised using a UV light box (BioDoc-It, imaging system, USA).

2.6.4 Purification of PCR products

The purification and isolation of PCR fragments were performed to eliminate all impurities such as primer-dimers dNTPs, Mg ions and restriction enzymes, as these could interfere with subsequent manipulations such as DNA sequencing and ligation. A Qiagen QIA-quick PCR purification kit that is based on the selective binding properties of a proprietary silica-gel membrane was used according to the manufacturer's protocol.

2.6.5 Cloning into TA vector

Jacob2 gene was cloned into pGEM-T-Easy plasmid, that contains thymidine overhangs that allow the hybridization of the complementary PCR product and the plasmid (Figure 2.3).

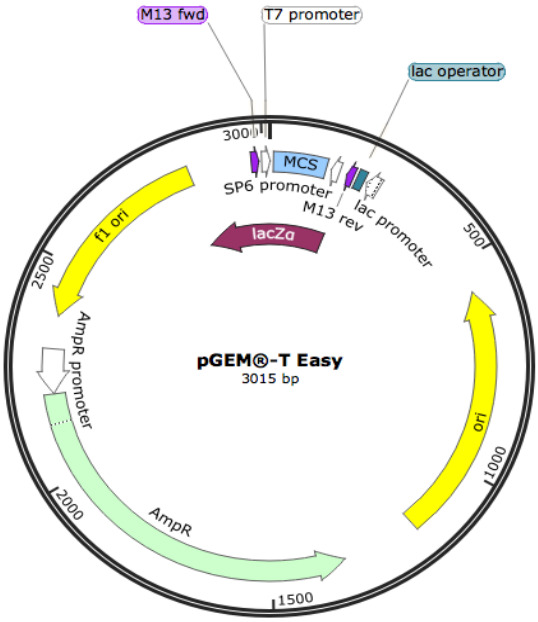

Figure 2. 3 The general cloning vector pGEM-T-Easy showing the multiple cloning site (MCS) that comes after the T7 promoter site, Ampicillin resistance gene. Figure created using SnapGene.

2.6.5.1 Ligation

Ligation was performed according to the manufacturer's protocol as follow:

• **2x rapid ligation buffer**	**5 µl**
• **pGEM-T-Easy vector (50 ng/ µl)**	**1 µl**
• **Purified PCR product (100-150 ng/µl)**	**3 µl**
• **T4 ligase (3 U/µl)**	**1 µl**
• **Final volume (H_2O)**	**10 µl**

Ligation mixtures were pipetted up-forth gently, centrifuged for 5 seconds to collect the mix at the bottom of the tube, and incubated in a baker filled with water inside the

fridge (4 °C). The ligation mix was optimized using the vector: insert ratio of 3:1 as follow:

$$\frac{\boldsymbol{ng\ of\ vector \times kb\ size\ of\ insert}}{\boldsymbol{kb\ of\ the\ vector}} \times \frac{\boldsymbol{insert}}{\boldsymbol{vector}} = \boldsymbol{ng\ of\ insert}$$

For example: Jacob2 length is 1.2 kb, the vector length and concentration are 3 kb and 50 ng respectively.

$\boldsymbol{so,}\ \frac{\mathbf{50\ ng \times 1.2\ kb}}{\mathbf{3\ kb}} \times \frac{\mathbf{3}}{\mathbf{1}} = \mathbf{60\ ng}$ of Jacob2 was used for the ligation experiment.

2.6.5.2 Transformation

After the cloning of EiJacob2, transformation into *E. coli* DH5α competent cells was carried out using a heat shock method following the instructions of the cloning protocol. Approximately 5-8 µl of ligation mix were transferred into 100 µl of *E. coli* competent cells, mixed gently by the tip of the pipette, kept on ice for 30 minutes, heat shocked by placing the mix in water bath at 42 °C for 45 seconds, then kept on ice again for 2 minutes. About 900 µl of LB broth were added to the mix and incubated in shaker incubator at 37 ºC for 1 hour. One hundred microliters of transformed cells were plated onto LB agar with ampicillin (100 mg/ml) and incubated overnight at 37 °C, and the remaining 900 µl was centrifuged for one minute at full speed and the pellet was plated onto another plate.

2.6.5.3 Colony PCR

Several colonies were picked and tested by colony PCR. Colonies were resuspended in 50 µl of water, and 5 µl of this suspension used for colony PCR using GoTaq DNA polymerase (Promega), the rest of the dilution were used for plasmid DNA extraction.

2.6.5.4 Plasmid DNA extraction

As mentioned in the colony PCR section, positive colonies were picked and resuspended in 50 µl of water, 45 µl were transferred into 5 ml of LB broth plus ampicillin (100mg/ml) and grown for 16-18 hours. Overnight cultures were purified using the QIAprep Spin Miniprep Kit (QIAgen, Germany) following the manufacturer's protocol. The constructs were checked by restriction digestion using *Eco*RI enzyme, and then sent for sequencing to Eurofins MWG Operon.

2.6.6 Cloning into pET-14b expression vector

In order to produce recombinant protein, genes were cloned into the expression vector pET-14b, which contains the T7 promoter and the N-terminal His-tag for affinity purification, followed by a thrombin cleavage site for removal of the His-tag after protein purification. The vector contains three cloning sites for introduction of the gene of interest. It contains an ampicillin resistant gene for selection. See Figure 2.4 for more details.

2.6.6.1 Targeted genes amplification

*Ei*Jacob2 was PCR amplified from pGEM-T-Easy (Promega), using a forward primer with an *Xho*I restriction site and a reverse primer with a *Bam*HI restriction sites, following the manufacturer's protocol. EiJacob1, EiJacob3, and *Ei*Jessie3a were PCR amplified from genomic DNA using primers with *Xho*I/*Bam*HI restriction sites. *EiJessie*3b was amplified from genomic DNA and *Nde*I restriction sites were added to the ends of the gene. Primers were designed by Dr Mark van der Giezen. A high fidelity KOD Hot Start DNA Polymerase (Merck Millipore) was used.

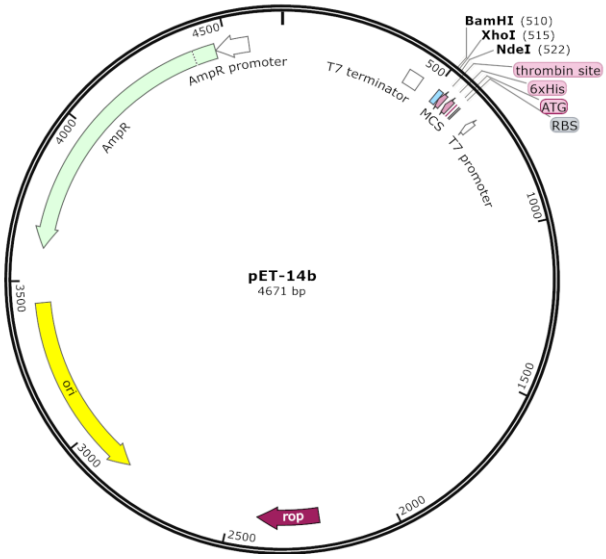

Figure 2. 4 Gene expression vector pET-14b, showing a backbone size of 4.6 kb, the multiple cloning sites with NdeI, XhoI and BamHI restriction sites used in this study, antibiotic resistance site and the T7 forward sequencing primer. Figure drawn using SnapGene.

2.6.6.2 Restriction digestion of DNA fragments and expression vector

Double digestion with *Xho*I/*Bam*HI was performed on EiJacob1-3, EiJessie3a and pET-14b using cut smart buffer (New England Biolabs). While, *Ei*jessie3a was digested by *Nde*I only using cut smart buffer. All digestions were done at 37 °C for 2 hours. New England Biolabs' double digest calculator program (https://nebcloner.neb.com/#!/redigest) was used to determine the double-digest conditions. Initially, a digestion with *Dpn*I was done only on Jacob2 to exclude the TA cloning vector carry over created by PCR, then proceeded to the double digestion steps as follow:

- Digestion with *Dpn*I:
    - DNA 8 µl (2 µg)
    - NEB CutSmart buffer 10X 4 µl
    - *Dpn*I enzyme 2 µl (20 U)
    - Free water, Nuclease up to 40 µl

Samples were mixed gently by pipetting and incubated at 37 °C for 1 hr, followed by heat inactivation at 80 °C for 5 min. All 40 µl of the digested PCR products were used in the double digestion.

- Double digestion:

  Plasmid DNAPCR products

- DNA 38 µl (2 µg) 40 µl (2 µg)

- NEBuffer CutSmart or 1 (10X) 5 µl 5 µl
- Restriction enzymes 2 µl (20 U) 2 µl (20 U)
- Free water, Nuclease 5 µl 3 µl
- Total volume 50 µl 50 µl

The Reaction mixtures were incubated at 37 °C for 2 hours. DNA samples were purified using the PCR Purification Kit (QIAgen). Purified products were quantified using NanoDrop 2000c (Thermo Fisher Scientific), and visually inspected using gel electrophoresis. The purified digestion product was either stored at -20 °C or directly used in subsequent ligation reactions.

2.6.6.3 Ligation and transformation

DNA fragments and pET-14b vector were ligated using T4 ligase (New England Biolabs). Ligation ratios were calculated by NEBio calculator from New England Biolabs (http://nebiocalculator.neb.com/#!/ligation) using 1:3 ratio, as follow:

- DNA (68 ng) 1.5 µl
- Vector (27 ng) 1 µl
- 10x buffer 1 µl
- T4 ligase (5 U) 0.5 µl
- Free water, Nuclease 6µl
- Final volume 10 µl

Ligation mixtures were pipetted up and down gently, spun for 5 s and incubated in a beaker filled with water at 4 °C.

2.6.6.4 Transformation of competent cells with plasmid DNA

Transformation was performed using *E. coli* α-select (Bioline). Competent cells were thawed on ice for 5 min. Between 1-8 µl of the plasmid construct were added to 50-100 µl of competent cells in 1.5 ml Eppendorf tube and flicked gently. Tubes were placed on ice for 30 minutes and heat shocked in water bath preheated at 42 °C for 40-45 seconds. Afterward, tubes were re-placed on the ice for another 2-5 minutes. Around 1 ml of LB medium were added and incubated in a shaker incubator (220 rpm) at 37 °C for 1 hour. Afterwards, 100 µl and 50 µl of the mixture were plated on LB agar plates containing the required antibiotic, with Isopropyl-β-D-thiogalactopyranoside (IPTG, Thermo-Scientific), and 5-Bromo-4-Chloro-3-Indolyl β-D-Galactopyranoside (X-gal, Thermo-Scientific) for cells that needs blue-white screening. Finally, plates were Incubated at 37 °C overnight for 16-18 hrs.

2.6.6.5 Colony PCR

Following bacterial transformation, individual colonies were picked using a sterile technique and re-suspended in 50 µl of sterile water. PCR was performed using 5 µl of the suspended colony as the template DNA. PCR was done using GoTaq DNA polymerase.

2.6.6.6 Plasmid DNA extraction (Miniprep)

Around 5 ml of LB broth containing the transformed cells with Ampicillin (100 mg /ml) were allowed to grow overnight in shaking incubator (200-250 rpm) at 37 °C. Plasmid DNA was isolated from the cultures using the QIAquick Spin Miniprep Kit according to the manufacturer's instructions. This procedure depends on the alkaline lysis of the competent cells; the lysed cells were neutralized and centrifuged to remove proteins and cells debris. The last step involves the loading of the DNA onto a silica membrane to remove impurities and elute with elution buffer or distilled water. DNA was stored until use at - 20°C.

2.6.6.7 Long term storage of bacterial clones

Glycerol stocks were made from recombinant cultures and mixed with 50% autoclaved glycerol at ratio 1:1. The mixture was then vortexed and stored at -80 °C.

2.6.6.8 DNA sequencing

To verify the desired constructs, Plasmids DNA were sent for sequencing. Sequencing was performed by Eurofins MWG Operon. The pGEM-T-Easy based construct were sequenced using the universal M13 forward (-43) and M13 reverse (-29) primers. pET14b based constructs were sequenced using the T7 forward and T7 terminator.

2.6.7 Gene expression

2.6.7.1 Transformation of constructs

Competent *E. coli* BL21 (DE3) (New England BioLabs Inc.) and Rosetta cells (Novagen) were used for gene expression. The competent cells were thawed on ice for 10 min. Tow µl of the plasmid construct were added to 50 µl of competent cells in 1.5 ml Eppendorf tube, flicked gently and incubated on ice for 30 minutes. Then cells were shocked in water bath preheated at 42 °C for 40-45 seconds before cooling them on ice for 2 minutes. About 200 µl of LB medium was added and cells were incubated at 37 ºC with shaking at 220 rpm for one hour. Afterwards, the cells were plated out onto LB plates containing Ampicillin and incubated at 37 °C overnight.

2.6.7.2 Protein induction

Next day, colonies were picked and used to inoculate an overnight starter culture at 37 °C with shaking at 220 rpm in 10 ml of LB with 100 mg/ml of ampicillin. The following day, glycerol stocks produced and stored in -80 ºC. Then 1 ml from this culture was transferred to 500 ml and 1 L of pre-warmed LB containing 100 mg/ml ampicillin. The culture was grown with shaking at 220 rpm at 37 °C. After three to four hours of incubation, optical density (OD_{600nm}) readings were taken periodically until OD_{600nm} reached between 0.4-0.8. IPTG was added at different concentrations (0.025, 0.050, 0.1, 0.2 and 0.4 M) to find out which concentration need to induce gene expression, followed by overnight (18-20 hours) incubation at different temperatures (30 °C and 20 °C, as not yet know the preferred temperature) with

constant shaking at 220 rpm. The cultures were then harvested by centrifugation at 4,700 *g* for 30 minutes at 4 °C. Finally, the cell pellet was re-suspended in 25 ml of nickel column wash buffer (20 mM Tris-HCl pH 8, 500 mM NaCl) per 0.5 L of culture. Cell suspension was processed immediately for sonication or kept at -20 °C.

For autoinduction experiments, ZYM media was used instead of LB after the overnight starter culture step, and when the OD_{600nm} became between 0.4-0.8 the containers were transferred into another shaking incubator at 220 rpm at 20 ºC overnight. Next day, the cultures were harvested same as above.

2.6.7.3 Cell lysis by sonication

The cell suspension was sonicated on ice to lyse cells using a Soniprep 150 Sonicator (MSE, London, UK), by six cycles of 25 seconds on and 35 seconds resting at a frequency of 25 kHz and 60% amplitude. Lysed cells solution was centrifuged to separate the insoluble fraction from soluble one at 20,000 *g* for 30 minutes at 4 °C. Then samples were prepared to analyse by SDS-PAGE to find out whether these samples have any protein to processed for purification or not.

2.6.7.4 Sodium dodecyl sulphate polyacrylamide gel electrophoresis (SDS-PAGE)

The insoluble and soluble fractions were analysed by SDS-PAGE gels (Express plus TM Page Gels, GenScript. 4 - 20%) to separate proteins by size for visualization. The fractions were diluted in an equal volume of 2x SDS-PAGE buffer (100 mM Tris-HCl pH 6.8, 4% (w/v) SDS, 0.2% (w/v) bromophenol blue, 20% (w/v) glycerol, and

2% (v/v) ß-mercaptoethanol) to denature the protein, by mixing 20 µl of protein samples and 20 µl of the buffer. The samples were heated at 95 °C for 10 min then cooled and loaded with Spectra Multicolor Broad Range Protein Ladder (Thermo-Scientific) on the SDS-PAGE gel using a Mini-Protean Electrophoresis System (Bio-Rad, UK) at 150 V and 60 min. Gels were stained with InstantBlue stain (Expedeon) for 1 hour, washed with water to remove the excess dye, and visualised using a UV light box.

Chapter 3 - The Influence of Chitin and Chitosan on The Dynamics of *E invadens* Membrane Lipids

3.1 Introduction

The cell membrane is an outer membrane of the cell that separates the internal cell compartment from its outside environment and helps the cell to interact with its environment in a controlled way. Cells need to exclude, take in, and excrete various substances, all in specific amounts. In addition, they need to communicate with other cells, identifying themselves and sharing information; and in all these functions the plasma membrane is involved. The plasma membrane consists of a bilayer of lipids, cholesterol and a protein network known as the cytoskeleton. Table 3.1 below provides information about the types of lipids present in *E. invadens* and the proportions of each type in whole cell extracts compared to plasma membrane extracts as reported in (Van Vliet *et al*., 1976). The lipid composition varies between cells, depending on their function (Krapf, 2018). The phospholipids are the most abundant lipid type in most cell membranes. Some of the membrane proteins are integral proteins, embedded in the phospholipid bilayer, and in some cases extending through both layers, while others are peripheral proteins, attached to the inner or outer surface of the phospholipid bilayer. The carbohydrates are found on the outer surface of the plasma membrane and are attached to proteins, forming glycoproteins, or lipids, forming glycolipids (Figure 3.1) (Robertson, 1981).

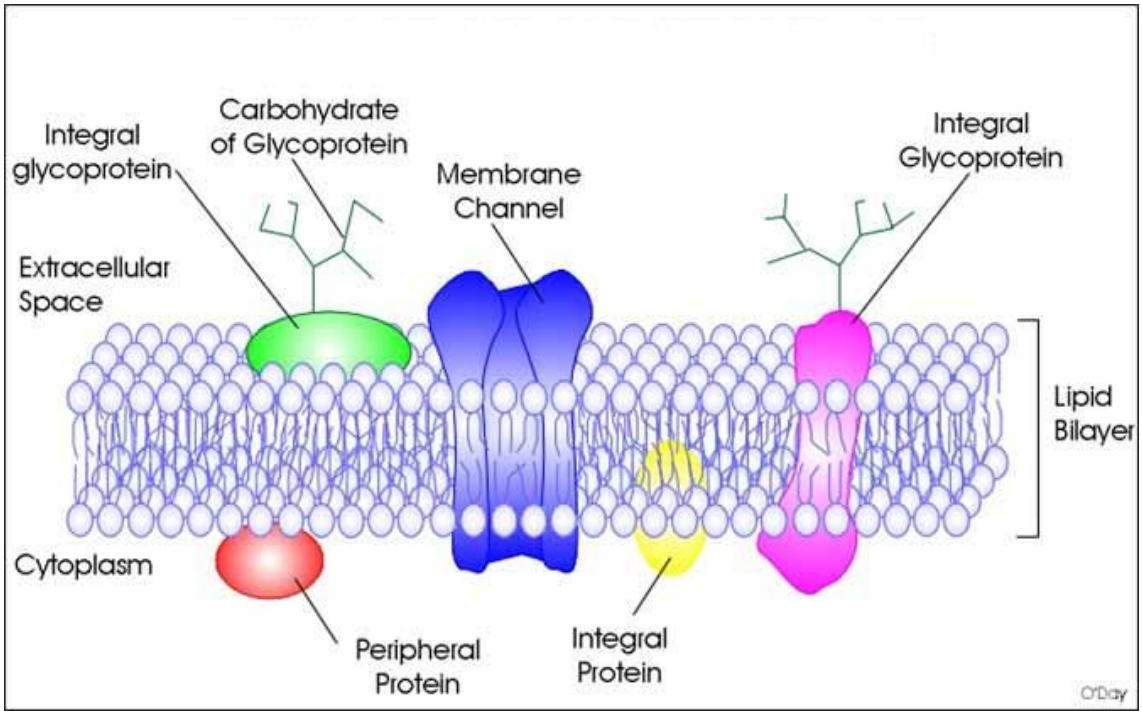

Figure 3. 1 Plasma membrane structure: It consists of a phospholipids bilayer, proteins and carbohydrates. Transmembrane (integral) and peripheral proteins are also shown. The carbohydrates are present on the outer surface of the plasma membrane and are attached to proteins, forming glycoproteins, or lipids, forming glycolipids. The image has been taken from APSUbiology.org.

The phospholipids have a hydrophilic head group and two hydrophobic tails. Phospholipid bilayers arrange as a result of the hydrophobic interactions between the lipid tails, to make a barrier between the inside and the outside of the cell. The arrangement occurs so that the hydrophilic head groups are arranged on the inside and outside of the cell and the hydrophobic region in between, to decrease the interactions between the hydrophobic tails and the surrounding water molecules (King, 2016). The head group of a phospholipid molecule involves either a glycerol or sphingosine base, and also two fatty acid chains. Phospholipids are characterised by their head group and, also, by the number, length and degree of saturation of the

fatty acid chains. The lipid head group size and the level of fatty acid chains saturation will affect their arrangement across the membrane and shape the curvature of the membrane (Hamilton, 2003).

Table 3. 1 Lipid composition of *E. invadens* from whole cells and from plasma membranes (Van Vliet *et al*., 1976).

Lipids	Whole cell (%)	PML (%)
Phosphatidylethanolamine	25.4	30.1
Phosphatidylcholine	33.7	38.3
Sphingomyelin	4.0	9.3
Phosphatidylserine	7.1	8.4
Ceramidephosphorylinositol	17.3	7.6
Phosphatidylinositol	3.3	3.7
Phosphatidic acid	3.6	1.4

Another component of the plasma membrane is cholesterol which is an amphipathic lipid molecule containing a hydrophilic region and a lipophilic region. Cholesterol is classified as a sterol, with a network of hydrocarbon rings that easily intercalates into the lipid bilayer. It is a crucial component of cell membranes and is also used by the cell to synthesise other steroids (Bagatolli *et al*., 2010). Cholesterol decreases the permeability of the membrane by increasing the hydrophobicity of the barrier to polar molecules and also helps strengthen the bilayer. It is also important for the formation of domains within biological membranes. Cholesterol has the ability to shift rapidly between the two leaflets of the membrane, due to a lower free-energy barrier compared to phospholipids. Cholesterol also interacts with sphingolipids, another

lipid molecule found in the cell membrane, which have longer, more saturated hydrocarbon chains (Hamilton, 2003).

The structure and function of the cell depend on the mechanical properties of a cell membrane. Addressing these mechanical properties would reveal the physiological properties of the membrane. These properties are important for studying the effects of disease or administration of drugs. In this study, I investigated the interaction of the membrane with chitin and chitosan. I used RBC as a generic model of biological plasma membrane, as its mechanical properties are well understood, RBC consists of a representative cell membrane encapsulating a haemoglobin solution, and supported by the cytoskeleton, ensuring the mechanical integrity of the membrane (Bokori-Brown *et al*., 2016). Therefore, I can use it as a model to investigate the effect of chitin/chitosan on its membrane mechanical properties.

The cell membrane is typically composed of two interacting monolayers. Although there are difficulties in accurately comparing the properties of monolayers and bilayers, lipid monolayers are often used as model systems in research, especially to study interactions between membranes and biologically active molecules. The lipid monolayers can be used to study the outer and the inner leaflet of the cell membrane (Jewell *et al*., 2015; Pinto and Disalvo, 2019).

The plasma membrane of *Entamoeba* plays a key role in the encystation process beside the other functions mentioned above. During *Entamoeba* encystation, cyst wall components are synthesized and transferred to the cell surface, where they bind to the plasma membrane to form the cyst (Herman *et al*., 2017). Chitin and chitosan are the first components to appear at the cell surface during the encystation process

(Chatterjee, Sudip K. Ghosh, *et al*., 2009; Das, Van Dellen, *et al*., 2006). Chitin synthesis is controlled by chitin synthase, an essential membrane enzyme that mediates the transfer of GlcNAc from UDP-GlcNAc to chitin chain, whereas chitin degradation is mediated by chitinases, where the latter can hydrolyse the β-(1-4) linkages in polymers of chitin. These enzymes are found in a wide variety of organisms, including viruses, bacteria, plants and animals (Yang and Zhang, 2019). Chitin is a long-chain N-acetylglucosamine polymer and is found in the exoskeleton of arthropods and insect vectors of human diseases, cell wall of fungi and yeast. Chitin is the main component of some protozoan's cyst walls such as *Entamoeba* (Samuelson *et al*., 2013) and *Acanthamoeba* (Magistrado-Coxen *et al*., 2018) and also of the egg shell and gut lining of parasitic nematodes such as *Ascaris* spp (Dubinský *et al*., 1986). Chitosan, the deacetylated form of chitin, is mainly found in shrimp shells and other crustaceans (Schmitz *et al.*, 2019). Since chitin does not exist in humans and other vertebrates, this has been identified as a potential drug target against some internal and external parasitic and fungal diseases (Fanelli *et al*., 2005; Geoghegan and Gurr, 2017; Samuelson *et al*., 2013). Scarce studies have been performed on the relationship between chitin and cyst formation. At the end of the last century, two groups were sought to study the role of chitin as a potential encystation blocker (Avron *et al*., 1982) demonstrated that polyoxin D and nikkomycin, structural analogs of a substrate for chitin synthase, inhibited the cyst formation when added to *Entamoeba* culture in a dose-dependent manner. However, the effect of polyoxin D and Nikkomycin on encystation was refuted by Das and Gillin (1991). Later on, the role of chitin metabolism during encystation was well studied by Samanta and Ghosh (2012), in which all putative genes encoding for chitin

metabolism were highly upregulated during cyst formation. The addition of glucosamine-6-phosphate isomerase and glycogen phosphorylase inhibitor, enzymes involved in chitin metabolism, to *Entamoeba in vitro* culture led to chitin synthesis blocking and decreased cyst formation (Samanta and Ghosh, 2012). However, the association between chitin synthesis and cyst formation is still unsupported and more studies are needed.

As *Entamoeba* (and other micro-organisms) plasma membrane is elastic and flexible, while the cyst wall is solid and constant, the transitions between these two states that occur during encystation are important to be understood. The process of cyst formation is based on the hypothesis that encystation goes through three phases called the "wattle-and-daub" model (Chatterjee *et al.*, 2009). Firstly, the foundation phase (early encystation phase) includes constitutive expression of the plasma membrane Gal/GalNAc lectins followed by the binding of Jacob lectins (glycoprotein containing Gal) to the surface of the encysting amebae. Secondly, in the wattle phase (mid-encystation phase), Jacob lectins cross-link with chitin fibrils deposited on the surface of encysting amebae. Thirdly, the daub phase (late phase) includes the aggregation of Jessie3 lectin, that binds the chitin and the cyst wall becomes solid as a result of self- C-terminal domain, making them impenetrable to small molecules (Marta Frisardi *et al*., 2000; Wang *et al*., 2003).

I aimed to investigate the changes in the membrane elasticity that occur during encystation. I hypothesised that interactions between proteins at the surface of the membrane and the lipid bilayer will cause changes in rigidity and elasticity of plasma membrane that makes it impermeable and to protect the parasite from harsh environment after shedding.

In order to achieve this, I first characterized the plasma membrane lipids and the interactions of lipids molecules with each other. Lipids were extracted from whole *E. invadens* cells and from the plasma membrane only, and where characterised using a Langmuir trough. I then studied the effect of chitin and chitosan on the mechanical properties of PML using the Langmuir trough. Langmuir trough experiment can only assess the dilatation modules of PML monolayer, therefore, I used thermal fluctuation analysis to investigate the effect of chitin and chitosan on the membrane bending module using RBCs as a generic model of bilayer plasma membrane.

3.2 Materials and methods

3.2.1 *E. invadens*

Entamoeba invadens-IP-1 strain was maintained and grown in LYI-S medium supplemented with 5% adult bovine serum (ABS) and 2% vitamin mixture (complete medium) in borosilicate tubes at room temperature with an angle of 35^{o}. For subculture and maintenance, 100 µl of *E. invadens* trophozoites, grown until the logarithmic phase, were seeded in 13 ml of complete LYI-S medium and kept at room temperature (Clark and Diamond, 2002; Diamond and Cunnick, 1991). For lipid extraction and plasma membrane isolation, *E. invadens* trophozoites, were grown at room temperature in 250 ml flasks containing complete LYI-S medium for 8 – 10 days.

3.2.2 Plasma membrane isolation

E. invadens trophozoites grown for 8-10 days in 250 ml LYI-S medium were harvested at 500*g* for 5 min, washed twice with phosphate buffer solution (PBS tablets, Fisher scientific) and centrifuged at 500 g for 5 min. After that, the pellet was re-suspended in cold sucrose solution (1 mM EDTA, 10 mM $NaHCO_3$ and 10% sucrose, adjusted at pH 7.0) then homogenized by 10-15 strokes using a loose fitting Dounce homogenizer. Samples were then centrifuged at 500*g* for 10 min, in order to separate the nuclei and cell debris from the other parts of the cell. Afterward, the supernatant was transferred into a new tube and centrifuged at 4500*g* for 20 min (the floated layer that contain phagolysosomes was disposed) and centrifuged again at 1500*g* for 10 min. The supernatant which contains the microsomes was disposed. Subsequently, the pellet was washed twice using 10 % sucrose solution at 1500*g* for 10 min, then the pellet which contains the crude plasma membrane was re-suspended in 10 % sucrose solution. Five sucrose solutions of increasing concentrations (30%-50%) were prepared, and 2 ml of each concentration were added carefully into a 14 ml ultracentrifuge tube (Ultra-Clear tubes, Beckman), by placing a long syringe needle to the tube bottom and loading the gradients in which the lightest gradient concentration is loaded first to make a continuous sucrose gradient layer. The final pellet with 10 % sucrose solution was laid down on the continuous sucrose gradients and centrifuged at 25200 rpm for 150 minutes using an ultracentrifuge (Beckman SW 40 Ti rotor, USA). The main part of the plasma membranes that were lined at 47 % sucrose was collected and stored at -20°C for the subsequent experiments (Van Vliet *et al*., 1976).

3.2.3 Lipid extraction

In order to extract lipids from whole cells (WCL) and from plasma membranes (PML), harvested cells or plasma membranes were homogenized 20 times in chloroform/methanol (2:1 ratio) solution and shaken for 15 – 20 min at room temperature (Infors-HT Shaker incubator, multitron, Switzerland). The homogenate was filtered using Whatman quantitative filter paper, washed with 0.9 % NaCl solution (4 ml for 20 ml), vortexed and centrifuged at 600*g* for 10 min to separate the two phases (chloroform and methanol). The upper methanol phase was removed, and the interface was washed two times with methanol/water (1:1) solution. The lower chloroform phase containing the lipids was evaporated under a nitrogen stream. Lipids dried on the wall of the tube were collected by rinsing the tube with 1 ml of chloroform. The mixture (chloroform/lipids) was aliquoted in small glass vials and stored at -80°C for the subsequent experiments (Folch *et al*., 1957).

3.2.4 Langmuir trough

Langmuir trough apparatus (Kibron Inc, Micro Trough S, Filmware version 2.41, Finland) was used to characterize the WCL and PML, and then to investigate the effect of chitin and chitosan on the elasticity of the lipid monolayer of the PML. WCL or PML of *E. invadens* was spread over the surface of the sub-phase (60 ml of purified water) between the two barriers, to allow for compression and relaxation of the monolayer, which directly controls the surface concentration (area/molecule) (Figure 3.2). The layer was left to equilibrate for one hour and to be sure the solvent

(chloroform) was evaporated. In the chitin and chitosan experiments, their solutions were added separately to the monolayer of PML using a syringe with a long needle underneath the monolayer. A magnetic stir bar was used to mix the chitin/ chitosan molecules in the sub-phase.

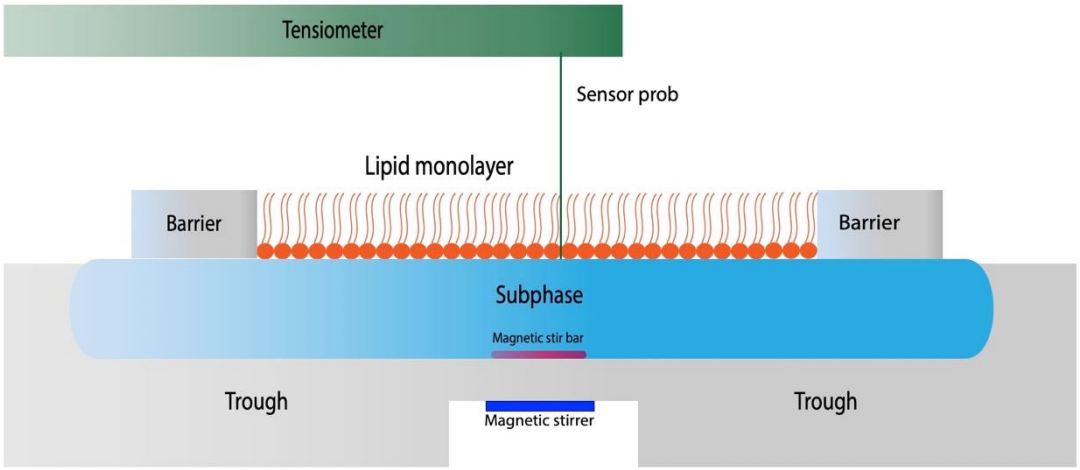

Figure 3. 2 Illustration of a Langmuir Trough system showing the trough, two moving barriers, subphase of purified water and pressure probe. Image was modefied from Abdul Rahman (2008).

The barriers were moved by a stepper motor and a wire probe was used to measure the surface pressure. During monolayer compression, the two barriers are moved towards each other, the average molecular area decreases, the surface density of the lipid molecules increases, resulting in increase in the surface pressure, and the lipid molecules rearrange and orientate in a specific way depending on the interactions between them, and vice versa during the relaxation process. The surface pressure (π) is the difference between the surface tension of the pure sub-phase, and the surface tension of the Langmuir film (King, 2016).

$$\pi = \gamma_0 - \gamma$$

in which $\gamma 0$ is the surface tension of the subphase in the absence of the monolayer and γ is the surface pressure when the lipid monolayer is present at the interphase. Surface tension is measured from the applied force on a probe at the air-water interface. The probe must be wetted by the surface of the film *e.g.* a contact angle of zero, to exclude errors arising from the contact angle of the meniscus at the probe. The surface pressure and area per lipid molecule are plotted against each other to produce a pressure-area isotherm.

The dilatational modulus that characterises the monolayer elasticity with respect to area change was calculated from the gradient of the isotherms to collect information about the elasticity of the lipid monolayer by the following formula:

$$\varepsilon = -A\frac{d\pi}{dA}$$

where ε is the dilatational modulus, A is the area and π is the surface pressure.

3.2.5 Thermal fluctuation analysis

Thermal fluctuation analysis was used to investigate the effect of chitin and chitosan on the elasticity of the plasma membrane of red blood cells (RBCs) which were used as a model for lipids bilayer. Briefly, five microliters of fresh human blood were suspended in 1 ml of PBS (same preparation as in section 2.2.) mixed with 1 mg/ml bovine serum albumin (Sigma-Aldrich, UK). After that, 50 µl from the suspension were mounted onto a clean microscope slide and covered by a coverslip which was fixed to the slide by two strips of Parafilm on the long slide edges to construct an

open sided observation chamber (Hale *et al*., 2011). Once the RBCs stabilized at the bottom of the slide chamber, the buffer was exchanged with 1000 µl of buffer containing 100 µg/ml of either chitin or chitosan. Videos of RBCs were recorded during a time series as follows: immediately before buffer exchange, 0, 5, 10 and 20 minutes after buffer exchange. These videos were recorded using fast-video phase contrast microscopy (Leica DMLFS upright microscope equipped with a 63x PL Phase-contrast objective) and Moticam 2000 2 MP progressive scan digital video camera (Motic, Hong Kong) at a typical frame rate of 60 fps. The videos were then analysed using special software developed in the Biophysics Group at the University of Exeter to extract 2D contours, which were used to obtain the thermal fluctuation spectrum of the cell. The theoretical dependence of the mean squared fluctuation amplitudes on the mode number was then fitted to the experimental fluctuation spectrum to obtain the membrane bending elastic modulus.

3.2.6 Solutions

3.2.6.1 Chitin

Short-chain chitin was kindly donated by Prof. Sarah Gurr and this originated initially form Prof. Hengo Yin laboratory, the Dalian Institute of Chemical Physics in China. For the Langmuir trough experiments 500 µl of chitin solution with 1 mg/ml concentration was used to give 0.0042 mg/ml concentration in the trough. In the cell fluctuation experiments, 1 ml of chitin solution with 100 µg/ml concentration was used.

3.2.6.2 Chitosan (deacetylated chitin)

For this study chitosan, a solution of 1 mg/ml was prepared by dissolving chitosan powder (Sigma-Aldrich) in distilled water. Few drops of 1 M HCl were added to the solution since chitosan is soluble in aqueous acidic solutions. This was followed by the addition of 1 M NaOH to neutralize the solution (pH 7). Subsequently, 500 µl of this solution was used in the Langmuir trough experiments to give 0.0042 mg/ml concentration in the trough. While in the cell fluctuation experiments, 1 ml of chitosan solution with (100 µg/ml) concentration was used.

3.3 Results

3.3.1 Characterisation of *Entamoeba invadens* lipids monolayer

3.3.1.1 Characterisation of *E. invadens* whole cell lipids

Twenty-five pressure–area isotherms of *E. invadens* monolayer lipids of the whole cell (WCL) were recorded using the Langmuir trough and twenty-one of them were reproducible. The compression isotherms exhibited a transition between 22-25 mN/m, possibly between a liquid expanded and a liquid condensed phase (Figure 3.3).

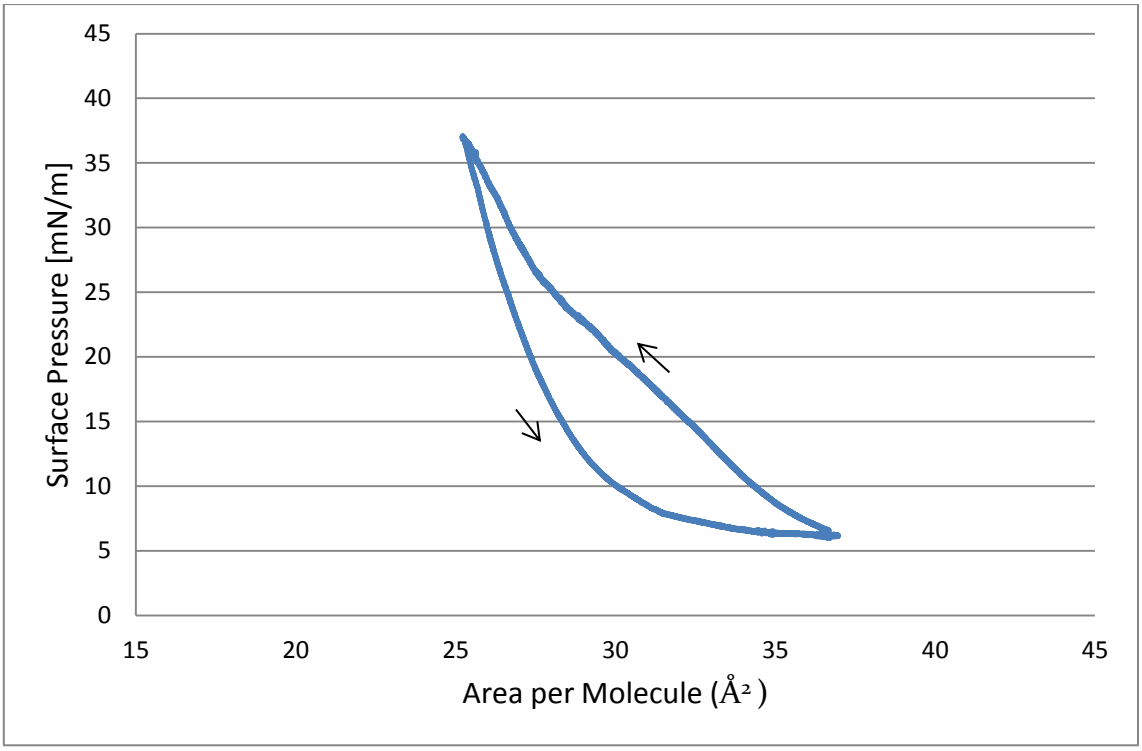

Figure 3. 3 Pressure - area isotherm of *E. invadens* lipids. Ascending arrow shows the compression, and descending arrow shows the relaxation of the WCL pressure area isotherm.

The dilatational modulus revealed a peak in the compression isotherm between 22-25 mN/m, which is further evidence for a phase transition (Figure 3.4).

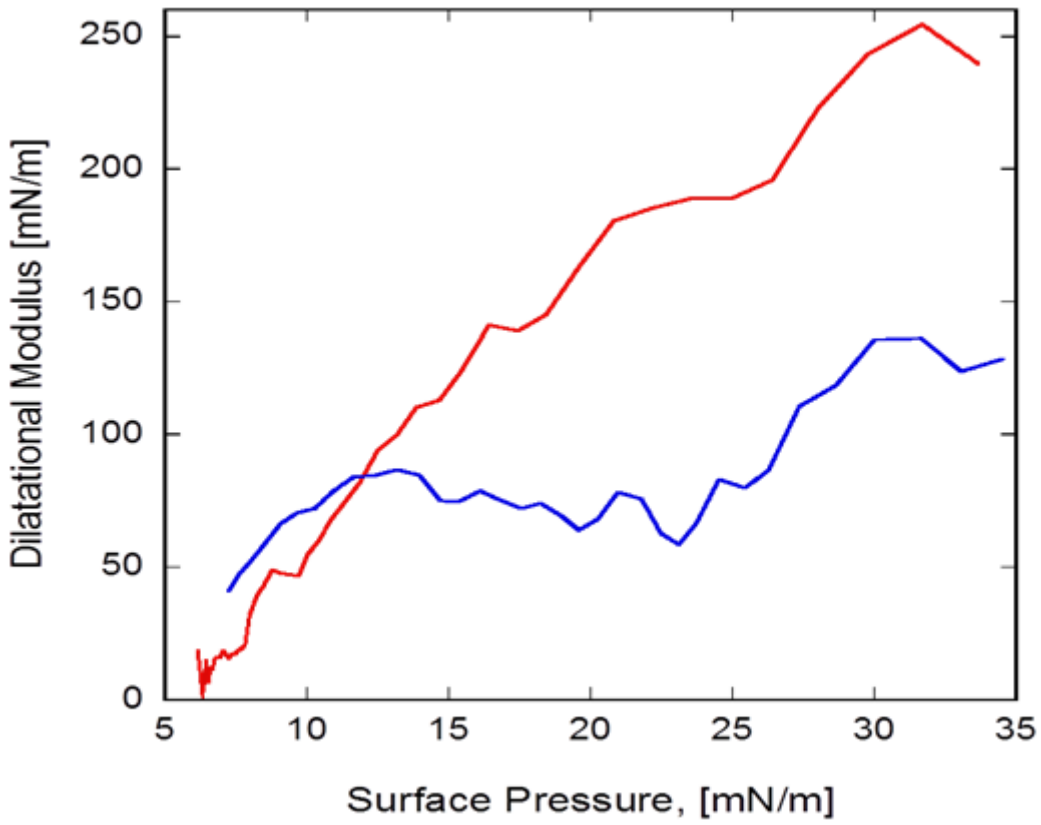

Figure 3. 4 Dilatational modulus for *E. invadens* lipids Pressure - area isotherm from Figure 3.3. The compression curve (blue) shows a phase transition between 22-25 mN/m, whereas the relaxation curve (red) does not show any phase transition. The experiment was repeated 25 times but 21 were reproducible.

3.3.1.2 Characterisation of *E. invadens* plasma membrane lipids

Twenty-three pressure area isotherms of *E. invadens* plasma membrane lipids (PML) were recorded. The compression isotherms showed no transition which means the monolayer of *E. invadens* PML remain in the same phase (Figure 3.5). The hysteresis was much smaller in this case compared to the isotherm obtained from WCL (Figure 3.3) which suggests faster lateral rearrangement of the lipid

molecules. The dilatational modulus shows a gradual increase with pressure for both compression and relaxation with no evidence of phase changes (Figure 3.6).

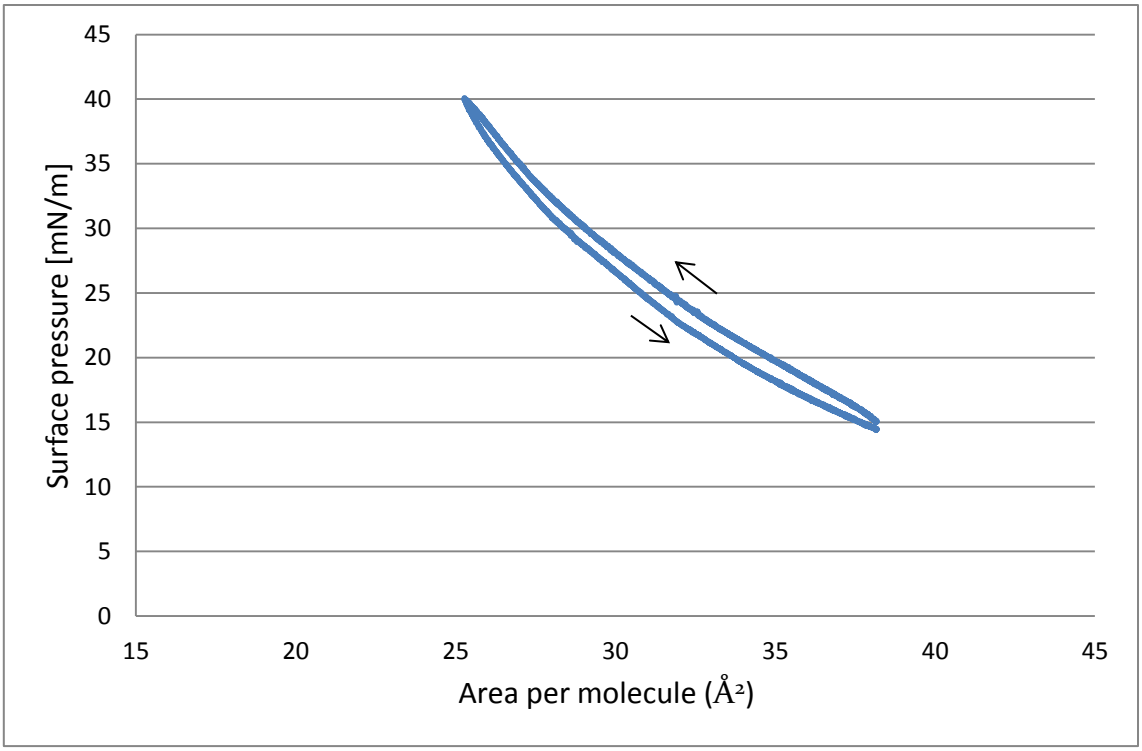

Figure 3. 5 Pressure – area Isotherm of *E. invadens* plasma membrane lipids (PML). The ascending arrow refers to compression and the descending refers to relaxation isotherm. No transmission phases were observed. This experiment was recorded twenty three times.

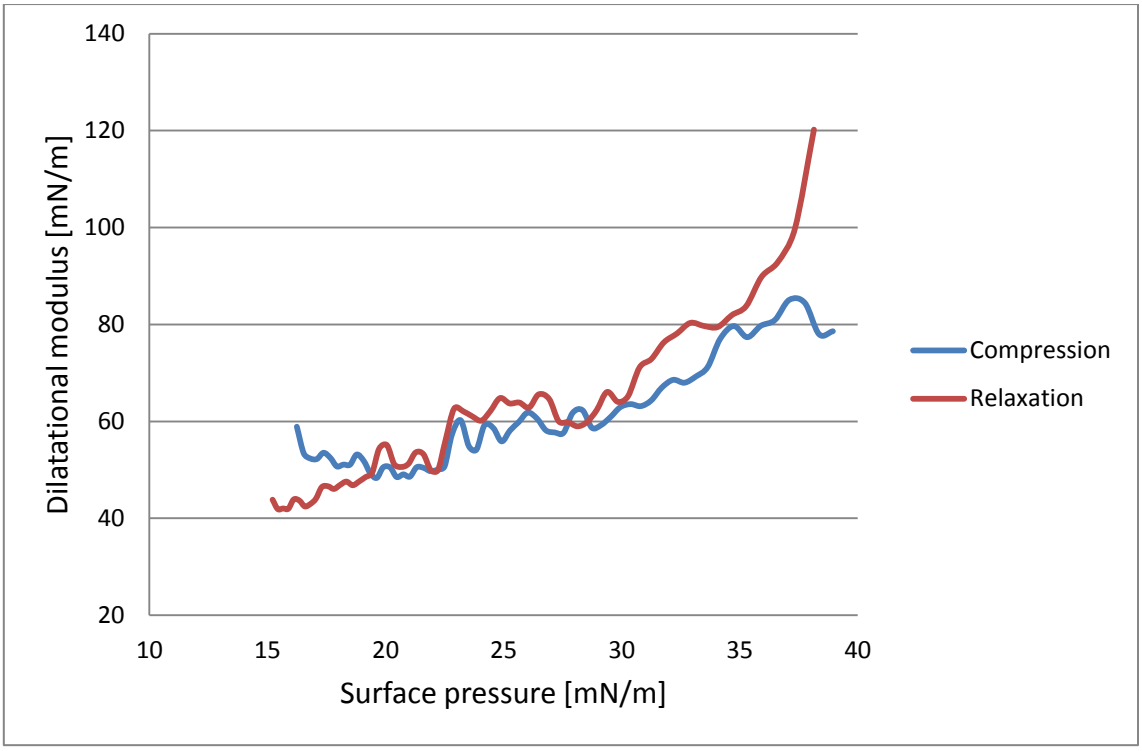

Figure 3. 6 Dilatational modulus of the compression and relaxation of *E. invadens* plasma membrane lipids (PML) for the Pressure – area Isotherm in Figure 3.5.

The dilatational modulus of WCL appears to be higher than PML, where the dilatational modulus of the compression of the WCL reached 140 mN/m and of the relaxation was 250 mN/m. While the dilatational modulus of the compression of the PML recorded more than 80 mN/m and of the relaxation reached 120 mN/m (Figure 3.4 and Figure 3.6).

3.3.2 Effect of chitin and chitosan on the elastic behaviour of plasma membrane lipids monolayer

3.3.2.1 Chitin

The interaction between chitin molecules and PML monolayers was investigated at 500 µl of chitin solution (1 mg/ml), which were added in two aliquots (250 µl each) to a monolayer of *E. invadens* PML. The chitin addition and the changes in the pressure after adding the chitin are shown in Figure 3.7. The chitin molecules appear to insert into the PML monolayer, which was observed as slight increases of pressure after the addition of chitin. Twelve pressure area isotherms were recorded after the addition of chitin to compare between the isotherms with and without chitin. Figure 3.8 illustrates two isotherms of PML, one of them before adding chitin (blue colour) and the other one after adding chitin (red colour).

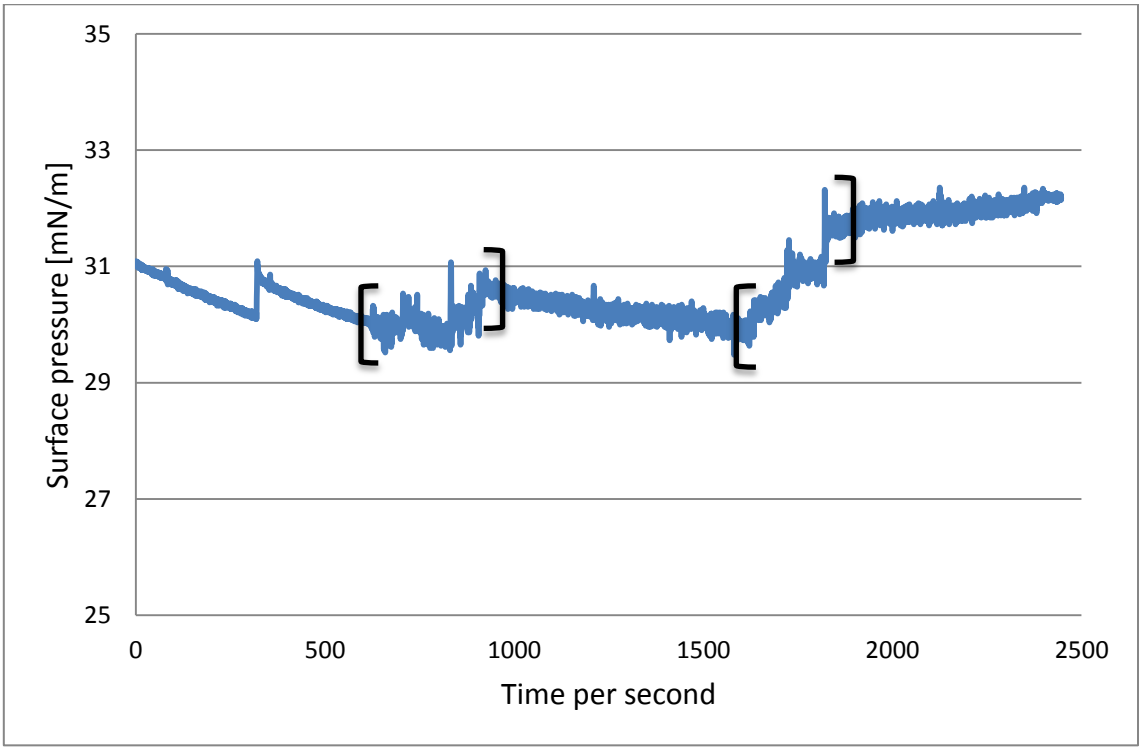

Figure 3. 7 Pressure – time dependence of chitin addition beneath an *E. invadens* plasma membrane lipids (PML) monolayer. The area between the brackets indicates the point at which 250 µl of the chitin solution were added.

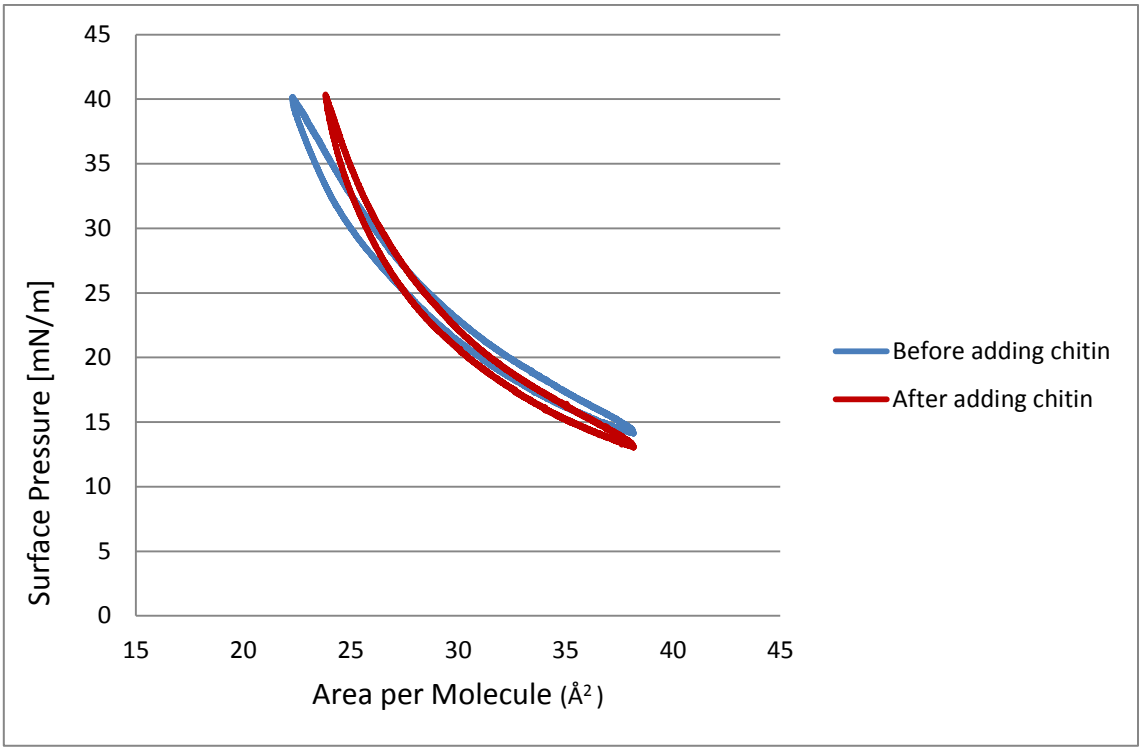

Figure 3. 8 Pressure – area isotherm of *E. invadens* plasma membrane lipids, before and after adding chitin. This experiment was recorded twelve times.

The dilatational modulus of the compression before and after adding chitin is shown in Figure 3.9. The PML monolayer became more rigid after adding chitin and the dilatational modulus value rose from 70 to 130 mN/m at high pressures.

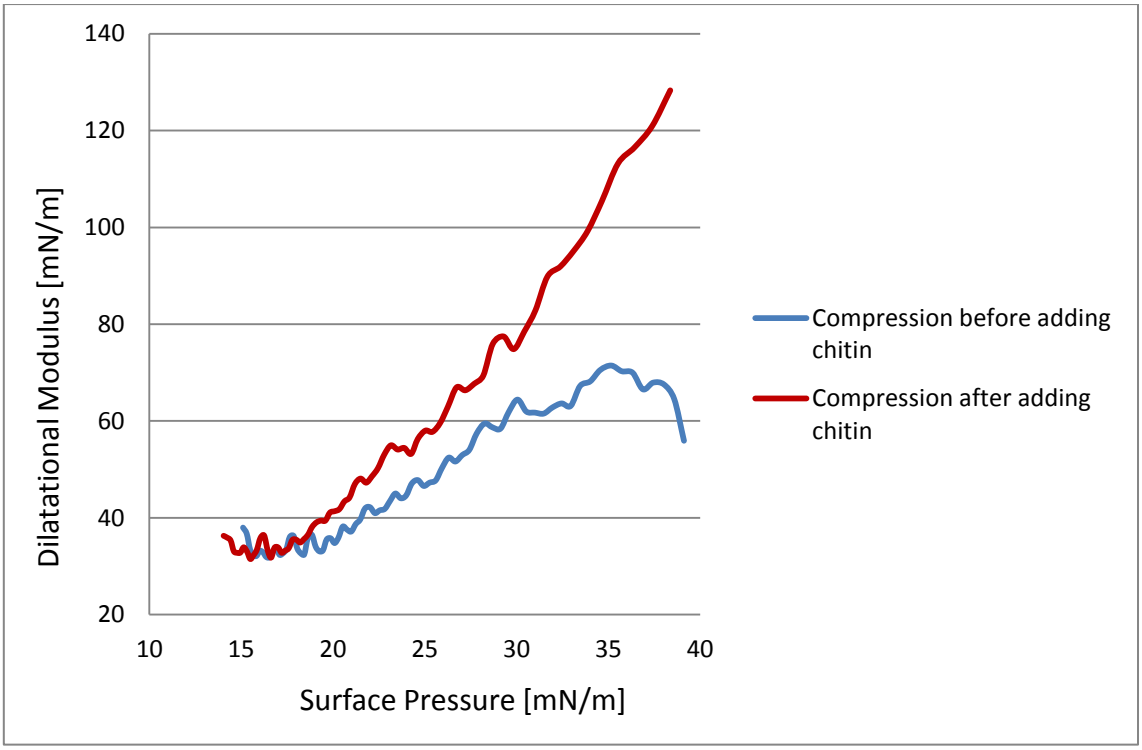

Figure 3. 9 Compression dilatational modulus of plasma membrane lipids monolayer in Figure 3.8 before and after adding the chitin.

The same interaction is observed in the dilatational modulus of the relaxation after adding chitin, where the stiffness of the PML monolayer also increased from 110 mN/m to180 mN/m as is shown in Figure 3.10.

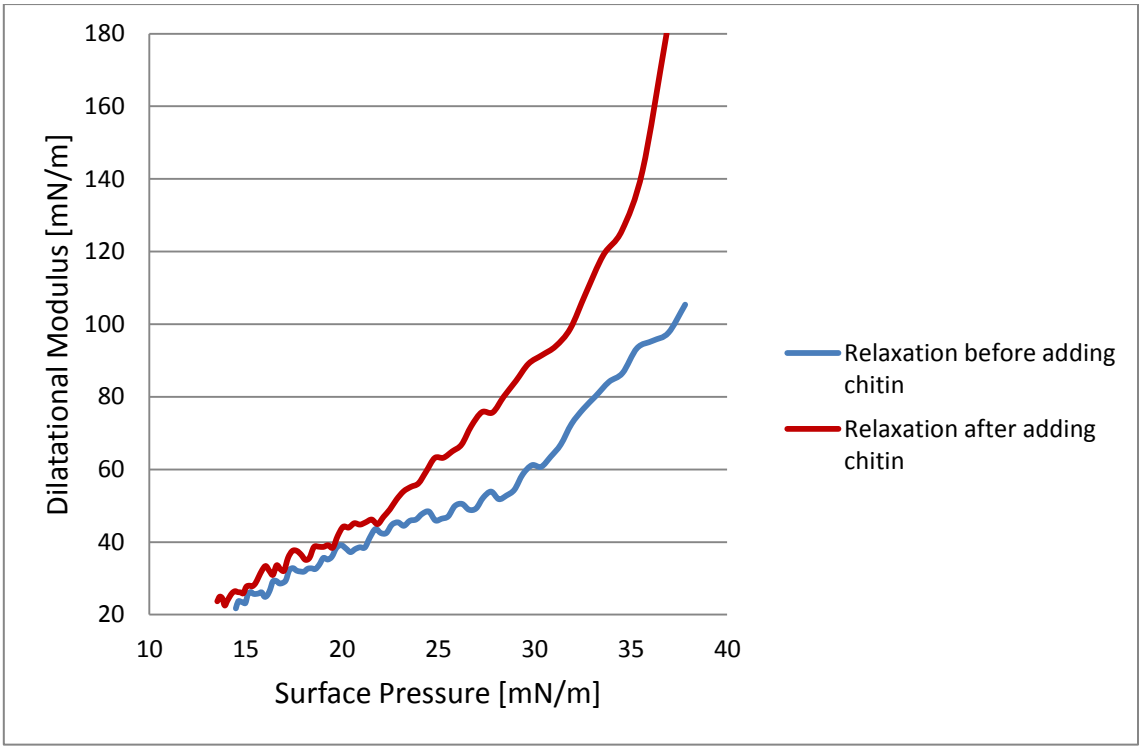

Figure 3. 10 Relaxation dilatational modulus of *E. invadens* plasma membrane lipids monolayer in Figure 3.8 before and after chitin addition.

3.3.2.2 Chitosan

To investigate the effects of the chitosan on PML, chitosan solution was added gradually to the PML in different concentrations to reach a detectable interaction between chitosan molecules and PML. The interaction point was obtained at 500 µl of chitosan with a concentration of 1 mg/ml, which were added in two aliquots of 250 µl underneath a monolayer of *E. invadens* PML. The pressure increased after the chitosan addition as a result of the interaction between chitosan molecules and PML monolayer (Figure 3.11).

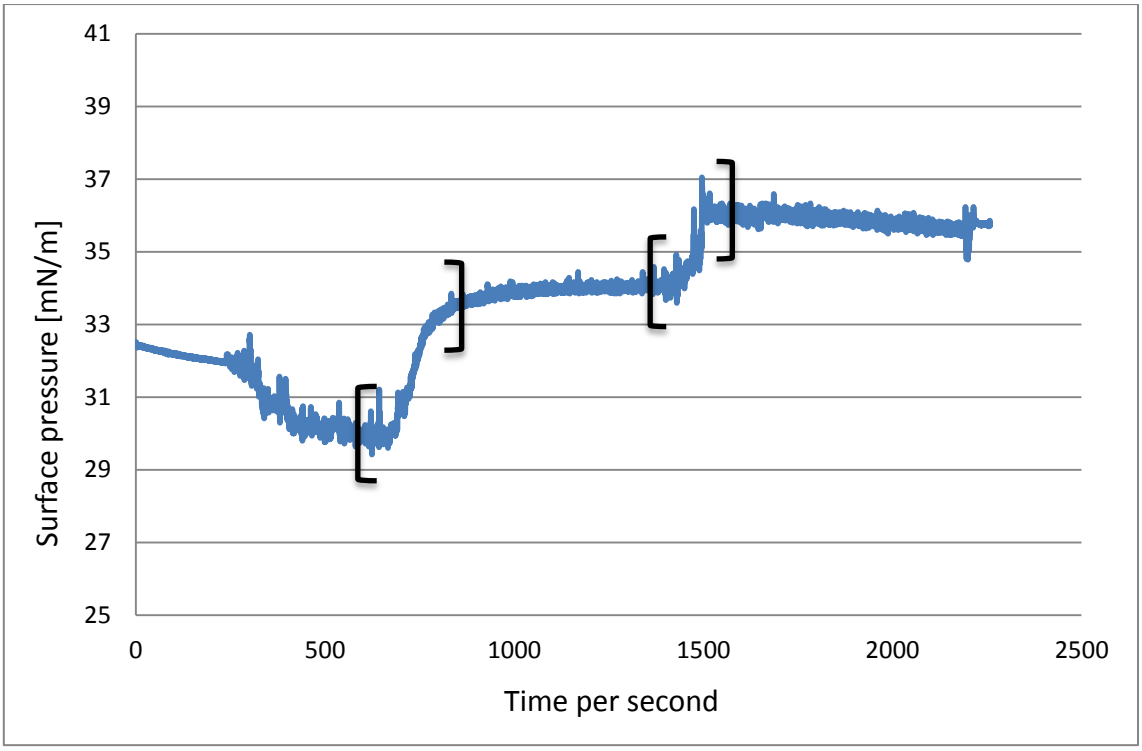

Figure 3. 11 Pressure – time dependence of chitosan addition to *E. invadens* plasma membrane lipids (PML). The brackets show when chitosan was added beneath the plasma membrane lipids monolayer of *E. invadens*.

Twelve pressure area isotherms were recorded, to compare between the isotherms before and after chitosan addition. The chitosan addition caused a change in the isotherms, suggesting the chitosan interacts and intercalates with the lipid molecules, which led to a shift in the pressure – area isotherms from 24 Å to 27 Å Figure 3.12.

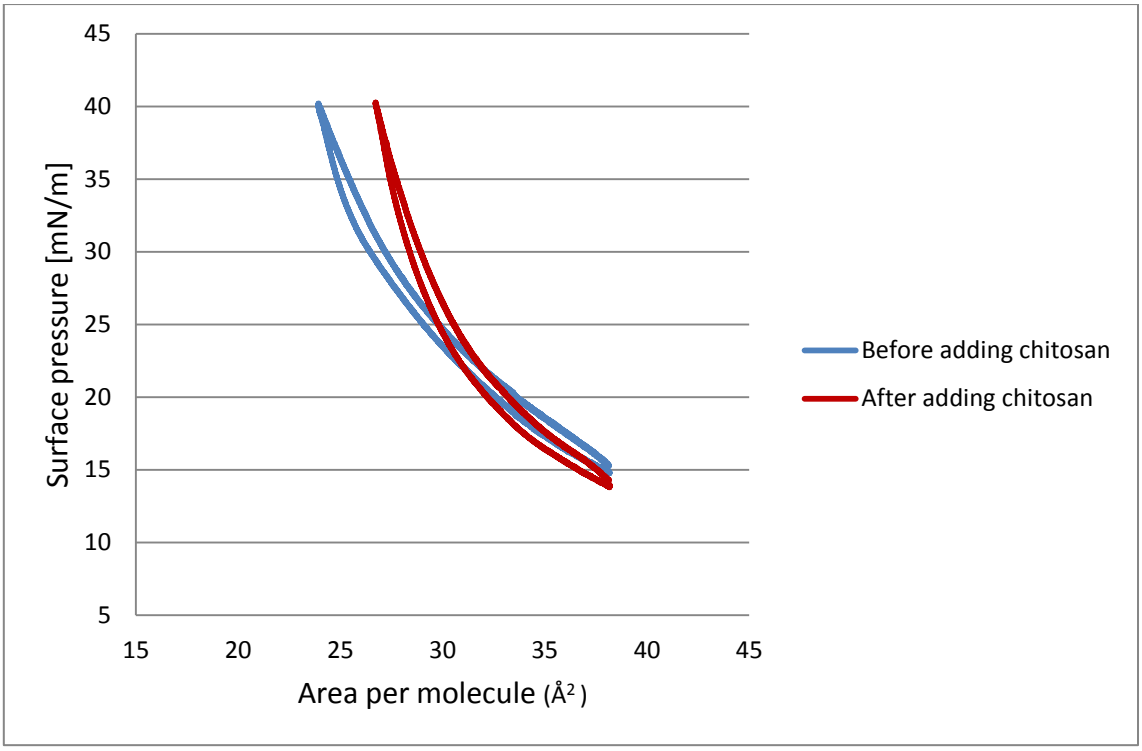

Figure 3. 12 Pressure – area isotherms of *E. invadens* plasma membrane lipids before and after adding chitosan. This experiment was repeated twelve times.

The compression and relaxation dilatational moduli of *E. invadens* PML monolayer show that the monolayer of PML became more rigid after adding chitosan. The compression dilatational modulus after chitosan addition increased by 70 mN/m (from 90 mN/m to 158 mN/m) at surface pressure of 40 mN/m (Figure 3.13), and the relaxation dilatational modulus also increased after chitosan addition by 75 mN/m (from 145 mN/m to 220 mN/m) at surface pressure of 40 mN/m (Figure 3.14).

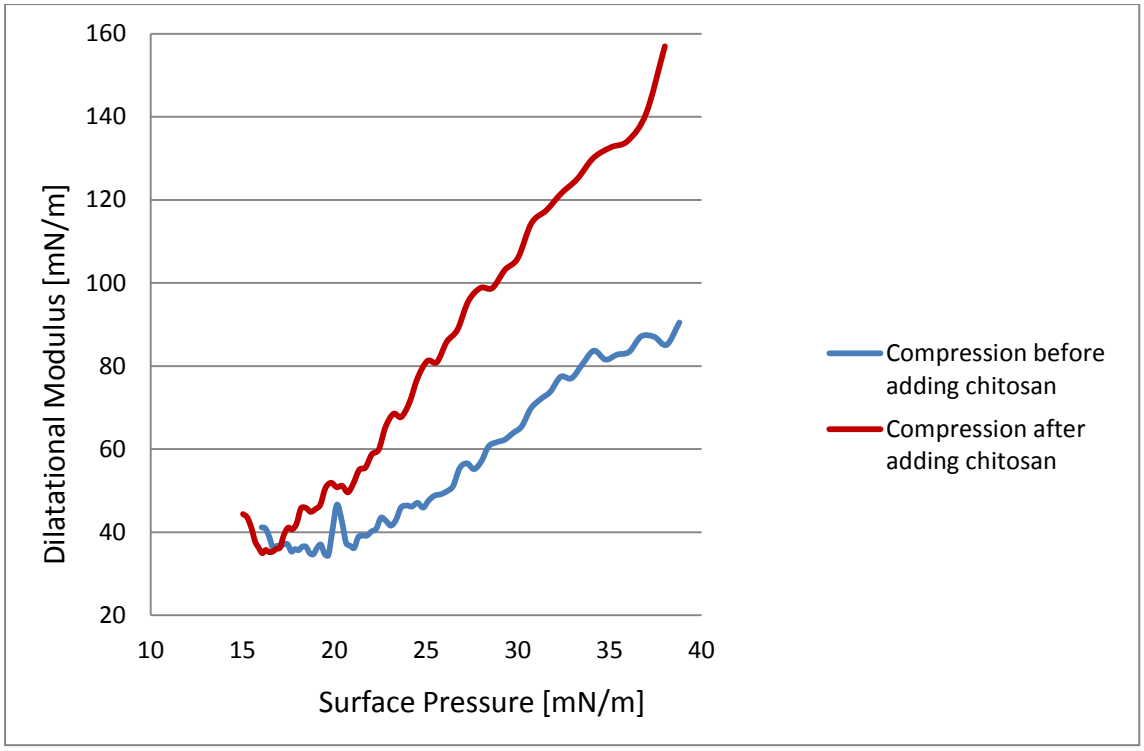

Figure 3. 13 Comparison between the dilatational modulus of the compression from Figure 3.12, before and after adding chitosan.

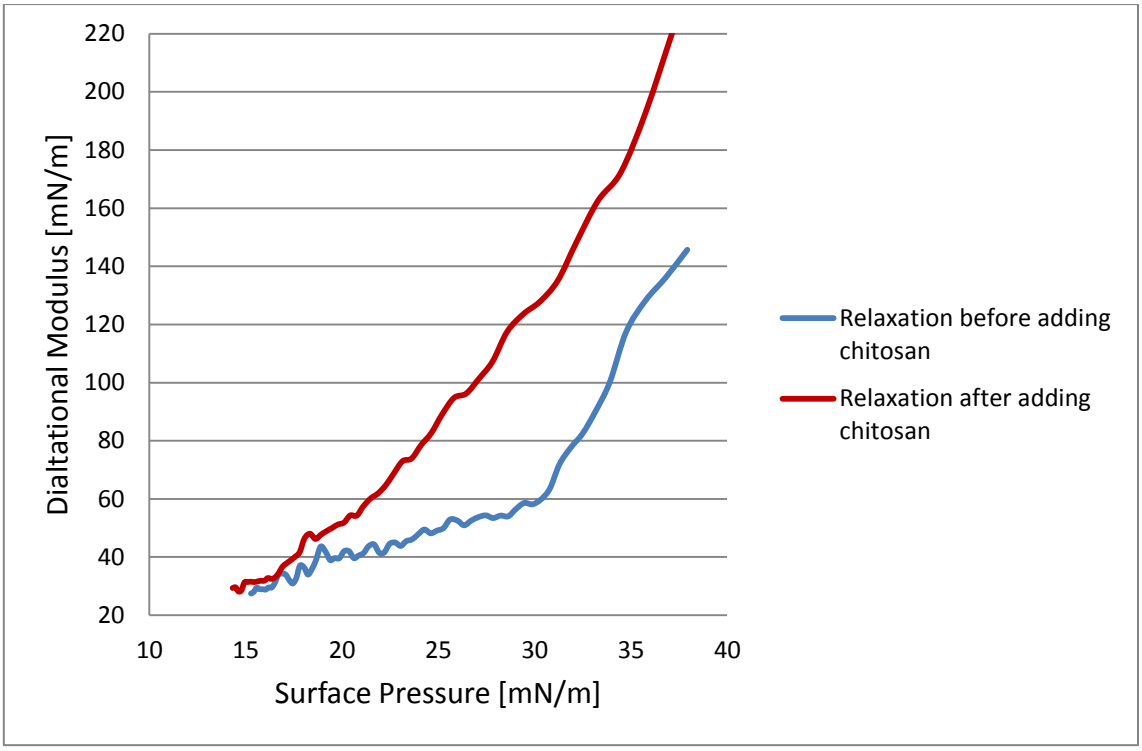

Figure 3. 14 Comparison between the dilatational modulus of the relaxation from Figure 3.12, before and after adding the chitosan.

3.3.3 Effect of chitin and chitosan on the elastic behaviour of plasma membranes lipid bilayer (Thermal fluctuation analysis)

3.3.3.1 Chitin

To study the interaction between chitin and plasma membrane of red blood cells (RBCs), thermal fluctuation analysis was used. The interaction between RBCs membrane and chitin molecules takes place relatively quickly after changing the buffer. The analysis reveals that RBCs membrane bending stiffness increased after changing the chitin containing buffer (Figure 3.15).

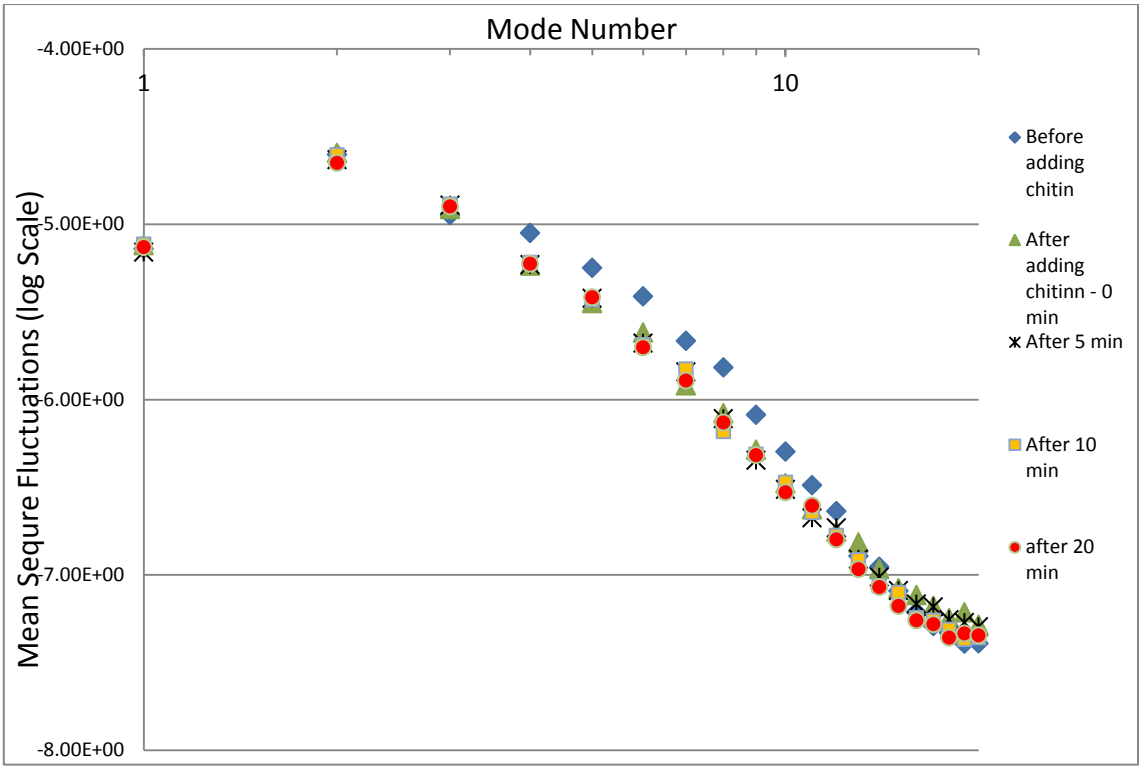

Figure 3. 15 Fluctuation spectra of a red blood cell before and after adding chitin. This experiment was repeated 7 times using different cells.

Values of the bending elastic moduli of 7 RBCs before and after adding the chitin at different points of time are illustrated in Table 3.2. The bending stiffness of the cell membrane increases after chitin addition. Generally, there was an increase in the RBCs elastic modulus immediately after addition of chitin (0 min). Some cells exhibited an increase at all time points, but others showed a decrease in bending rigidity after 5 and 10 minutes, then all cells showed increase at 20 minutes post addition.

Table 3. 2 Values (in k_BT) of the bending elastic moduli before and after chitin addition

Cell No.	Before	0 min	After 5 min	After 10 min	After 20 min
1	136 ± 7	150 ± 13	210 ± 8	200 ± 10	206 ± 8
2	97 ± 31	189 ± 22	173 ± 27	145 ± 30	178 ± 14
3	115 ± 11	202 ± 24	264 ± 8	146 ± 25	187 ± 13
4	105 ± 25	281 ± 19	198 ± 18	235 ± 32	238 ± 15
5	109 ± 30	299 ± 8	254 ± 14	264 ± 13	250 ± 17
6	123 ± 8	98 ± 33	160 ± 23	153 ± 35	181 ± 9
7	156 ± 14	218 ± 13	182 ± 18	191 ± 21	194 ± 27
Average	120 ± 3	205 ± 10	206 ± 6	191 ± 7	205 ± 4

3.3.3.2 Chitosan

At the beginning, cell fluctuation experiments were carried out using different amounts of the chitosan changing buffer (600 µl and 700 µl) with different concentration of chitosan (60 µg/ml and 70 µg/ml). The analysis showed no changes in the RBCs membrane bending stiffness after adding chitosan at 0 and 5 minutes (Figure 3.16).

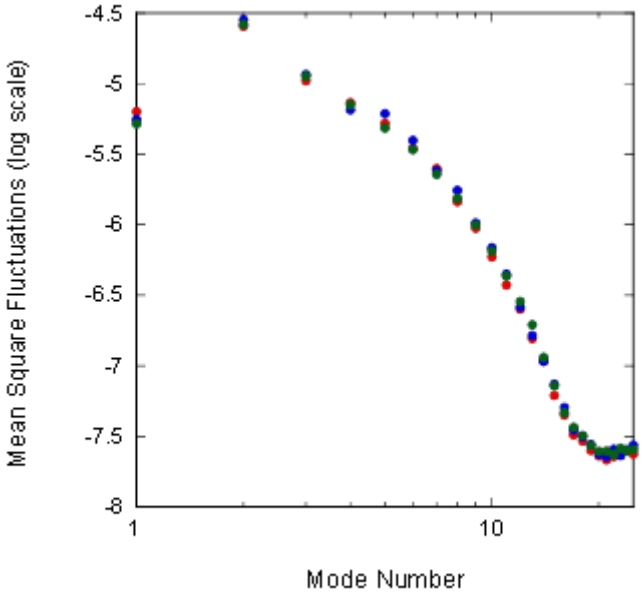

Figure 3. 16 Fluctuation spectra of a red blood cell before and after chitosan addition (red colour: before adding the chitosan solution; blue colour: immediately after adding the chitosan solution; green colour: 5 min after addition). 700 µl of chitosan changing solution was used and 70 µg/ml concentration of chitosan.

Further cell fluctuation experiments were carried out using more concentrated chitosan changing solution (100 µg/ml) and in larger quantities (1000 µl). Videos were recorded at different time points (before and after changing the buffer, at 0, 5, 10 and 20 minutes). The results reveal that there was an interaction between the chitosan and the RBC membrane. The bending stiffness of RBC membranes after the addition of chitosan was increased as shown in Figure 3.17.

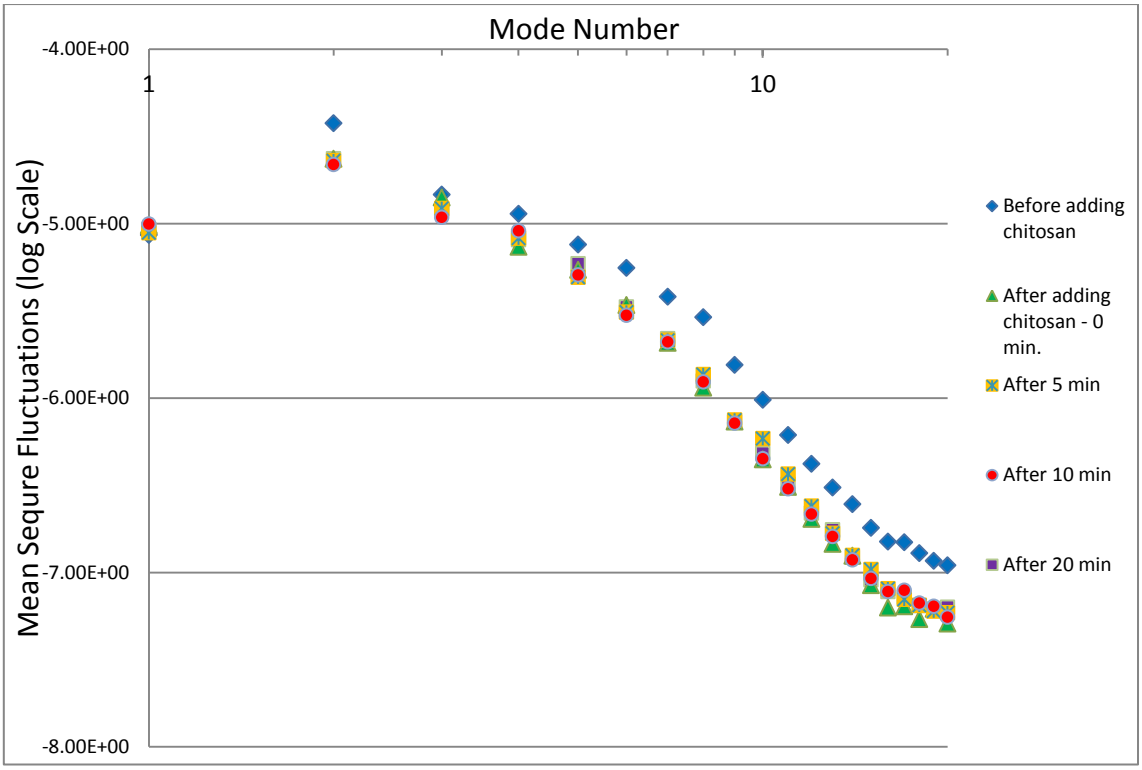

Figure 3. 17 Fluctuation spectra of a red blood cell before and after chitosan addition. This experiment was repeated 7 times using different cells.

The bending elastic moduli of 5 RBCs before and after adding chitosan are shown in Table 3.3 and indicate changes in the bending stiffness of RBC membranes after adding chitosan. The average of values of the bending elastic moduli after introducing chitosan appeared to be higher than in chitin at all time points (Table 3.2 and Table 3.3).

Table 3. 3 Values (in k_BT) of the bending elastic moduli before and after chitosan addition.

Cell No.	Before	0 min	After 5 min	After 10 min	After 20 min
1	79 ± 10	193 ± 38	161 ± 11	136 ± 21	143 ± 14
2	168 ± 15	254 ± 18	276 ± 26	Bad fit	Bad fit
3	137 ± 32	272 ± 38	333 ± 43	360 ± 31	345 ± 49
4	220 ± 13	Bad fit	281 ± 63	361 ± 24	Bad fit
5	134 ± 20	223 ± 22	223 ± 23	195 ± 18	266 ± 35
Average	148 ± 10	236 ± 9	255 ± 13	263 ± 29	251 ± 34

3.4 Discussion

In this study I investigated the behaviour of membrane lipids of *E. invadens* in the presence and absence of the cyst wall components, chitin and chitosan. In order to do this, I extracted lipids from the whole *E. invadens* cells (WCL) and from the plasma membrane (PML) only and characterised their interactions with chitin and chitosan using the Langmuir trough technique. These components of the cell wall caused an increase in the stiffness and rigidity of the monolayer and bilayer lipids.

The pressure – area isotherms of WCL revealed that the there is a transition area between 22-25 mN/m and the dilatational modulus have confirmed this, whereas no transition area was recorded in the PML pressure – area isotherms during the compression and the relaxation processes of PML. This might be attributed to the differences in the lipid composition of WCL and PML monolayers (Van Vliet *et al*., 1976). The lack of transition area in PML pressure – area isotherms was reported in

other studies (King, 2016; Gzyl-Malcher *et al* 2017 and Mottola *et al* 2019) which studied phospholipid monolayers including phosphatidylcholine, phosphatidylethanolamine, phosphatidylserine, and phosphatidylinositol, which are also found in PML of *E. invadens.*

The addition of chitin and chitosan to PML has increased its stiffness. This was confirmed by the dilatational modulus, for both compression and relaxation.The increase in the stiffness of PML monolayer after adding chitin and chitosan is compatible with the process of encystation, where the deposition of chitin and chitosan to *Entamoeba* plasma membrane cause an increase in the stiffness of plasma membrane. Additionally, the accumulation of chitin binding proteins (Jacob and Jessie) make the cyst solid and impermeable (Das, Van Dellen, *et al*., 2006; Samuelson and Robbins, 2011; Chatterjee, Sudip K. Ghosh, *et al*., 2009).

The effect of chitin and chitosan on the bilayer membrane was also studied using thermal fluctuation analysis and RBCs as a model. The fluctuation spectra and the bending elastic moduli before and after adding chitin and chitosan revealed that both chitin and chitosan increased the bending rigidity of RBC membrane. According to table 3.2 and 3.3, the values of the bending elastic moduli are higher following the addition of chitosan than chitin, which suggest that chitosan increases the rigidity of RBCs membrane to a greater extent than chitin, and this may justify why *Entamoeba* changes chitin to chitosan during the transition from trophozoite to cyst (Das, Van Dellen, *et al*., 2006). An increase in bending modulus of the red blood cell membrane also occurs in cells exposed to oxidative stress (Hale *et al.*, 2011) and this may also

occur after adding chitin since it has been reported to induce oxidative stress in *Pseudomonas aeruginosa* cells (Gurunathan *et al*., 2012).

The hydrogen bonding is possibly participating in the mechanism of chitin/chitosan interactions with the lipid monolayer. Studies have shown that chitosan has a strong interaction with the cholesterol and fatty acids monolayer, where chitosan has caused changes in the monolayer morphology and induced cholesterol monolayer expansion. This was attributed to the hydrogen-bonding between the hydroxyl and amine groups from chitosan and the hydroxyl groups of cholesterol (Wydro *et al*., 2007; Pavinatto *et al*., 2005).

Hydrophobic interactions could have a role in the interaction between chitin /chitosan and lipid mono/bilayer. The most likely explanation is that the lipid hydrophobic tails might encourage the adsorption of the chitin/chitosan molecules which reorganize themselves to maximize the hydrophobic interactions with lipid (Pavinatto *et al*., 2005; de Oliveira Pedro *et al*., 2020). It was noted that the chitosan caused an expansion in lipid monolayer when added to the dipalmitoyl phosphatidyl choline (DPPC) and dipalmitoyl phosphatidyl glycerol (DPPG) and his might be attributed to the hydrophobic interactions (Pavinatto *et al*., 2010; de Oliveira Pedro *et al*., 2020).

Further, electrostatic interactions might also have an important role in the interaction between the positively charged chitosan and some of the negatively charged lipid in PML (like Phosphatidylserine, Phosphatidylinositol and Phosphatidic acid) and RBCs (which has a negative overall charge). Studies have reported a strong interaction between the chitosan and DPPG monolayer and weak interaction with DPPC, which might be due to the electrostatic interactions between the positive charges of

chitosan and the anionic head of the monolayers. The difference in the interaction between DPPG and DPPC, is that the latter has a zwitterionic character, which is responsible for the small expansion in the lipid monolayer (Krajewska *et al*., 2013; Pavinatto *et al*., 2016; de Oliveira Pedro *et al*., 2020). However, the interaction between the neutral chitin and mono/bilayer might be attributed to hydrophobic interactions and hydrogen bonding. Another report aimed to study the effect of chitosan and a positively charged polymer (poly allylamine hydrochloride; PAH) found that the electrostatic interactions are not enough to explain the action of chitosan on DPPG and DPPC; where the elasticity of DPPC and DPPG monolayers were considerably affected by chitosan, despite the fact that PAH has positive charge like chitosan (Pavinatto *et al.*, 2010).

To summarise, the dilatational modulus of lipids monolayers from the Langmuir trough experiments and the bending modulus of lipid bilayer from the cell fluctuation experiments, both were increased as a result of the interaction between the lipids mono/bilayer and chitin/chitosan. This might be attributed to either the electrostatic (for chitosan), hydrophobic forces or depend on the hydrogen bond between chitin/chitosan and lipids mono/bilayer. Finally, the monolayer and bilayer experiments provided preliminary knowledge on the chitin/chitosan-lipid interacting systems and further studies for proteins-lipids interaction are needed.

Chapter 4 - Gene Expression and Protein Purification

4.1. Introduction

Entamoeba life cycle involves two developmental stages, a mobile proliferative trophozoite and a chitin-walled dormant cyst which is the infective stage and the transition from trophozoite to cyst is called encystation, a critical process for the development of disease (Aguilar-Díaz *et al.*, 2011). Encystation involves decrease of the cell size, reduction of metabolism, increase in transcription and DNA content and encapsulation to protect the parasite from severe environmental conditions and preventing it from adhering to the intestinal mucosa (Dey *et al*., 2009). The cyst wall is mainly composed of chitin (a polymer of N-acetylglucosamine, GlcNAC) and its deacetylated form, chitosan (Das, Dellen, *et al*., 2006). In addition to chitin there are three protein families with chitin binding domains (CBDs) that are associated with the cyst wall named Jacob, Jessie and chitinase (Chatterjee *et al.*, 2009). Chitin producing organisms synthesize chitin in a specific vesicle by chitin synthase, which is a conserved membrane-bound type 2 glycosyltransferase. Chitin biosynthesis is a complex process and controlled by nucleotide sugar transporters which are transmembrane proteins found in all eukaryotes, responsible for the transport of activated nucleotide sugars from cytoplasm to other organelles (Nayak and Ghosh, 2019a). The *E. invadens* chitinase forms around 20% of cyst wall proteins and is composed of a single N-terminal CBD containing eight cysteine residues, a low complexity spacer, and a C-terminal enzymatic domain. Three chitinases might be involved in the remodeling of the walls during encystation or in the degrading of the walls during excystation (Van Dellen *et al*., 2002).

Jacob lectin is the most abundant protein in the *E. invadens* cyst wall, and it is a glycoprotein containing five tandemly arranged CBDs. CBDs contain six conserved cysteine residues and several conserved aromatic amino acids (Figure 4.1). *E. invadens* has seven Jacobs (Jacob1-7) form 30% of the cyst wall proteins, Jacob1-3 are the most abundant ones in the cyst wall (Van Dellen *et al.*, 2006). Five Jessie3 lectins, compose 50% of the protein mass of the *E. invadens* cyst wall. Jessie lectins contain a single N-terminal 8-cysteine CBD like that of *E. invadens* chitinase, followed by a low complexity spacer, and a C-terminal domain with unidentified function (Chatterjee *et al.*, 2009;Van Dellen *et al*., 2006).

Jacob lectin binds galactose lectins of plasma membrane, and cross-links chitin fibrils in the same way that CBDs of insect peritrophins cross-links chitin fibrils in insect and plants. Although they contain similar six or eight cysteines, there is no sequence homology between them (Frisardi *et al*., 2000). Chitinases are involved in remodelling cyst wall components during encystation or in degrading during excystation (Van Dellen *et al.*, 2006). Chitinase and Jessie lectin have a unique, N-terminal CBD that contains eight conserved cysteine residues (Nayak and Ghosh, 2019) (Figure 4.1). Although neither chitin synthase nor chitinase are present in *E. invadens* trophozoites, both enzymes are expressed by encysting amoebae (Herman *et al*., 2017). Chitinases show hydrophilic heptapeptide repeats between an N-terminal signal sequence and a C-terminal glycohydrolase domain. These repeats are similar between species of *Entamoeba* (Van Dellen *et al.*, 2002).

According to the “wattle-and-daub” model hypothesis, encystation occurs in three phases (Chatterjee *et al.*, 2009). Firstly: the foundation phase or early encystation

includes the expression of the plasma membrane Gal/GalNAc lectins and binding of Jacob lectins to the surface of the encysting plasma membrane., Secondly: the wattle phase or the mid encystation, where the Jacob lectins cross-link with chitin fibrils.

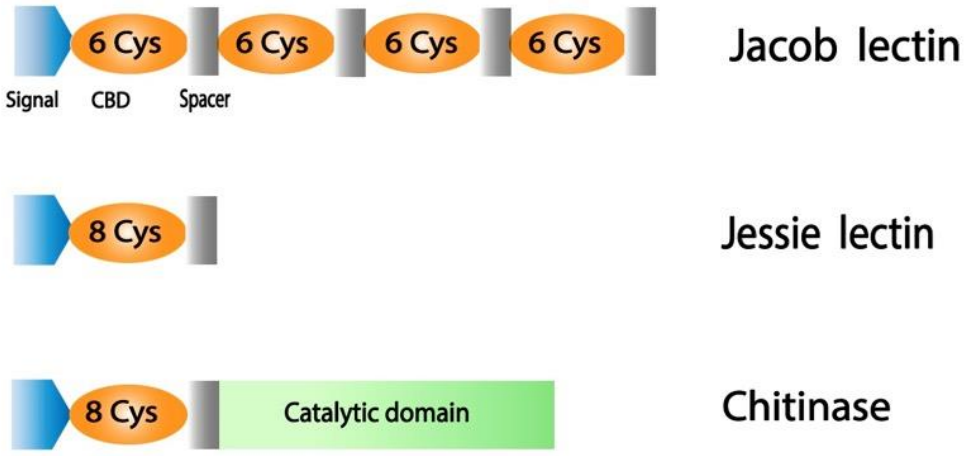

Figure 4. 1 Illustration of *Entamoeba* lectins with characterized chitin binding domains CBDs. 6-Cys CBDs in Jacob and 8-Cys Jessie and chitinase. Modified from Van Dellen *et al* 2002.

Thirdly: the daub phase or late encystation induced by the addition of the Jessie3 lectin, that binds the chitin, Jessie increases the stiffness of the cyst wall making them impenetrable to small molecules (Marta Frisardi *et al*., 2000; Wang *et al*., 2003).

The development of new approaches to control *E. histolytica* encystation is essential to stop amoebiasis. The interruption of the life cycle is important through the impairment of stage transition that can stop cyst formation and block the spread of the disease. In the last years, several researchers have studied the molecules that

are associated with stage transition such as: Gal-lectin production (García *et al.*, 2015), catecholamine pathway signalling (Coppi, *et al*., 2002), cholesterol sulphate synthesis (Mi-Ichi *et al*., 2016), heat shock protein 90 (Singh *et al*., 2015), chitin metabolism (Chatterjee *et al*., 2009), proteolytic systems (Makioka *et al*., 2002), and enolase (Herman *et al.*, 2017). Little known about the role of Jacob and Jessie lectins during encystation, therefore, in this study I tried to express and purify these proteins, to study their interaction with the *Entamoeba* plasma membrane lipids (PML) using a Langmuir trough apparatus. I also like to study their interaction with red blood cell membranes as a model for the lipid bilayer.

4.2. Materials and methods

4.2.1. DNA extraction

Trophozoites of *E. invadens* strain IP-1 were grown at room temperature, in 50 ml flasks containing LYI-S medium (Liver digest, Yeast extract, Iron and Serum), 15% adult bovine serum and 2% Diamond vitamin mix, as described in Chapter 2. When the culture reached the logarithmic phase, cells were harvested at 4000 g for 5 minutes and washed twice with PBS. DNA was extracted according to Ali *et al* (2005). Briefly, trophozoites were re-suspended in 250 µl lysis buffer (0.25% SDS in 0.1 M EDTA, pH 8.0) and 100 µg/ml of proteinase K (3 µl from a 10 mg/ml stock) (Sigma – Aldrich) and incubated at 55 °C for 15 minutes. Afterward, 75 µl of 3.5 M NaCl was added and mixed, followed by the addition of 42 µl of 10% CTAB/0.7 M NaCl (heated to 55 °C), mixed and incubated at 65 °C for 10 minutes. Inside a fume hood, 400 µl of chloroform was added, mixed well by inversion and centrifuged at full

speed in a micro-centrifuge for 5 minutes. The supernatant was removed and transferred into a new tube (inside a fume hood) and 400 µl of phenol: chloroform: isoamyl alcohol were added, mixed well by inversion and centrifuged at full speed in a micro-centrifuge for 5 minutes. Subsequently, the supernatant was then transferred to a new tube, followed by the addition of two volumes of 100% ethanol, mixed gently, incubated at room temperature for 5 minutes and centrifuging for 10 minutes at full speed. The resulting supernatant discarded carefully from the pellet and the pellet was then washed in 200 µl of 70% ethanol by centrifuging for 5 minutes as above. The pellet was air dried and then re-suspended in 50 µl of sterile water (overnight at 4°C is best). Finally, DNA was quantified using a NanoDrop 2000c (Thermo-scientific), visualized using agarose gel electrophoresis and stored at -20 ^{o}C.

4.2.2. Amplification and cloning of the targeted genes

The genes encoding *E. invadens* cyst wall proteins were all amplified from genomic DNA. EiJacob2 (GenBank accession number DQ324634.2) was amplified from *E. invadens* genomic DNA using the forward primer (5'-ATG ATA CTA CTG TTT TTG G) and reverse primer (5'-TTA ATT CTT CTT TGC CCA G). Primers were designed by Dr Mark van der Giezen. Genes were amplified using GoTaq G2 Hot Start Green Master Mix (Promega) which adds an adenine overhang to the PCR product which is utilised for cloning into a TA cloning vector containing a complementary thymine overhang. The thermal cycler was programmed using the recommended parameters for GoTaq G2 Hot Start Green Master Mix. The following parameters were used: an

initial step of denaturation at 95 °C for 5 min, followed by 35 cycles of denaturation at 95 °C for 45 s, annealing at 46 °C for 45 s, extension at 72 °C for 1 min and a final extension at 72 °C for 5 min. EiJacob2 gene was TA-cloned into the pGEM-T-Easy plasmid, that contains thymidine overhangs that allow the hybridization of the complementary PCR product and the plasmid (Figure 4.2). Constructs were verified by the DNA sequencing (MWG-Eurofins, Germany), using the universal M13 forward (-43) and M13 reverse (-29) primers. EiJacob2 was re-amplified TA cloning vector, and *Xho*I and *Bam*HI restriction sites were added to either end of the gene for cloning into pET14b the expression vector(Figure 4.4). An *Xho*I restriction site was incorporated into the 5' terminus of the forward primer and a *Bam*HI site into the 5' terminus of the reverse primer. The EiJacob1 (AF175527), EiJacob3 (DQ324635.2), EiJessie3a (DQ324645.1) and EiJessie3b (DQ324646.2) genes were amplified from the *E. invadens* genomic DNA using primers with restriction sites for the cloning into the expression vector pET14b (Figure 4.3 and 4.5). Primers are described in Table 4.1.

Table 4. 1 Primers for Jacob and Jessie genes with restriction sites. Underlined letters represent the restriction sites, uppercase indicate homologous sequence and lowercase indicate nonsense sequence.

Protein	Primers
Ei_Jacob1-XhoI-F	aga aga CTC GAG ATG TTA TCT TTT ATA TTG TTC
Ei_Jacob1-BamHI-R	tct tct gga tcc TTA GAT CTT CTT CCC CCA AG
Ei_Jacob2-XhoI-F	aga aga CTC GAG ATG ATA CTA CTG TTT TTG G
Ei_Jacob2-BamHI-R	tct tct GGA TCC TTA ATT CTT CTT TGC CCA GG
Ei_Jacob3-XhoI-F	aga aga CTC GAG ATG TTG ATA CTA CTG TTA CTG G
Ei_Jacob3-BamHI-R	tct tct gga tcc TTA CCA CTC TGT TTG GTC C
Ei_Jessie3a-XhoI-F	aga aga CTC GAG ATG AAA ATC ACT TTC ATT GTA C
Ei_Jessie3a-BamHI-R	tct tct GGA TCC TCA CTT ATT TAT TGT GTA ATT C
Ei_Jessie3b-NdeI-F	aga aga CAT ATG ATG AAC AGA GCG ATT ATA AC
Ei_Jessie3b-NdeI-R	tct tct CAT ATG TCA TTT GCA TAA GTT CTT TC

A high fidelity KOD DNA polymerase (Merck-Millipore) was used to amplify these genes (to reduce the possibility of mutation), using a gradient PCR machine (Bio-Rad T100 Thermal Cycler, USA) to reveal the optimal annealing temperature. The following parameters were used: an initial step of denaturation at 95 °C for 2 min, followed by 30 cycles of denaturation at 95 °C for 20 s, annealing at 59-65 °C for 10 s, extension at 70 °C for 20 sec. and a final extension at 72 °C for 5 min. To verify the desired constructs, Plasmids DNA were sent for sequencing. Sequencing was performed by Eurofins MWG Operon, using the T7 forward and T7 terminator.

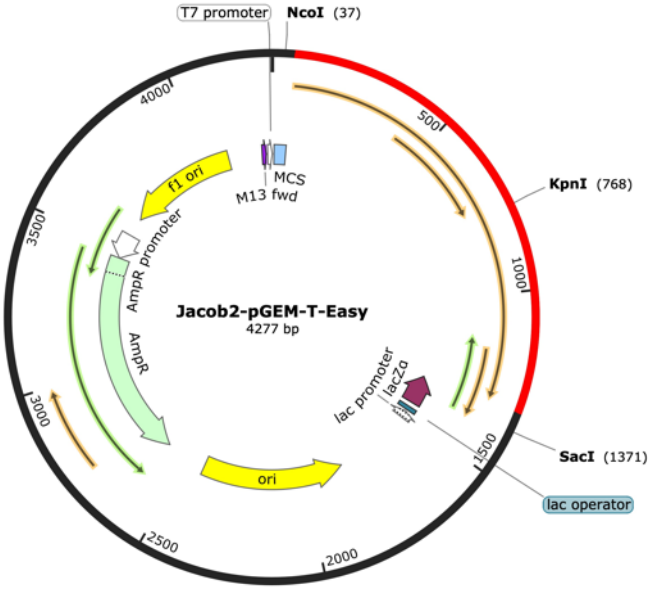

Figure 4. 2 Showing EiJacob2 (red) cloned into the TA cloning vector pGEM-T-Easy. Figure created using SnapGene.

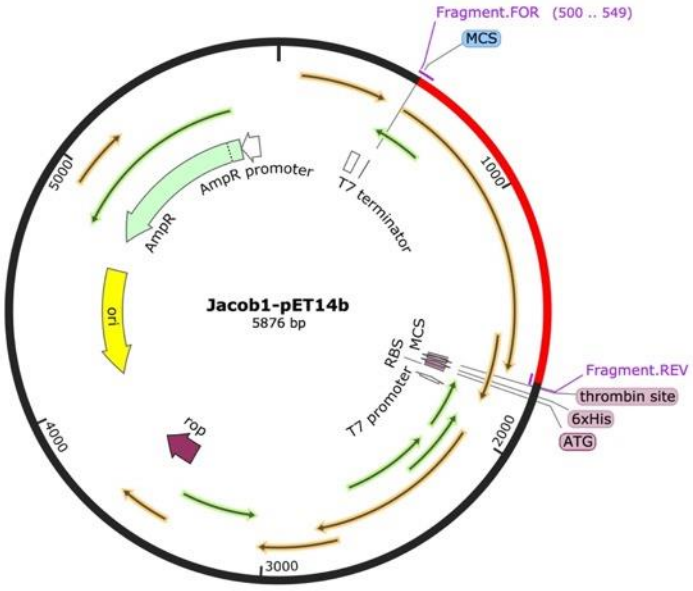

Figure 4. 3 Showing EiJacob1 (red) cloned into pET14b expression vector. Figure created using SnapGene.

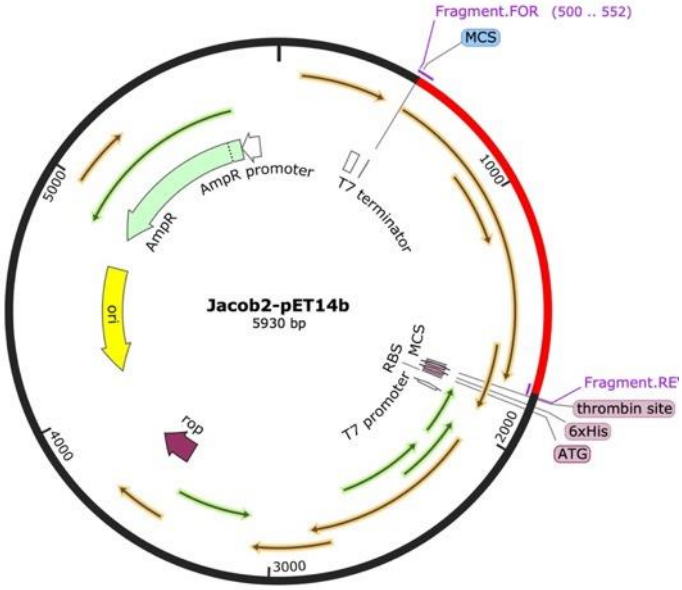

Figure 4. 4 Showing EiJacob2 (red) cloned into pET14b expression vector. Figure created using SnapGene.

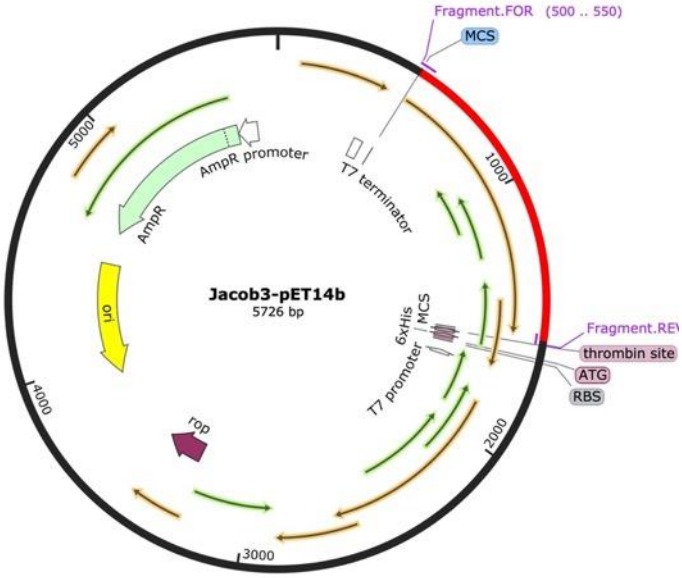

Figure 4. 5 Showing EiJacob3 (red) cloned into pET14b expression vector. Figure created using SnapGene.

4.2.3. Gene expression

For gene expression, two types of competent cells were used: *E. coli* BL21 (DE3) (New England BioLabs Inc.) and Rosetta cells (Novagen) were used and according to the manufacturer protocol. Briefly, 2 µl of the plasmid DNA were added to 50 µl of competent cells, flicked gently and incubated on ice for 30 minutes. The cells were heat-shocked in water bath at 42 °C for 40-45 seconds followed by 2 minutes cooling on ice. Subsequently, the cells were flooded by 200 µl of LB medium and incubated at 37 ºC with shaking at 220 rpm for one hour. Finally, the cells were plated out onto LB plates containing ampicillin (100 µg/ml) and incubated at 37 °C overnight.

The next day, positive colonies were used to start an overnight culture at 37 °C with shaking at 220 rpm in 10 ml of LB with 100 µg/ml of ampicillin. The following day, 1 ml from this culture was transferred to 500 ml and 1 L of LB medium containing 100 µg /ml ampicillin and incubated. The culture was grown for 3-4 hours with shaking at 220 rpm at 37 °C. The optical density (OD_{600nm}) readings were taken hourly until OD_{600nm} reached between 0.4-0.8. To induce gene expression, IPTG at different concentrations 0.025, 0.050, 0.1, 0.2 and 0.4 M was added, and incubated for 18-20 hours at 30 °C and 20 °C / 220 rpm. For autoinduction experiments, ZYM media was used instead of LB after the overnight starter culture step, and when the OD_{600nm} became between 0.4-0.8 the containers were transferred into another shaking incubator at 220 rpm at 20 ºC overnight. The cultures were then pelleted at 4,700 g for 30 minutes at 4 °C and re-suspended in 25 ml of nickel column wash buffer (20 mM Tris-HCl pH 8, 500 mM NaCl) per 0.5 L of culture.

On ice, cell suspension was lysed by sonication using a Soniprep 150 Sonicator (MSE, London, UK). Six cycles of 25 seconds on and 35 seconds resting at a frequency of 25 kHz and 60% amplitude were used. To separate the insoluble fraction from soluble one, the lysed cells was centrifuged at 20,000 g for 30 minutes at 4 °C.

For SDS-PAGE analysis, the insoluble and soluble fractions were diluted in an equal volume of 2x SDS-PAGE buffer (100 mM Tris-HCl pH 6.8, 4% (w/v) SDS, 0.2% (w/v) bromophenol blue, 20% (w/v) glycerol, and 2% (v/v) ß-mercaptoethanol) to denature the protein, by mixing 20 µl of protein samples and 20 µl of the buffer. The samples were heated at 95 °C for 10 min then cooled and loaded with Spectra Multicolour Broad Range Protein Ladder (Thermo-Scientific) on the SDS-PAGE gel (Express plus TM Page Gels, GenScript. 4-20%) to separate proteins by size for visualization using a Mini-Protean Electrophoresis System (Bio-Rad, UK) at 150 V/60 min. Gels were stained with InstantBlue stain (Expedeon) for 1 hour and visualised using a UV light box.

4.3. Results

The DNA genes coding for EIJacob1-3, EiJessie3a and EiJessie3b were PCR amplified directly from the genomic DNA of *E. invadens* IP-1. Gel electrophoresis analysis shows the bands of the amplified EIJacob1 with the predicted size of 1200 bp, EIJacob2 gene with the predicted size of 1260 bp, EIJacob3a with the predicted size of 1030 bp, EiJessie3a gene with the predicted size of 1840 bp and EiJessie3b with the predicted size of 1760 bp (Figure 4.6). A proofreading Pfu DNA polymerase:

High fidelity KOD DNpolymerase) (Merck) was used to minimize the chance of mutation and to add primers containing *Kpn*I and *Bam*HI restriction sites (see 4.2.1). Following double digestion with restriction enzymes, the fragments were incorporated into pET14b expression vector. Cloned constructs were confirmed by the DNA sequencing (MWG-Eurofins, Germany).

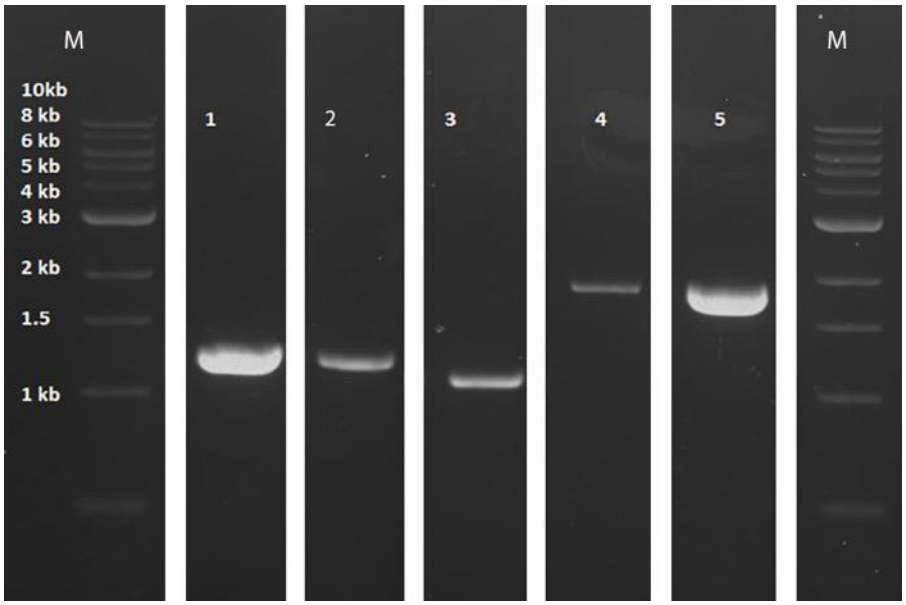

Figure 4. 6 PCR amplification of *E. invadens* Jacob1 (1), Jacob2 (2), Jacob3 (3) Jessie3a (4), and Jessie3b (5). DNA marker from New England Biolabs (NEB).

According to the sequencing results, EiJacob1-3 and EiJessie3b were successfully cloned in the C-terminus of His-tag in the pET14b expression vector. Sequence comparison of Jacob1-3, EiJessie3b and EiJessie3a were performed by the Clustal method using BioEdit software (BioEdit 7.0). These sequences were checked against part of pET14b vector, EiJacob1-3 EiJessie3b and EiJessie3a sequences obtained from GenBank. Analysis showed that all sequences are identical to the GenBank sequences (Figure 4.7 - 4.10), except for EiJessie3a that indicated PCR

artefacts (change in the nucleotide T to A at the position 553), which would lead to changes in amino acid sequences, so these clones were discarded (Figure 4.11).

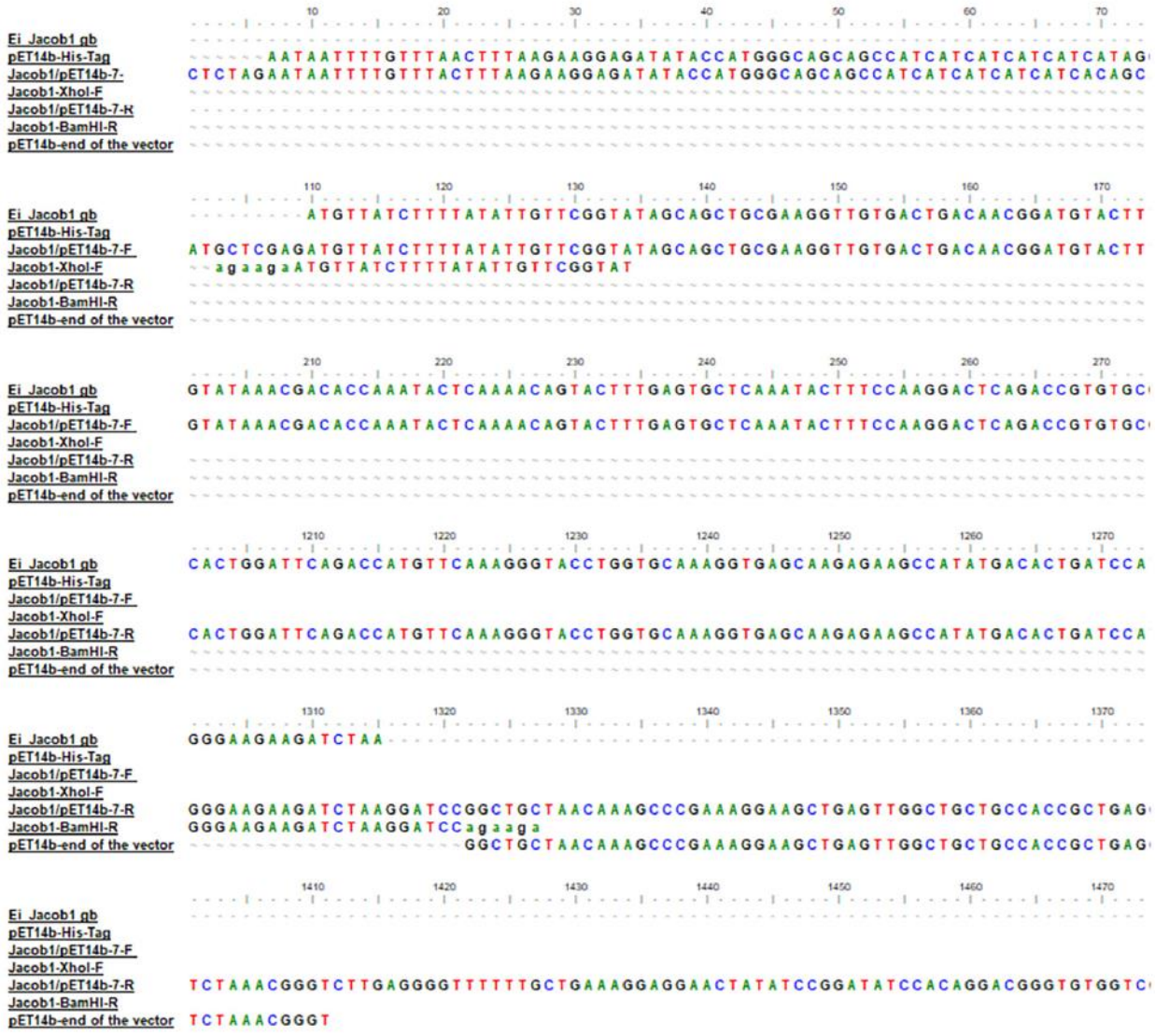

Figure 4. 7 Sequence comparison of (EiJacob1) aligned with EiJacob1 obtained from GenBank, primers used for cloning and the His tag sequence.

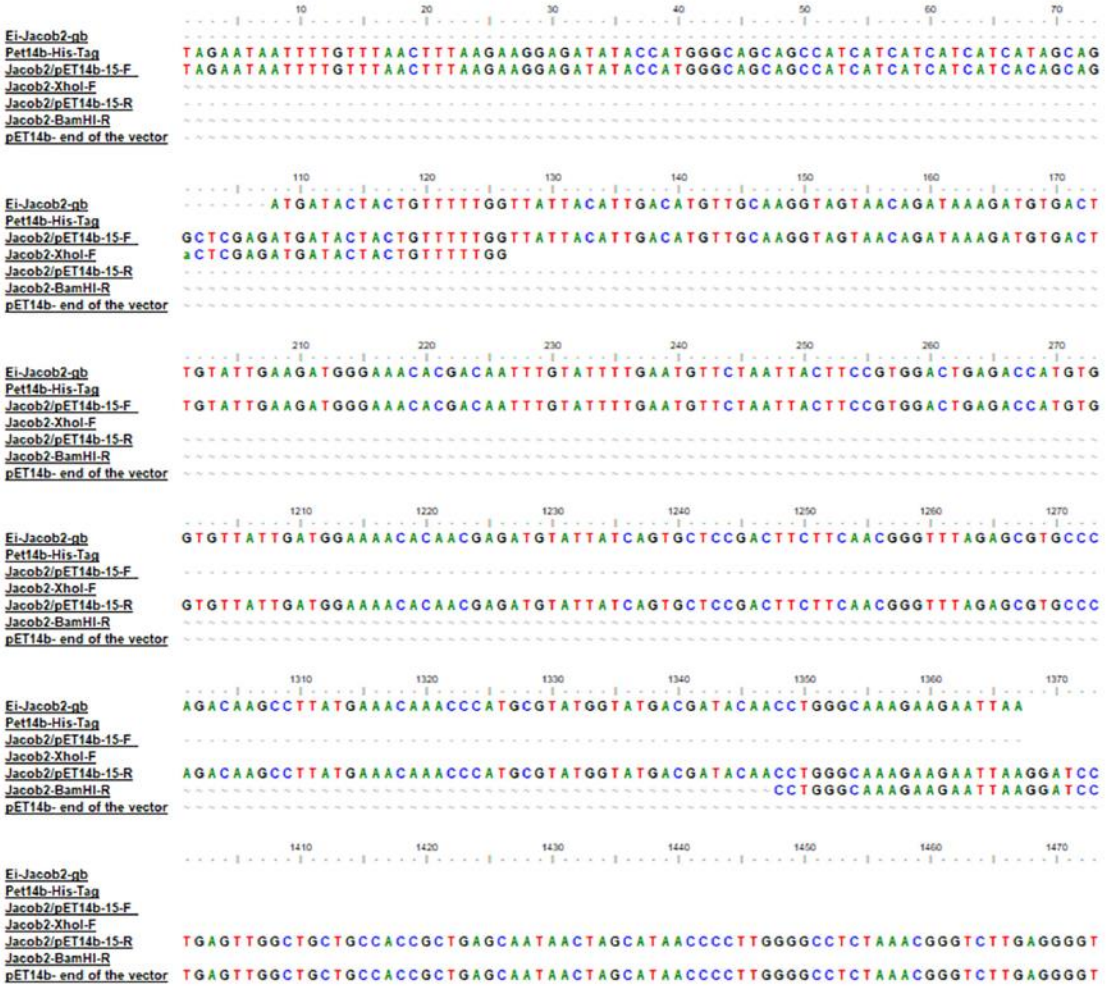

Figure 4. 8 Sequence comparison of (EiJacob2) aligned with EiJacob2 obtained from GenBank, primers used for cloning and the His tag sequence.

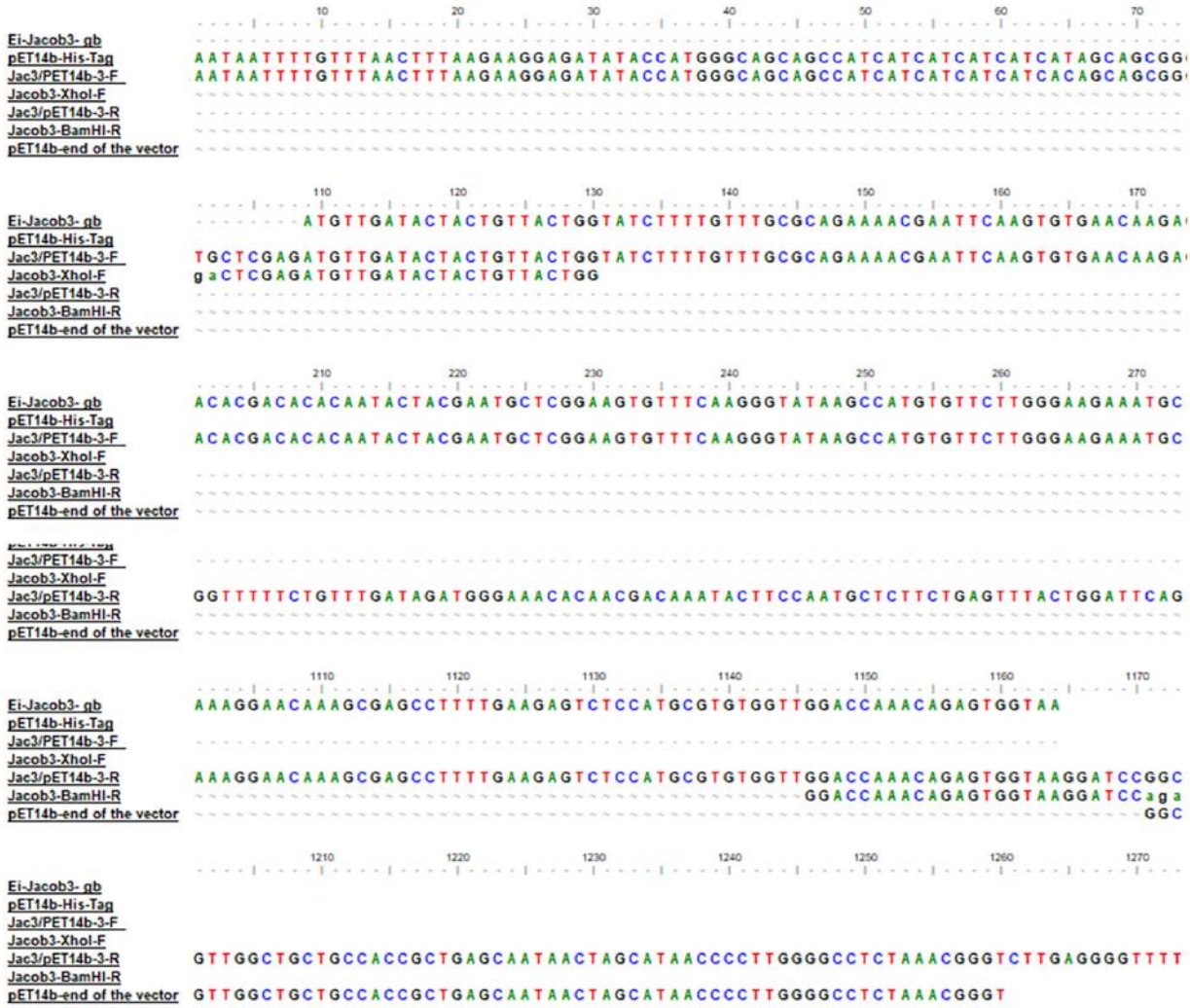

Figure 4. 9 Sequence comparison of (EiJacob3) aligned with EiJacob3 obtained from GenBank, primers used for cloning and the His tag sequence.


Jess3b GeneBank
His-tag
A-184266_H2-F
A-184266_A3-F2
A-184265_G10-R
A-184265_H10-R2

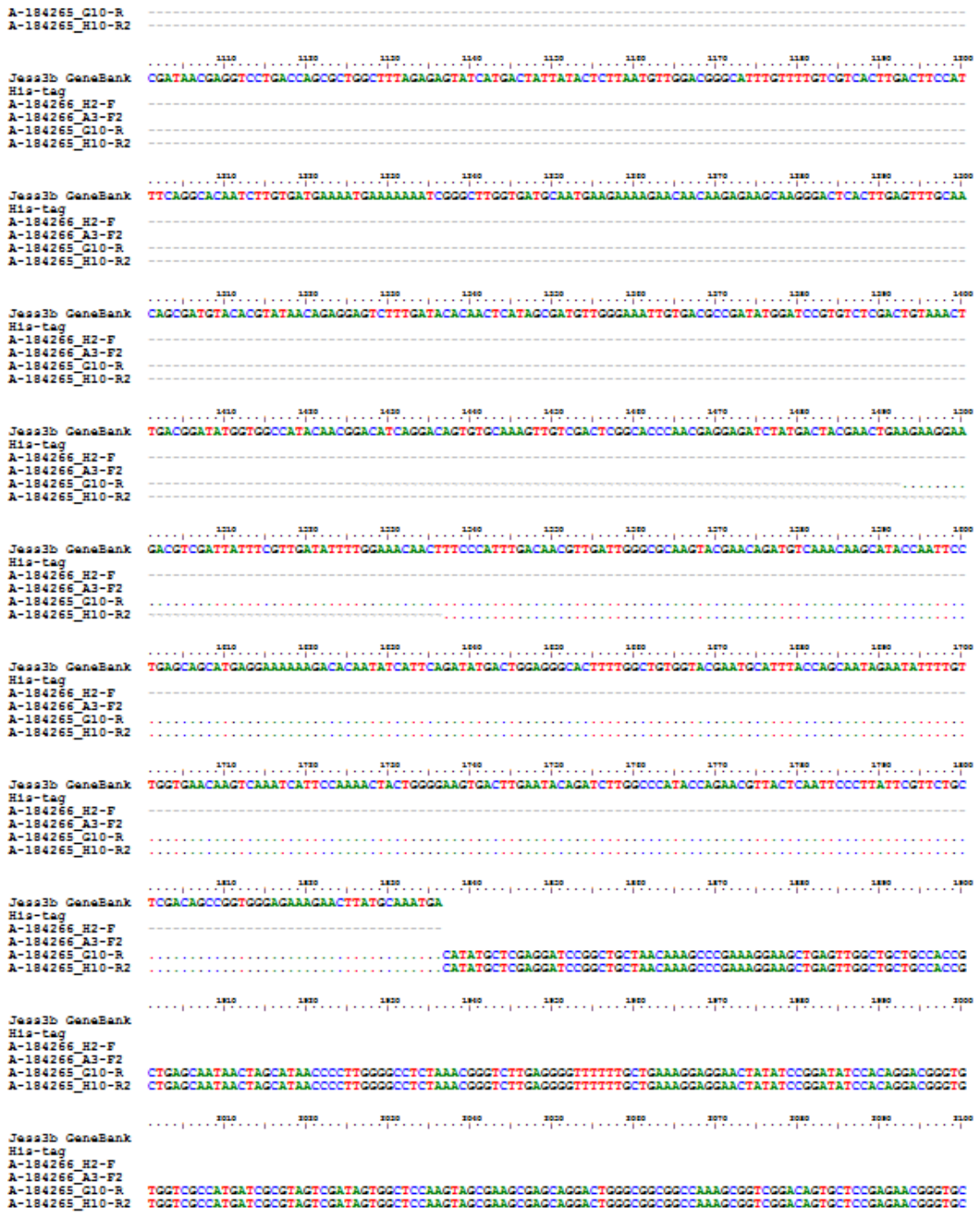

Figure 4. 10 Sequence comparison of (EiJessie3b) aligned with EiJessie3b obtained from GenBank, primers used for cloning and the His tag sequence.

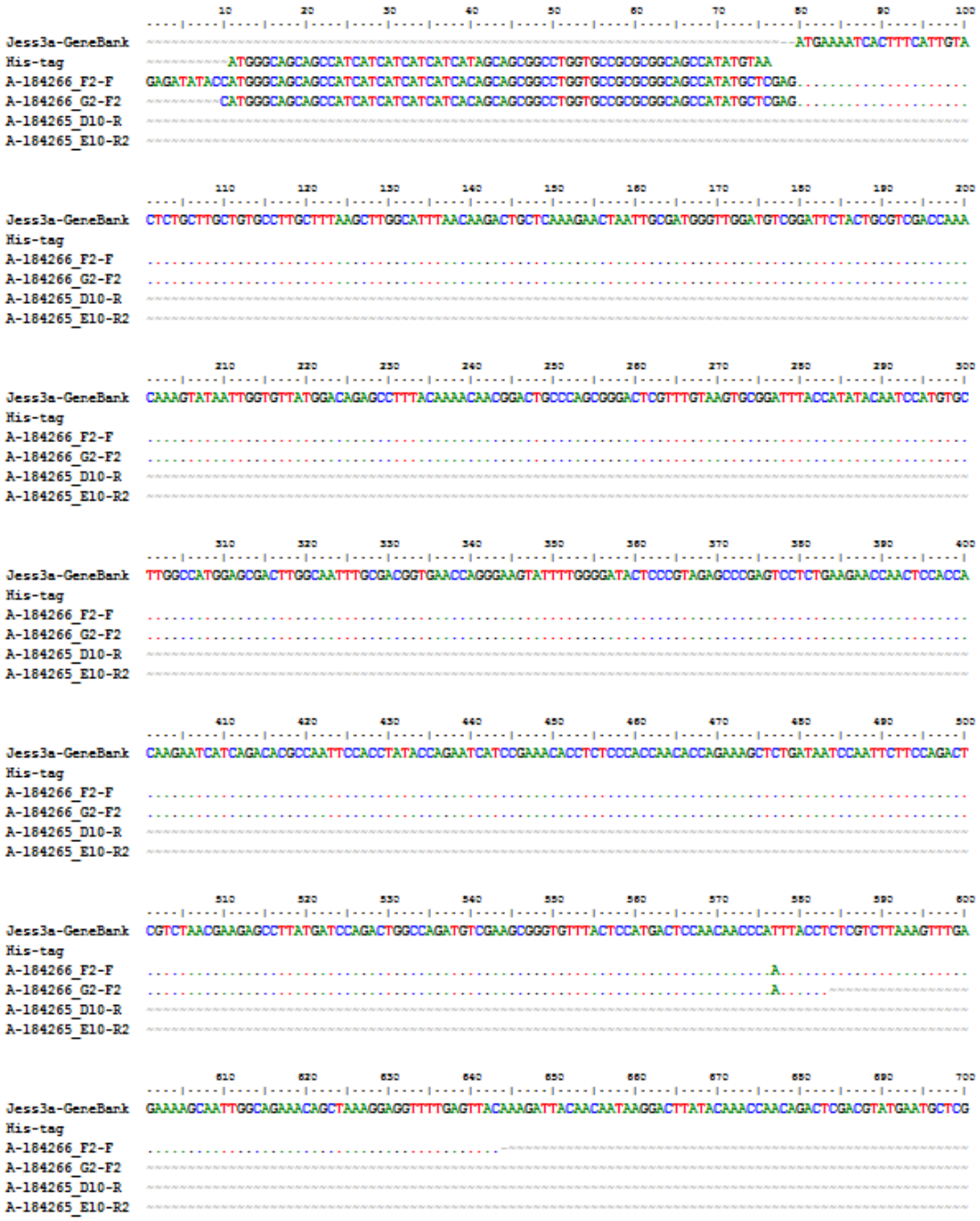

Figure 4. 11 Sequence comparison of (EiJessie3a) aligned with EiJessie3a obtained from GenBank, primers used for cloning and the His tag sequence. Showing PCR artifact in the position 553.

To purify Jacob 1-3, different approaches were carried out; two strains like *E. coli* BL21 (DE3) and Rosetta were used, at different concentrations of IPTG (0.025, 0.050, 0.1, 0.2 and 0.4 M) and two different temperatures at 30 °C and 20 °C for an overnight incubation after the IPTG induction. In spite of all these different conditions, the production of protein was unsuccessful. Figures 4.12 – 4.14 represent examples of some attempts.

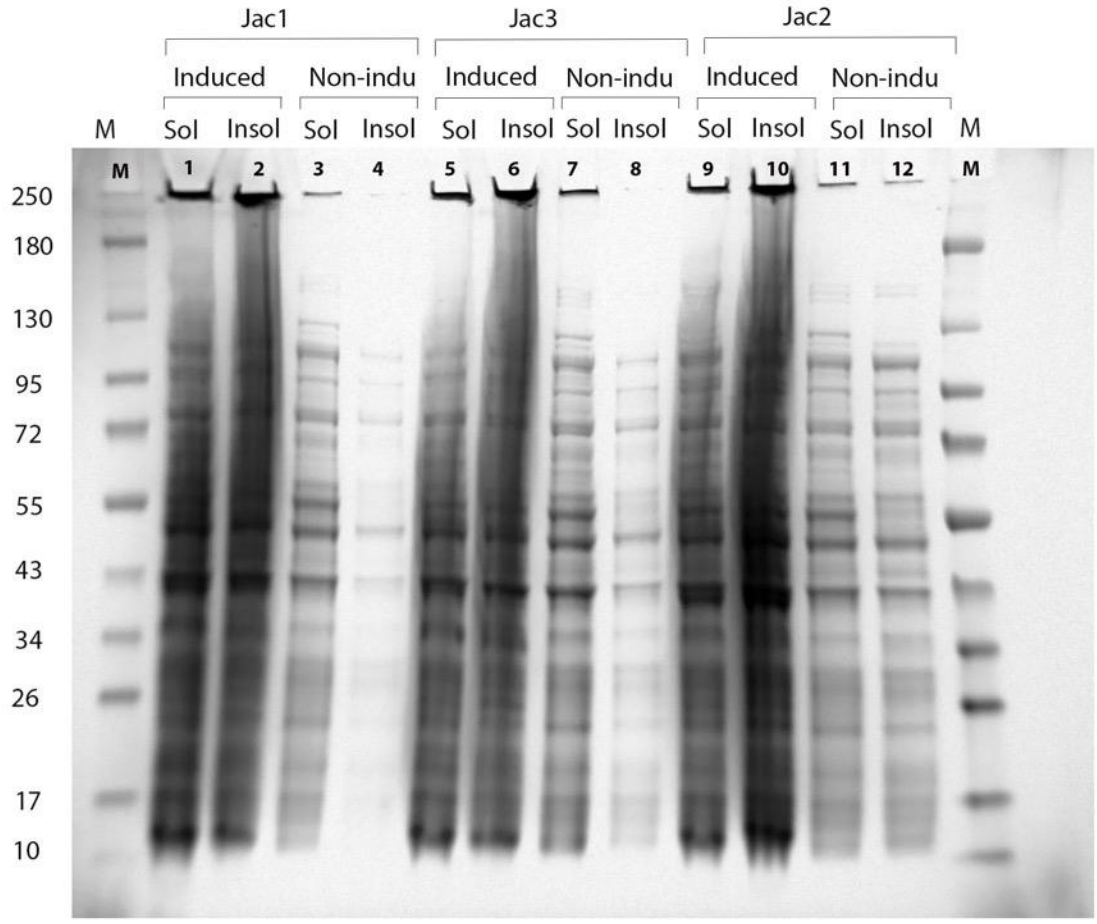

Figure 4. 12 SDS gel of several expression trials of *Entamoeba invadens* Jacob1-3-pET-14b constructs in *E. coli* BL21. Lanes 1-2: Represents EiJacob1-pET-14b soluble and insoluble proteins induced 20 °C with IPTG concentration

200 uM. Lanes 3-4: Represents EiJacob1-pET-14b insoluble and soluble proteins, auto induced using ZYM medium at 20 °C. Lanes 5-6: Represents EiJacob3-pET-14b soluble and insoluble proteins induced 20 °C with IPTG concentration 200 uM. Lanes 7-8: Represents EiJacob1-pET-14b insoluble and soluble proteins, auto induced using ZYM medium at 20 °C. Lanes 9-10: Represents EiJacob2-pET-14b soluble and insoluble proteins induced 20 °C with IPTG concentration 200 uM. Lanes 311-12: Represents EiJacob2-pET-14b insoluble and soluble proteins, auto induced using ZYM medium at 20 °C. M represents molecular weight marker.

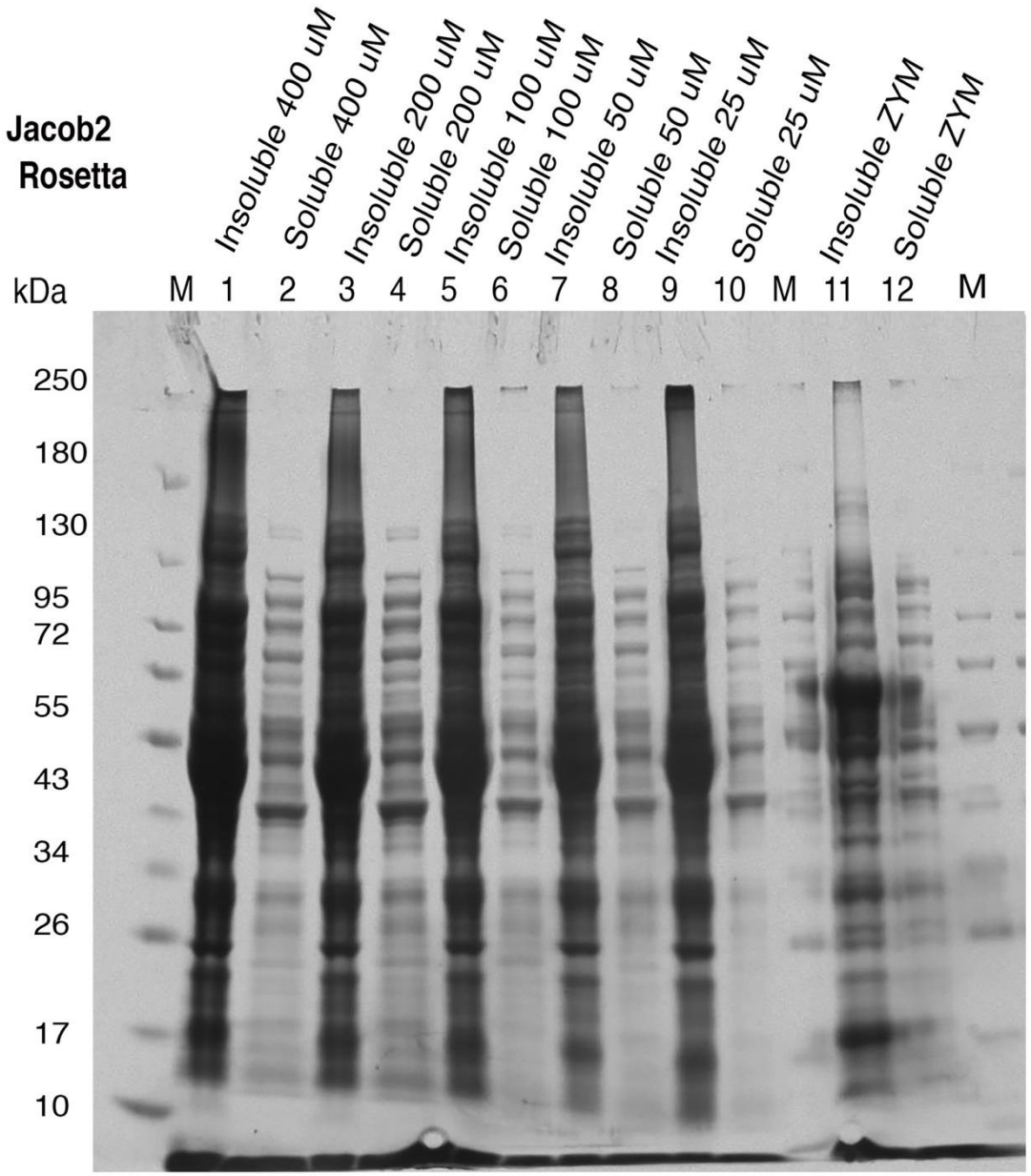

Figure 4. 13 SDS gel of several expression trials of *Entamoeba invadens* Jacob2-pET-14b construct in *E. coli* Rosetta. Lane1-10: Represents EiJacob2-pET-14b insoluble and soluble proteins induced at 20 °C with different IPTG concentration 400-25 uM, respectively. Lanes 11 and 12: Represents EiJacob2-pET-14b insoluble and soluble proteins, auto induced using ZYM medium at 20 °C. M represents molecular weight marker.

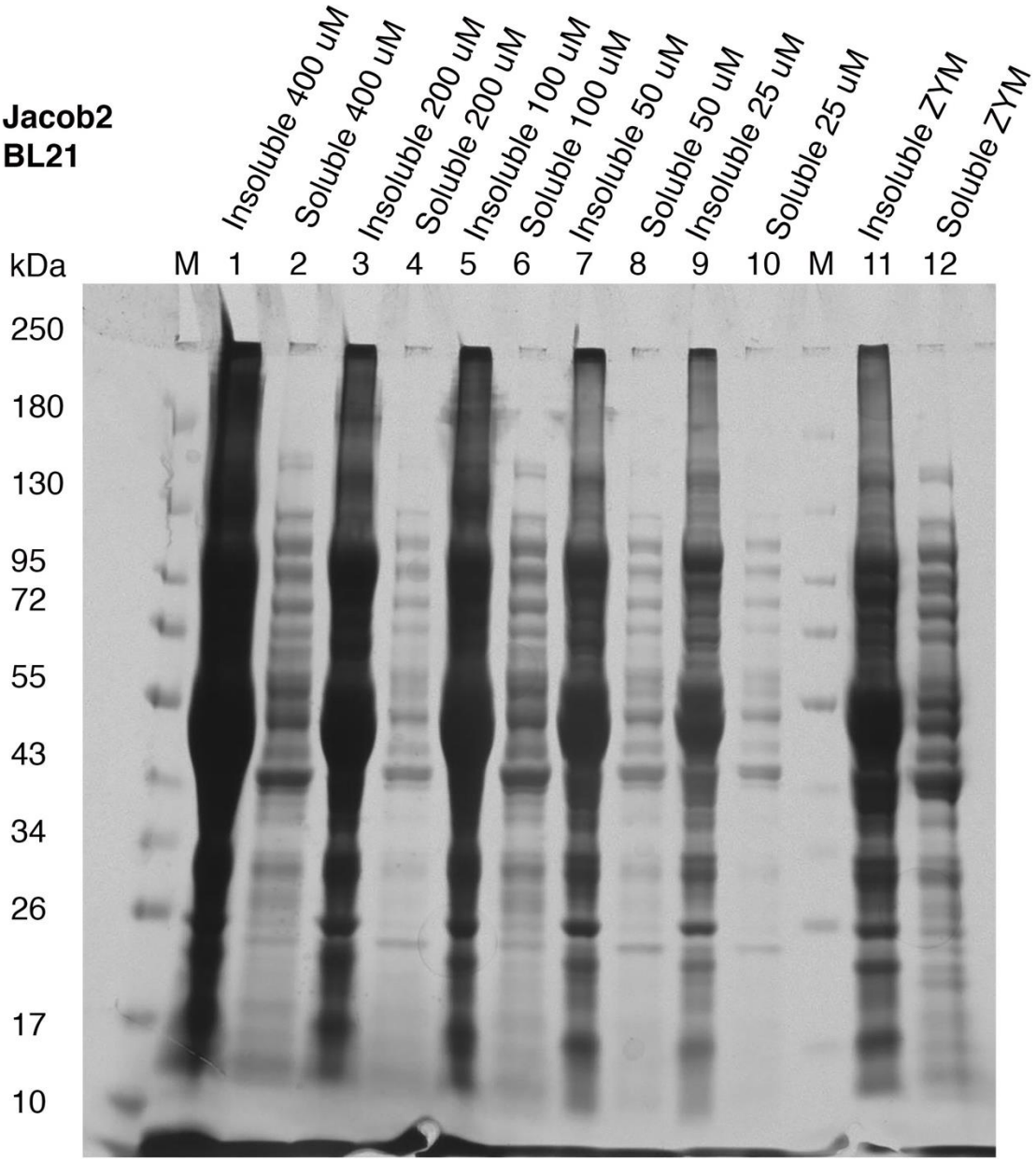

Figure 4. 14 SDS gel of several expression trials of *Entamoeba invadens* Jacob2-pET-14b construct in *E. coli* BL21. Lane1-10: Represents EiJacob2-pET-14b insoluble and soluble proteins induced at 20 °C with different IPTG concentration 400-25 uM, respectively. Lanes 11 and 12: Represents EiJacob2-pET-14b insoluble and soluble proteins, auto induced using ZYM medium at 20 °C. M represents molecular weight marker.

4.4. Discussion

This chapter aimed to characterize the *Entamoeba invadens* cyst wall lectins: Jacob and Jessie. The cyst wall is mainly composed of chitin and its deacetylated form chitosan and 30:70 mix of Jacob and Jessie lectins and chitinase (Das *et al.,* 2006). Previous researchers reported an increase in mRNAs encoding Jacobs, and Jessies, during *E. invadens* encystation (Chatterjee *et al*., 2009). *Entamoeba invadens* genome encoded for seven predicted copies of Jacob and five Jessie lectins, but only three copies of Jacob and two of Jessie were the most abundantly expressed during encystation (Van Dellen *et al*., 2006). In this study, I chose Jacob 1-3 and jessie3a and Jessie3b. I aimed to clone these proteins in a pET14b expression vector, in order to purify them and study their physical and biochemical properties. pET14b vector is designed for high levels of protein production and works under the control of a T7 promoter induced by IPTG. It contains a Histidine tag (His-tag) sequence before the *Nde*I cloning site, thus generating a recombinant protein containing a sequence of six His residues at the N-terminus to facilitate its purification.

Only Jacob 1-3 and Jessie3b were successfully cloned in the expression vector. Jessie3a had and artifact during amplification that led to change in one amino acid. Purifying a membrane associated proteins such as Jacob and Jessie were a challenging process. Several trials have been performed to obtain the protein. Several approaches were applied, including using two types of *E. coli* (BL21 and Rosetta) and different concentrations of the inducer (IPTG). The orientation of the

gene in the plasmid, the codons, and the selection of the suitable expression vector (pET14b) have also been checked. At the end I decided not to continue the expression as there was no yield and this might be due to that the protein is toxic to the cells, or the protein needs post-translational modification, which doesn't exist in *the E. coli* expression system. Therefore, it has been suggested that using an alternative expression system such as mammalian or insect cells (William, 2009), maybe needed to achieve the objective of expressing these proteins. However, due to unavailability of such systems at the university and time limitation I couldn't perform experiments.

For unknown reasons, *E. coli* cells sometimes fail to express the recombinant proteins of genes cloned into some expression vectors. These may include protein toxicity to *E. coli*, plasmid or protein instability, inefficient transcription or translation, inefficient posttranslational modification, and presence in the cloned gene of inadequate or non-used codon sequences by the *E. coli* host cells (Brondyk, 2009). The expression of some membrane proteins was still toxic in the *E. coli* BL21 C41(DE3) strain, C43(DE3) was derived from C41(DE3) by selecting resistance to the F-ATPase b subunit gene. Thus, C43(DE3) is able to express various set of toxic membrane proteins than C41(DE3) (Kopanic *et al*., 2013).

To summarize, *E. invadens* cyst wall lectins Jacob and Jessie were amplified and successfully cloned into pET14b expression vector. Numerous trials were performed to express and purify these proteins in the *E. coli* host were unsuccessful. The reason may be due to proteins toxicity to the host cell, protein instability, inefficient transcription or translation, inefficient posttranslational modification.

Chapter 5 - Conclusions and Future Work

5.1 Conclusions

Amoebiasis is the third-leading cause of death due to parasitic diseases. it is caused by *Entamoeba histolytica* that infect human, animals and other primates, producing various clinical signs ranging from asymptomatic carriers to symptomatic invasive amoebiasis (Pritt and Clark, 2008). The spread of amebiasis in poor countries makes it a serious health problem (Nath *et al*., 2015). Metronidazole is the drug of choice for the treatment of this disease. However, some reports have raised concerns about the development of metronidazole-resistance in *Entamoeba* strains (Quintanilla-Licea *et al.*, 2014). Identification and characterization of novel drug targets unique to *E. histolytica* are therefore needed to design better therapeutics against amebiasis. Researchers are developing new strategies focusing on blocking encystation which has the potential to stop the transmission of the disease (Herman *et al*., 2017). Cyst wall components are the main drug target that have been studied over time (Mi-Ichi *et al.*, 2016) but the process of encystation remains poorly understood. This study was aimed to address this knowledge gap by investigating the mechanism of encystation using *E. invadens* as a model.

Data presented here showed that the addition of chitin and chitosan to the monolayer of plasma membrane lipids (PML) increases its stiffness. These two components have the same effect when added to red blood cells (RBCs) membrane, resulting in increased RBCs membrane rigidity. Studies reported that all cyst components including chitin biosynthesis pathway genes and other cyst components genes such as Jessie as Jacob were reported to be highly expressed during

encystations (Chatterjee *et al.*, 2009; De Cádiz *et al*., 2013; Herman *et al*., 2017; Samuelson and Robbins, 2011) Therefore, chitin might represent a good potential drug target against amoebiasis since it does not have homologues in humans (Samuelson *et al*., 2013).

To investigate the interaction between cyst wall components and PML of *E. invadens* plasma membrane, PML was extracted, and characterized using Langmuir trough apparatus for the first time to identify the interactions and changes after the addition of cyst wall components (Chapter 3). The pressure area isotherm of PML revealed that there is no transition area during the compression and the relaxation of PML.

For studying the interactions between cyst wall components and the PML of *E. invadens,* chitin and chitosan were added to PML monolayer. Chitin and chitosan insertion caused an increase in the overall surface pressure of the PML monolayers, and also elevated the stiffness of PML. These data indicates that the deposition of chitin and its deacetylated form on the plasma membrane during encystation would cause changes that increase cyst wall stiffness.

Thermal fluctuation analysis was used to study the interaction between chitin / chitosan and RBCs membrane (as a model for lipids bilayer) and the bending elastic moduli was calculated as well after the addition of chitin /chitosan (Chapter 3). Thermal fluctuation and bending elastic moduli revealed that RBCs membrane rigidity has been increased after the addition of chitin and chitosan.

Cyst wall lectins, Jacobs and Jessies were amplified from *E. invadens* gDNA, cloned into pET14b expression vector to get expressed and purified (Chapter 4). Numerous

attempts and approaches were carried out to express the proteins, but no yield was obtained. This might be due to that the protein is toxic to the cells, or the protein requires post-translational modification, which are absent in *the E. coli* expression system.

In summary, my results provide evidence that chitin and chitosan interact with lipids mono/bilayer lipids to increase their stiffness and rigidity. This direct interaction between chitin / chitosan and lipids mono / bilayer is the first important step in cyst formation. These data would provide a basic knowledge about the behaviour of *Entamoeba* plasma membrane during encystation. More studies would be necessary to investigate the effect of chitin binding proteins on lipids mono / bilayer.

5.2 Future work

The expression and purification experiments for Jacob and Jessie were unsuccessful. Therefore, the first priority for future work is to express and purify these lectins using alternative systems, for example mammalian or insect expressing system. The techniques that have been used in this thesis can be applied to simulate the *Entamoeba* encystation process. First, I would suggest performing various experiments by adding each cyst wall components to the PML using a Langmuir trough. I would start adding Jacob protein to the PML in one experiment and add Jessie proteins in another, to study the individual effects of these proteins on *Entamoeba* lipids. Furthermore, I would do more experiments by adding each protein with chitin / chitosan, to monitor their effect on the elasticity of the membrane, as well

as all cyst wall components together to the PML to mimic the encystation process. Together, these data would enable the characterisation of the individual and combined function of each component, allowing for a better understanding of the encystation process.

To study the effect of cyst wall components on biological cell membranes such as RBCs, to further investigate its biocompatibility, it would be interesting to investigate the effect of Jacob and Jessie proteins on the cell fluctuation of RBCs, as a bilayer model. I would start by studying the interaction of Jacob and Jessie, respectively, with the RBCs membrane lipids, followed by their effect after the addition of chitin and chitosan, respectively. Moreover, study the effect of the whole cyst wall components on the cell fluctuation of RBCs bilayers lipid membrane.

This study has shown that chitin and chitosan have altered the mechanical properties of lipid membranes. These data were supported by other studies in which chitin and chitosan were shown to be essential for life cycle transition in *Entamoeba* and can be potentially used as a drug target (Mi-Ichi *et al*., 2016; Chatterjee *et al*., 2009; De Cádiz *et al*., 2013). CRISPR/Cas9 technology can be used to edit or delete genes responsible for chitin synthesis and modification during encystation such as chitin synthase and chitinase. The same technology can be applied on other cyst components Jacobs and Jessies after characterizing them and study their interaction with plasma membrane lipids.

Fluorescence microscopy using fluorescently tagged lipids would help to monitor PML interaction with other components (Rodgers and Glaser, 1991). Fluorescently tagged lipids can be introduced into the PML to allow monitoring of lipid and their

distribution within the monolayer. This technique could be used to determine changes in PML microdomain organisation after the addition any or all of cyst wall components.

Together, the proposed future work offers the potential to explore in detail the role of individual genes, components of the cyst wall and their interactions for the process of encystation and therefore the identification of the best targets for drug development in the future.

Chapter 6 - Bibliography

Bibliography

Abdul Rahman, I.B., 2008. Mesoscopic structure and surface behaviour of the tear film lipid layer. University of Exeter. School of Physics, UK.

Aguilar-Díaz, H., Carrero, J.C., Argüello-García, R., Laclette, J.P. and Morales-Montor, J., 2011. Cyst and encystment in protozoan parasites: Optimal targets for new life-cycle interrupting strategies? *Trends in Parasitology*, 27(10), pp.450–458.

Aguilar-Díaz, H., Díaz-Gallardo, M., Laclette, J.P. and Carrero, J.C., 2010. In vitro induction of *Entamoeba histolytica* cyst-like structures from trophozoites. *PLoS Neglected Tropical Diseases*, 4(2): e607.

Ali, I.K., Zaki, M. and Clark, G., 2005. Use of PCR Amplification of tRNA Gene-Linked Short Tandem Repeats for Genotyping *Entamoeba histolytica. Journal of Clinical Microbiology*, 43(12), pp.5842–5847.

Alvarado-Esquivel, C., Sanchez-Anguiano, L.F., Hernandez-Tinoco, J., Estrada-Martinez, S., Perez-Alamos, A.R., Ramos-Nevarez, A., Cerrillo-Soto, S.M. and Guido-Arreola, C.A., 2017. *Entamoeba histolytica* Infection in Female Sex Workers: A Matched Case-Control Study in Durango, Mexico. *Journal of Clinical Medicine Research*, 9(7), pp.624–629.

Arroyo-Begovich, A., Cárabez-Trejo, A. and Ruíz-Herrera, J., 1980. Identification of the structural component in the cyst wall of *Entamoeba invadens*. *Journal of. Parasitology.*, 66(5), pp.735–741.

Avron, B., Deutsch, R.N. and Mirelman, D., 1982. Chitin synthesis inhibitors prevent cyst formation by *Entamoeba* trophozoites. *Biochemical and Biophysical Research Communications*, 108(2), pp.815–821.

Bagatolli, L.A., Ipsen, J.H., Simonsen, A.C. and Mouritsen, O.G., 2010. An outlook on organization of lipids in membranes: Searching for a realistic connection with the organization of biological membranes. *Progress in Lipid Research*, 49(4), pp.378–389.

Bernet Sánchez, A., Bellés Bellés, A., Aramburu Arnuelos, J., Jover Sanz, A., Sesé Abizanda, E., Vallverdú Vidal, M. and García González, M., 2019. *Entamoeba histolytica* liver abscess case: could stool PCR avoid it? *Diagnosis*. 7(1):69-73

Billet, A.C., Salmon Rousseau, A., Piroth, L. and Martins, C., 2019. An underestimated sexually transmitted infection: Amoebiasis. *BMJ Case Reports*, 12(5): e228942.

Bokori-Brown, M., Petrov, P.G., Khafaji, M.A., Mughal, M.K., Naylor, C.E., Shore, A.C., Gooding, K.M., Casanova, F., Mitchell, T.J., Titball, R.W. and Winlove, C.P., 2016. Red blood cell susceptibility to pneumolysin: Correlation with membrane biochemical and physical properties. *Journal of Biological Chemistry*, 291(19), pp.10210–10227.

Brondyk, William H., 2009. *Chapter 11 Selecting an Appropriate Method for Expressing a Recombinant Protein*. 1st ed. Elsevier Inc.

Brondyk, William H, 2009. Selecting an appropriate method for expressing a recombinant protein. *Methods in enzymology*, 463, pp.131–147.

De Cádiz, A.E., Jeelani, G., Nakada-Tsukui, K., Caler, E. and Nozaki, T., 2013. Transcriptome analysis of encystation in *Entamoeba invadens*. *PloS one*, 8(9), p.e74840.

Casadidio, C., Peregrina, D.V., Gigliobianco, M.R., Deng, S., Censi, R. and Di Martino, P., 2019. Chitin and chitosans: Characteristics, eco-friendly processes, and applications in cosmetic science. *Marine Drugs*, 17(6): e369.

Chandnani, S., Udgirkar, S., Jain, S.S., Sonthalia, N., Contractor, Q., Rathi, P.M. and Chapekar, A., 2019. Massive lower gastrointestinal bleeding due to fulminant necrotizing Amebic colitis: A diagnostic and therapeutic challenge. *Journal of Association of Physicians of India*, 67(4), pp.79–81.

Chatterjee, A., Ghosh, Sudip K, Jang, K., Bullitt, E., Moore, L., Robbins, P.W., Samuelson, J. and Johnson, P.J., 2009. Evidence for a '"Wattle and Daub"' Model of the Cyst Wall of *Entamoeba*. *PLoS Pathogens*, 5(7): e1000498.

Clark, C.G. and Diamond, L.S., 2002. Methods for Cultivation of Luminal Parasitic Protists of Clinical Importance. *Clinical Microbiology Reviews*, 15(3), pp.329–341.

Coppi, A., Merali, S. and Eichinger, D., 2002a. The enteric parasite *Entamoeba* uses an autocrine catecholamine system during differentiation into the infectious cyst stage. *Journal of Biological Chemistry*, 277(10), pp.8083–8090.

Coppi, A., Merali, S. and Eichinger, D., 2002b. The Enteric Parasite *Entamoeba* Uses an Autocrine Catecholamine System during Differentiation into the Infectious Cyst Stage. *The Journal of biological chemistry*, 277(10), pp.8083–8090.

Cornick, S. and Chadee, K., 2017a. *Entamoeba histolytica*: Host parasite interactions at the colonic epithelium. *Tissue Barriers,* 5(1): e1283386.

Cruz, O.H.D. La, Marchat, L.A., Guillén, N., Weber, C., Rosas, I.L., DÍaz-Chávez, J., Herrera, L., Rojo-Domínguez, A., Orozco, E. and López-Camarillo, C., 2016. Multinucleation and Polykaryon Formation is Promoted by the EhPC4 Transcription Factor in *Entamoeba histolytica*. *Scientific Reports* 6(12), 19611.

Das, S., Van Dellen, K., Bulik, D., Magnelli, P., Cui, J., Head, J., Robbins, P.W. and Samuelson, J., 2006. The cyst wall of *Entamoeba invadens* contains chitosan (deacetylated chitin). *Molecular and biochemical parasitology*, 148(1), pp.86–92.

Das, S., Dellen, K. Van, Bulik, D., Magnelli, P., Cui, J., Head, J., Robbins, P.W., Samuelson, J., Van Dellen, K., Bulik, D., Magnelli, P., Cui, J., Head, J., Robbins, P.W., Samuelson, J., Dellen, K. Van, Bulik, D., Magnelli, P., Cui, J., Head, J., Robbins, P.W. and Samuelson, J., 2006. The cyst wall of *Entamoeba invadens* contains chitosan (deacetylated chitin). *Molecular and biochemical parasitology*, 148(1), pp.86–92.

Das, S. and Gillin, F.D., 1991. Chitin synthase in encysting *Entamoeba invadens*. *Biochemical Journal*, 280(3), pp.641–647.

Debnath, A., Rodriguez, M.A. and Ankri, S., 2019. Editorial: Recent Progresses in Amebiasis. *Frontiers in Cellular and Infection Microbiology*, 9, pp.1–4.

Deepak Krishnan, Santhoshi Nayak, S.K.G. 6, 2020. Novel insights into *Entamoeba* cyst wall formation and the importance of actin cytoskeleton. bioRxiv 2020.04.24.059360

Van Dellen, K., Ghosh, S.K., Robbins, P.W., Loftus, B. and Samuelson, J., 2002. *Entamoeba histolytica* lectins contain unique 6-Cys or 8-Cys chitin-binding domains. *Infection and Immunity*, 70(6), pp.3259–3263.

Van Dellen, K.L., Chatterjee, A., Ratner, D.M., Magnelli, P.E., Cipollo, J.F., Steffen, M., Robbins, P.W. and Samuelson, J., 2006. Unique posttranslational modifications of chitin-binding lectins of *Entamoeba invadens* cyst walls. *Eukaryotic Cell*, 5(5), pp.836–848.

Dey, T., Basu, R. and Ghosh, S.K., 2009. *Entamoeba invadens*: cloning and molecular characterization of chitinases. *Experimental Parasitology*, 123(3), pp.244–249.

Diamond, L.S., 1987. *Entamoeba, Giardia* and *Trichomonas*. In: A. Taylor and J. Baker, eds. *In vitro methods for parasite cultivation*. London: Academic Press Ltd, pp.1–27.

Diamond, L.S. and Cunnick, C.C., 1991. A Serum-free, Partly Defined Medium, PDM-805, for Axenic Cultivation of *Entamoeba histolytica* Schaudinn, 1903 and other *Entamoeba*. *The Journal of Protozoology*, 38(3), pp.211–216.

van Dooren, G.G., Reiff, S.B., Tomova, C., Meissner, M., Humbel, B.M. and Striepen, B., 2009. A Novel Dynamin-Related Protein Has Been Recruited for Apicoplast Fission in *Toxoplasma gondii*. *Current Biology*, 19(4), pp.267–276.

Dubinský, P., Ryboš, M. and Turcekova, L., 1986. Properties And Localization of Chitin Synthase in *Ascaris Suum* Eggs. *Parasitology*, 92(1), pp.219–225.

Duchêne, M., 2015. Metronidazole and the Redox Biochemistry of *Entamoeba*

histolytica. Amebiasis,. Tokyo: Springer Japan, pp.523–541.

Eichinger, D., 1997. Encystation of *Entamoeba* parasites. *Bioessays*, 19(7), pp.633–639.

Eichinger, D., 2001. A role for a galactose lectin and its ligands during encystment of *Entamoeba*. *Journal of Eukaryoict Microbiology*, 48(1), Pp: 17-21.

Espinosa-Cantellano, M. and Martínez-Palomo, A., 2000. Pathogenesis of intestinal amebiasis: From molecules to disease. *Clinical Microbiology Reviews*, 13(2), pp.318–331.

Fanelli, E., Di Vito, M., Jones, J.T. and De Giorgi, C., 2005. Analysis of chitin synthase function in a plant parasitic nematode, Meloidogyne artiellia, using RNAi. *Gene*, 349, pp.87–95.

Farthing, M.J.G., Ana-Maria Cevallos and Kelly, P., 2009. Intestinal protozoa: The sarcodina amoeba. In: G.C. (Gordon C. Cook, A. Zumla and P. Manson, eds. *Manson's tropical disease*. Saunders/Elsevier, pp.1375–1385.

Folch, J., Lees, M. and Sloane Stanley, G.H., 1957. A simple method for the isolation and purification of total lipides from animal tissues. *The Journal of biological chemistry*, 226(1), pp.497–509.

Frisardi, M., Ghosh, S.K., Field, J., Van Dellen, K., Rogers, R., Robbins, P. and Samuelson, J., 2000. The Most Abundant Glycoprotein of Amebic Cyst Walls (Jacob) Is a Lectin with Five Cys-Rich, Chitin-Binding Domains. *Infection and Immunity*, 68(7), pp.4217–4224.

Frisardi, Marta, Ghosh, S.K., Field, J., Dellen, K.V.A.N., Rogers, R., Robbins, P. and

Samuelson, J., 2000. The Most Abundant Glycoprotein of Amebic Cyst Walls (Jacob) Is a Lectin with Five Cys-Rich , Chitin-Binding Domains. *Infection and Immunity* 68(7), pp.4217–4224.

Gaechter, V., Schraner, E., Wild, P. and Hehl, A.B., 2008. The single dynamin family protein in the primitive protozoan *Giardia lamblia* is essential for stage conversion and endocytic transport. *Traffic*, 9(1), pp.57–71.

García, M.A., Gutiérrez-Kobeh, L. and Vancell, R.L., 2015. *Entamoeba histolytica*: Adhesins and lectins in the trophozoite surface. *Molecules*, 20(2), pp.2802–2815.

Geoghegan, I.A. and Gurr, S.J., 2017. Investigating chitin deacetylation and chitosan hydrolysis during vegetative growth in Magnaporthe oryzae. *Cellular Microbiology*, 19(1), 9(9): e12743

Gonçalves, I.R., Brouillet, S., Soulié, M.C., Gribaldo, S., Sirven, C., Charron, N., Boccara, M. and Choquer, M., 2016. Genome-wide analyses of chitin synthases identify horizontal gene transfers towards bacteria and allow a robust and unifying classification into fungi. *BMC Evolutionary Biology*, 16(1):252.

Green, M. and Sambrook, J., 2012. *Molecular Cloninig: A Laboratory Manual*. 4th ed. New York, USA: Cold Spring Harbor Laboratory Press.

Gurunathan, S., Han, J.W., Abdal Dayem, A., Eppakayala, V. and Kim, J.H., 2012. Oxidative stress-mediated antibacterial activity of graphene oxide and reduced graphene oxide in *Pseudomonas aeruginosa*. *International Journal of Nanomedicine*, 7, pp.5901–5914.

Gzyl-Malcher, B., Filek, M., Rudolphi-Skórska, E. and Sieprawska, A., 2017. Studies of Lipid Monolayers Prepared from Native and Model Plant Membranes in Their Interaction with Zearalenone and Its Mixture with Selenium Ions. *Journal of Membrane Biology*, 250(3), pp.273–284.

Hale, J.P., Winlove, C.P. and Petrov, P.G., 2011. Effect of hydroperoxides on red blood cell membrane mechanical properties. *Biophysical Journal*, 101(8), pp.1921–1929.

Ham, 2003. Fast flip-flop of cholesterol and fatty acids in membranes: implications for membrane transport proteins. *Current Opinion in Lipidology*], pp.263–271.

Haque, R., Huston, C.D., Hughes, M., Houpt, E. and Petri, W.A., 2003. Amebiasis. *The new england journal of medicine*, 348(16), pp.1565–1573.

Herman, E., Siegesmund, M.A., Bottery, M.J., van Aerle, R., Shather, M.M., Caler, E., Dacks, J.B. and van der Giezen, M., 2017. Membrane trafficking modulation during *Entamoeba* encystation. *Scientific Reports*, 7(1), p.12854.

Jewell, S.A., Titball, R.W., Huyet, J., Naylor, C.E., Basak, A.K., Gologan, P., Winlove, C.P. and Petrov, P.G., 2015. Clostridium perfringens α-toxin interaction with red cells and model membranes. *Soft Matter*, 11(39), pp.7748–7761.

Kaganer, V., Möhwald, H. and Dutta, P., 1999. Structure and phase transitions in Langmuir monolayers. *Reviews of Modern Physics*, 71(3), pp.779–819.

Kantor, M., Abrantes, A., Estevez, A., Schiller, A., Torrent, J., Gascon, J., Hernandez, R. and Ochner, C., 2018. *Entamoeba Histolytica*: Updates in Clinical

Manifestation, Pathogenesis, and Vaccine Development. *Canadian Journal of Gastroenterology and Hepatology*, 2(12):e4601420

King, K., 2016. *Phosphoinositide Phase Behavior in Complex Lipid Monolayer Systems*. Biophysical Journal, 90(9): 3176–3183.

Kopanic, J.L., Al-Mugotir, M., Zach, S., Das, S., Grosely, R. and Sorgen, P.L., 2013. An *Escherichia coli* strain for expression of the connexin45 carboxyl terminus attached to the 4th transmembrane domain. *Frontiers in Pharmacology*, 4 (8), pp.4–11.

Krapf, D., 2018. Compartmentalization of the plasma membrane. *Current Opinion in Cell Biology*, 53, pp.15–21.

Kumirska, J., Czerwicka, M., Kaczyński, Z., Bychowska, A., Brzozowski, K., Thöming, J. and Stepnowski, P., 2010. Application of spectroscopic methods for structural analysis of chitin and chitosan. *Marine Drugs*, 8(5), pp.1567–1636.

Lee, C.G., Da Silva, C.A., Dela Cruz, C.S., Ahangari, F., Ma, B., Kang, M.-J., He, C.-H., Takyar, S. and Elias, J.A., 2011. Role of Chitin and Chitinase/Chitinase-Like Proteins in Inflammation, Tissue Remodeling, and Injury. *Annual Review of Physiology*, 73(1), pp.479–501.

Loftus, B., Anderson, I., Davies, R., Alsmark, U.C.M., Samuelson, J., Amedeo, P., Roncaglia, P., Berriman, M., Hirt, R.P., Mann, B.J., Nozaki, T., Suh, B., Pop, M., Duchene, M., Ackers, J., Tannich, E., Leippe, M., Hofer, M., Bruchhaus, I., Willhoeft, U., Bhattacharya, A., Chillingworth, T., Churcher, C., Hance, Z., Harris, B., Harris, D., Jagels, K., Moule, S., Mungall, K., Ormond, D., Squares,

R., Whitehead, S., Quail, M.A., Rabbinowitsch, E., Norbertczak, H., Price, C., Wang, Z., Guillén, N., Gilchrist, C., Stroup, S.E., Bhattacharya, S., Lohia, A., Foster, P.G., Sicheritz-Ponten, T., Weber, C., Singh, U., Mukherjee, C., El-Sayed, N.M., Petri, W.A., Clark, C.G., Embley, T.M., Barrell, B., Fraser, C.M. and Hall, N., 2005. The genome of the protist parasite *Entamoeba histolytica*. *Nature*, 433(7028), pp.865–868.

Lozano, R., Naghavi, M., Foreman, K., Lim, S., Shibuya, K., Aboyans, V., Abraham, J., Adair, T., Aggarwal, R., Ahn, S.Y., AlMazroa, M.A., Alvarado, M., Anderson, H.R., Anderson, L.M., Andrews, K.G., Atkinson, C., Baddour, L.M., Barker-Collo, S., Bartels, D.H., Bell, M.L., Benjamin, E.J., Bennett, D., Bhalla, K., Bikbov, B., Abdulhak, A. Bin, Birbeck, G., Blyth, F., Bolliger, I., Boufous, S., Bucello, C., Burch, M., Burney, P., Carapetis, J., Chen, H., Chou, D., Chugh, S.S., Coffeng, L.E., Colan, S.D., Colquhoun, S., Colson, K.E., Condon, J., Connor, M.D., Cooper, L.T., Corriere, M., Cortinovis, M., de Vaccaro, K.C., Couser, W., Cowie, B.C., Criqui, M.H., Cross, M., Dabhadkar, K.C., Dahodwala, N., De Leo, D., Degenhardt, L., Delossantos, A., Denenberg, J., Des Jarlais, D.C., Dharmaratne, S.D., Dorsey, E.R., Driscoll, T., Duber, H., Ebel, B., Erwin, P.J., Espindola, P., Ezzati, M., Feigin, V., Flaxman, A.D., Forouzanfar, M.H., Fowkes, F.G.R., Franklin, R., Fransen, M., Freeman, M.K., Gabriel, S.E., Gakidou, E., Gaspari, F., Gillum, R.F., Gonzalez-Medina, D., Halasa, Y.A., Haring, D., Harrison, J.E., Havmoeller, R., Hay, R.J., Hoen, B., Hotez, P.J., Hoy, D., Jacobsen, K.H., James, S.L., Jasrasaria, R., Jayaraman, S., Johns, N., Karthikeyan, G., Kassebaum, N., Keren, A., Khoo, J.-P., Knowlton, L.M.,

Kobusingye, O., Koranteng, A., Krishnamurthi, R., Lipnick, M., Lipshultz, S.E., Ohno, S.L., Mabweijano, J., MacIntyre, M.F., Mallinger, L., March, L., Marks, G.B., Marks, R., Matsumori, A., Matzopoulos, R., Mayosi, B.M., McAnulty, J.H., McDermott, M.M., McGrath, J., Memish, Z.A., Mensah, G.A., Merriman, T.R., Michaud, C., Miller, M., Miller, T.R., Mock, C., Mocumbi, A.O., Mokdad, A.A., Moran, A., Mulholland, K., Nair, M.N., Naldi, L., Narayan, K.M.V., Nasseri, K., Norman, P., O'Donnell, M., Omer, S.B., Ortblad, K., Osborne, R., Ozgediz, D., Pahari, B., Pandian, J.D., Rivero, A.P., Padilla, R.P., Perez-Ruiz, F., Perico, N., Phillips, D., Pierce, K., Pope, C.A., Porrini, E., Pourmalek, F., Raju, M., Ranganathan, D., Rehm, J.T., Rein, D.B., Remuzzi, G., Rivara, F.P., Roberts, T., De León, F.R., Rosenfeld, L.C., Rushton, L., Sacco, R.L., Salomon, J.A., Sampson, U., Sanman, E., Schwebel, D.C., Segui-Gomez, M., Shepard, D.S., Singh, D., Singleton, J., Sliwa, K., Smith, E., Steer, A., Taylor, J.A., Thomas, B., Tleyjeh, I.M., Towbin, J.A., Truelsen, T., Undurraga, E.A., Venketasubramanian, N., Vijayakumar, L., Vos, T., Wagner, G.R., Wang, M., Wang, W., Watt, K., Weinstock, M.A., Weintraub, R., Wilkinson, J.D., Woolf, A.D., Wulf, S., Yeh, P.-H., Yip, P., Zabetian, A., Zheng, Z.-J., Lopez, A.D. and Murray, C.J., 2012. Global and regional mortality from 235 causes of death for 20 age groups in 1990 and 2010: a systematic analysis for the Global Burden of Disease Study 2010. *The Lancet*, 380(9859), pp.2095–2128.

Magistrado-Coxen, P., Aqeel, Y., Lopez, A., Haserick, J.R., Urbanowicz, B.R., Costello, C.E. and Samuelson, J., 2018. The most abundant cyst wall proteins of *Acanthamoeba castellanii* are three sets of lectins that bind cellulose and chitin and

localize to distinct structures in cyst walls. *Plose Neglected Tropical Diseases,* 13(5): e0007352

Makioka, A., Kumagai, M., Ohtomo, H., Kobayashi, S. and Takeuchi, T., 2002. Effect of proteasome inhibitors on the growth, encystation, and excystation of *Entamoeba histolytic*a and *Entamoeba invadens. Parasitology Research*, 88(5), Pp: 454-459.

Merzendorfer, H. and Zimoch, L., 2003. Chitin metabolism in insects: Structure, function and regulation of chitin synthases and chitinases. *Journal of Experimental Biology*, 206(24), pp.4393–4412.

Mi-Ichi, F., Miyamoto, T., Takao, S., Jeelani, G., Hashimoto, T., Hara, H., Nozaki, T. and Yoshida, H., 2015. *Entamoeba* mitosomes play an important role in encystation by association with cholesteryl sulfate synthesis. *Proceedings of the National Academy of Sciences of the United States of America*, 112(22): e2884-2890.

Mi-Ichi, F., Yoshida, H. and Hamano, S., 2016. *Entamoeba* Encystation: New Targets to Prevent the Transmission of Amebiasis. *PLoS Pathogens*, 12(10), p.e1005845.

Mohandas, N. and Evans, E., 1994. Mechanical prepotries of the red cells membrane in relation to molecular structure and genetic gefects. Annual Review of Biophysics and Biomolecular Structure, 23, pp.787–818.

Mottola, M., Caruso, B. and Perillo, M.A., 2019. Langmuir flms at the oil/water interface revisitedNo Title. *Scientific Reports*, 9(1), p.2259.

Mukherjee, C., Clark, C.G. and Lohia, A., 2008. *Entamoeba* shows reversible variation in ploidy under different growth conditions and between life cycle phases. *PLoS Neglected Tropical Diseases*, 2(8), e281.

Nageshan, R.K., Roy, N., Ranade, S. and Tatu, U., 2014. Trans-spliced Heat Shock Protein 90 Modulates Encystation in *Giardia lamblia*. *PLoS Neglected Tropical Diseases*, 8(5), e2829.

Naghavi, M., Wang, H., Lozano, R., Davis, A., Liang, X., Zhou, M., Vollset, S.E., Abbasoglu Ozgoren, A., Abdalla, S., Abd-Allah, F., Abdel Aziz, M.I., Abera, S.F., Aboyans, V., Abraham, B., Abraham, J.P., Abuabara, K.E., Abubakar, I., Abu-Raddad, L.J., Abu-Rmeileh, N.M.E., Achoki, T., Adelekan, A., Ademi, Z., Adofo, K., Adou, A.K., Adsuar, J.C., Ärnlov, J., Agardh, E.E., Akena, D., Al Khabouri, M.J., Alasfoor, D., Albittar, M., Alegretti, M.A., Aleman, A. V., Alemu, Z.A., Alfonso-Cristancho, R., Alhabib, S., Ali, M.K., Ali, R., Alla, F., Al Lami, F., Allebeck, P., AlMazroa, M.A., Al-Shahi Salman, R., Alsharif, U., Alvarez, E., Alviz-Guzman, N., Amankwaa, A.A., Amare, A.T., Ameli, O., Amini, H., Ammar, W., Anderson, H.R., Anderson, B.O., Antonio, C.A.T., Anwari, P., Apfel, H., Argeseanu Cunningham, S., Arsic Arsenijevic, V.S., Artaman, A., Asad, M.M., Asghar, R.J., Assadi, R., Atkins, L.S., Atkinson, C., Badawi, A., Bahit, M.C., Bakfalouni, T., Balakrishnan, K., Balalla, S., Banerjee, A., Barber, R.M., Barker-Collo, S.L., Barquera, S., Barregard, L., Barrero, L.H., Barrientos-Gutierrez, T., Basu, A., Basu, S., Basulaiman, M.O., Beardsley, J., Bedi, N., Beghi, E., Bekele, T., Bell, M.L., Benjet, C., Bennett, D.A., Bensenor, I.M., Benzian, H., Bertozzi-Villa, A., Beyene, T.J., Bhala, N., Bhalla, A., Bhutta, Z.A., Bikbov, B., Bin

Abdulhak, A., Biryukov, S., Blore, J.D., Blyth, F.M., Bohensky, M.A., Borges, G., Bose, D., Boufous, S., Bourne, R.R., Boyers, L.N., Brainin, M., Brauer, M., Brayne, C.E.G., Brazinova, A., Breitborde, N., Brenner, H., Briggs, A.D.M., Brown, J.C., Brugha, T.S., Buckle, G.C., Bui, L.N., Bukhman, G., Burch, M., Campos Nonato, I.R., Carabin, H., Cárdenas, R., Carapetis, J., Carpenter, D.O., Caso, V., Castañeda-Orjuela, C.A., Castro, R.E., Catalá-López, F., Cavalleri, F., Chang, J.C., Charlson, F.C., Che, X., Chen, H., Chen, Y., Chen, J.S., Chen, Z., Chiang, P.P.C., Chimed-Ochir, O., Chowdhury, R., Christensen, H., Christophi, C.A., Chuang, T.W., Chugh, S.S., Cirillo, M., Coates, M.M., Coffeng, L.E., Coggeshall, M.S., Cohen, A., Colistro, V., Colquhoun, S.M., Colomar, M., Cooper, L.T., Cooper, C., Coppola, L.M., Cortinovis, M., Courville, K., Cowie, B.C., Criqui, M.H., Crump, J.A., Cuevas-Nasu, L., Da Costa Leite, I., Dabhadkar, K.C., Dandona, L., Dandona, R., Dansereau, E., Dargan, P.I., Dayama, A., De La Cruz-Góngora, V., De La Vega, S.F., De Leo, D., Degenhardt, L., Del Pozo-Cruz, B., Dellavalle, R.P., Deribe, K., Des Jarlais, D.C., Dessalegn, M., De Veber, G.A., Dharmaratne, S.D., Dherani, M., Diaz-Ortega, J.L., Diaz-Torne, C., Dicker, D., Ding, E.L., Dokova, K., Dorsey, E.R., Driscoll, T.R., Duan, L., Duber, H.C., Durrani, A.M., Ebel, B.E., Edmond, K.M., Ellenbogen, R.G., Elshrek, Y., Ermakov, S.P., Erskine, H.E., Eshrati, B., Esteghamati, A., Estep, K., Fürst, T., Fahimi, S., Fahrion, A.S., Faraon, E.J.A., Farzadfar, F., Fay, D.F.J., Feigl, A.B., Feigin, V.L., Felicio, M.M., Fereshtehnejad, S.M., Fernandes, J.G., Ferrari, A.J., Fleming, T.D., Foigt, N., Foreman, K., Forouzanfar, M.H., Fowkes, F.G.R., Fra Paleo, U., Franklin, R.C., Futran, N.D., Gaffikin, L., Gambashidze, K., Gankpé, F.G., García-Guerra, F.A.,

Garcia, A.C., Geleijnse, J.M., Gessner, B.D., Gibney, K.B., Gillum, R.F., Gilmour, S., Ginawi, I.A.M., Giroud, M., Glaser, E.L., Goenka, S., Gomez Dantes, H., Gona, P., Gonzalez-Medina, D., Guinovart, C., Gupta, Rahul, Gupta, Rajeev, Gosselin, R.A., Gotay, C.C., Goto, A., Gouda, H.N., Graetz, N., Greenwell, K.F., Gugnani, H.C., Gunnell, D., Gutiérrez, R.A., Haagsma, J., Hafezi-Nejad, N., Hagan, H., Hagstromer, M., Halasa, Y.A., Hamadeh, R.R., Hamavid, H., Hammami, M., Hancock, J., Hankey, G.J., Hansen, G.M., Harb, H.L., Harewood, H., Haro, J.M., Havmoeller, R., Hay, R.J., Hay, S.I., Hedayati, M.T., Heredia Pi, I.B., Heuton, K.R., Heydarpour, P., Higashi, H., Hijar, M., Hoek, H.W., Hoffman, H.J., Hornberger, J.C., Hosgood, H.D., Hossain, M., Hotez, P.J., Hoy, D.G., Hsairi, M., Hu, G., Huang, J.J., Huffman, M.D., Hughes, A.J., Husseini, A., Huynh, C., Iannarone, M., Iburg, K.M., Idrisov, B.T., Ikeda, N., Innos, K., Inoue, M., Islami, F., Ismayilova, S., Jacobsen, K.H., Jassal, S., Jayaraman, S.P., Jensen, P.N., Jha, V., Jiang, G., Jiang, Y., Jonas, J.B., Joseph, J., Juel, K., Kabagambe, E.K., Kan, H., Karch, A., Karimkhani, C., Karthikeyan, G., Kassebaum, N., Kaul, A., Kawakami, N., Kazanjan, K., Kazi, D.S., Kemp, A.H., Kengne, A.P., Keren, A., Kereselidze, M., Khader, Y.S., Khalifa, S.E.A.H., Khan, E.A., Khan, G., Khang, Y.H., Kieling, C., Kinfu, Y., Kinge, J.M., Kim, D., Kim, S., Kivipelto, M., Knibbs, L., Knudsen, A.K., Kokubo, Y., Kosen, S., Kotagal, M., Kravchenko, M.A., Krishnaswami, S., Krueger, H., Kuate Defo, B., Kuipers, E.J., Kucuk Bicer, B., Kulkarni, C., Kulkarni, V.S., Kumar, K., Kumar, R.B., Kwan, G.F., Kyu, H., Lai, T., Lakshmana Balaji, A., Lalloo, R., Lallukka, T., Lam, H., Lan, Q., Lansingh, V.C., Larson, H.J., Larsson, A., Lavados, P.M., Lawrynowicz, A.E.B., Leasher, J.L., Lee, J.T., Leigh, J.,

Leinsalu, M., Leung, R., Levitz, C., Li, B., Li, Yichong, Li, Yongmei, Liddell, C., Lim, S.S., De Lima, G.M.F., Lind, M.L., Lipshultz, S.E., Liu, S., Liu, Y., Lloyd, B.K., Lofgren, K.T., Logroscino, G., London, S.J., Lortet-Tieulent, J., Lotufo, P.A., Lucas, R.M., Lunevicius, R., Lyons, R.A., Ma, S., Machado, V.M.P., MacIntyre, M.F., Mackay, M.T., MacLachlan, J.H., Magis-Rodriguez, C., Mahdi, A.A., Majdan, M., Malekzadeh, R., Mangalam, S., Mapoma, C.C., Marape, M., Marcenes, W., Margono, C., Marks, G.B., Marzan, M.B., Masci, J.R., Mashal, M.T., Masiye, F., Mason-Jones, A.J., Matzopolous, R., Mayosi, B.M., Mazorodze, T.T., McGrath, J.J., McKay, A.C., McKee, M., McLain, A., Meaney, P.A., Mehndiratta, M.M., Mejia-Rodriguez, F., Melaku, Y.A., Meltzer, M., Memish, Z.A., Mendoza, W., Mensah, G.A., Meretoja, A., Mhimbira, F.A., Miller, T.R., Mills, E.J., Misganaw, A., Mishra, S.K., Mock, C.N., Moffitt, T.E., Mohamed Ibrahim, N., Mohammad, K.A., Mokdad, A.H., Mola, G.L., Monasta, L., Monis, J.D.L.C., Montañez Hernandez, J.C., Montico, M., Montine, T.J., Mooney, M.D., Moore, A.R., Moradi-Lakeh, M., Moran, A.E., Mori, R., Moschandreas, J., Moturi, W.N., Moyer, M.L., Mozaffarian, D., Mueller, U.O., Mukaigawara, M., Mullany, E.C., Murray, J., Mustapha, A., Naghavi, P., Naheed, A., Naidoo, K.S., Naldi, L., Nand, D., Nangia, V., Narayan, K.M.V., Nash, D., Nasher, J., Nejjari, C., Nelson, R.G., Neuhouser, M., Neupane, S.P., Newcomb, P.A., Newman, L., Newton, C.R., Ng, M., Ngalesoni, F.N., Nguyen, G., Nguyen, N.T.T., Nisar, M.I., Nolte, S., Norheim, O.F., Norman, R.E., Norrving, B., Nyakarahuka, L., Odell, S., O'Donnell, M., Ohkubo, T., Ohno, S.L., Olusanya, B.O., Omer, S.B., Opio, J.N., Orisakwe, O.E., Ortblad, K.F., Ortiz, A., Otayza, M.L.K., Pain, A.W., Pandian, J.D., Panelo, C.I., Panniyammakal, J., Papachristou, C., Paternina

Caicedo, A.J., Patten, S.B., Patton, G.C., Paul, V.K., Pavlin, B., Pearce, N., Pellegrini, C.A., Pereira, D.M., Peresson, S.C., Perez-Padilla, R., Perez-Ruiz, F.P., Perico, N., Pervaiz, A., Pesudovs, K., Peterson, C.B., Petzold, M., Phillips, B.K., Phillips, D.E., Phillips, M.R., Plass, D., Piel, F.B., Poenaru, D., Polinder, S., Popova, S., Poulton, R.G., Pourmalek, F., Prabhakaran, D., Qato, D., Quezada, A.D., Quistberg, D.A., Rabito, F., Rafay, A., Rahimi, K., Rahimi-Movaghar, V., Rahman, S.U.R., Raju, M., Rakovac, I., Rana, S.M., Refaat, A., Remuzzi, G., Ribeiro, A.L., Ricci, S., Riccio, P.M., Richardson, L., Richardus, J.H., Roberts, B., Roberts, D.A., Robinson, M., Roca, A., Rodriguez, A., Rojas-Rueda, D., Ronfani, L., Room, R., Roth, G.A., Rothenbacher, D., Rothstein, D.H., Rowley, J.T.F., Roy, N., Ruhago, G.M., Rushton, L., Sambandam, S., Søreide, K., Saeedi, M.Y., Saha, S., Sahathevan, R., Sahraian, M.A., Sahle, B.W., Salomon, J.A., Salvo, D., Samonte, G.M.J., Sampson, U., Sanabria, J.R., Sandar, L., Santos, I.S., Satpathy, M., Sawhney, M., Saylan, M., Scarborough, P., Schöttker, B., Schmidt, J.C., Schneider, I.J.C., Schumacher, A.E., Schwebel, D.C., Scott, J.G., Sepanlou, S.G., Servan-Mori, E.E., Shackelford, K., Shaheen, A., Shahraz, S., Shakh-Nazarova, M., Shangguan, S., She, J., Sheikhbahaei, S., Shepard, D.S., Shibuya, K., Shinohara, Y., Shishani, K., Shiue, I., Shivakoti, R., Shrime, M.G., Sigfusdottir, I.D., Silberberg, D.H., Silva, A.P., Simard, E.P., Sindi, S., Singh, J.A., Singh, L., Sioson, E., Skirbekk, V., Sliwa, K., So, S., Soljak, M., Soneji, S., Soshnikov, S.S., Sposato, L.A., Sreeramareddy, C.T., Stanaway, J.D., Stathopoulou, V.K., Steenland, K., Stein, C., Steiner, C., Stevens, A., Stöckl, H., Straif, K., Stroumpoulis, K., Sturua, L., Sunguya, B.F., Swaminathan, S., Swaroop, M., Sykes, B.L., Tabb, K.M., Takahashi, K.,

Talongwa, R.T., Tan, F., Tanne, D., Tanner, M., Tavakkoli, M., Te Ao, B., Teixeira, C.M., Templin, T., Tenkorang, E.Y., Terkawi, A.S., Thomas, B.A., Thorne-Lyman, A.L., Thrift, A.G., Thurston, G.D., Tillmann, T., Tirschwell, D.L., Tleyjeh, I.M., Tonelli, M., Topouzis, F., Towbin, J.A., Toyoshima, H., Traebert, J., Tran, B.X., Truelsen, T., Trujillo, U., Trillini, M., Tsala Dimbuene, Z., Tsilimbaris, M., Tuzcu, E.M., Ubeda, C., Uchendu, U.S., Ukwaja, K.N., Undurraga, E.A., Vallely, A.J., Van De Vijver, S., Van Gool, C.H., Varakin, Y.Y., Vasankari, T.J., Vasconcelos, A.M.N., Vavilala, M.S., Venketasubramanian, N., Vijayakumar, L., Villalpando, S., Violante, F.S., Vlassov, V.V., Wagner, G.R., Waller, S.G., Wang, J.L., Wang, L., Wang, X.R., Wang, Y., Warouw, T.S., Weichenthal, S., Weiderpass, E., Weintraub, R.G., Wenzhi, W., Werdecker, A., Wessells, K.R.R., Westerman, R., Whiteford, H.A., Wilkinson, J.D., Williams, T.N., Woldeyohannes, S.M., Wolfe, C.D.A., Wolock, T.M., Woolf, A.D., Wong, J.Q., Wright, J.L., Wulf, S., Wurtz, B., Xu, G., Yang, Y.C., Yano, Y., Yatsuya, H., Yip, P., Yonemoto, N., Yoon, S.J., Younis, M., Yu, C., Yun Jin, K., Zaki, M.E.S., Zamakhshary, M.F., Zeeb, H., Zhang, Y., Zhao, Y., Zheng, Y., Zhu, J., Zhu, S., Zonies, D., Zou, X.N., Zunt, J.R., Vos, T., Lopez, A.D., Murray, C.J.L., Alcalá-Cerra, G., Hu, H., Karam, N., Sabin, N. and Temesgen, A.M., 2015. Global, regional, and national age-sex specific all-cause and cause-specific mortality for 240 causes of death, 1990-2013: A systematic analysis for the Global Burden of Disease Study. *The Lancet*, 385(9963), pp.117–171.

Nakada-Tsukui, K., Watanabe, N., Maehama, T. and Nozaki, T., 2019. Phosphatidylinositol Kinases and Phosphatases in *Entamoeba histolytica*. *Frontiers in Cellular and Infection Microbiology*, 6;(9):150.

Narayanasamy, R.K., Castañón-Sanchez, C.A., Luna-Arias, J.P., García-Rivera, G., Avendaño-Borromeo, B., Labra-Barrios, M.L., Valdés, J., Herrera-Aguirre, M.E. and Orozco, E., 2018. The *Entamoeba histolytica* TBP and TRF1 transcription factors are GAAC-box binding proteins, which display differential gene expression under different stress stimuli and during the interaction with mammalian cells. *Parasites and Vectors*, 11(1), pp.1–16.

Nath, J., Ghosh, S.K., Singha, B. and Paul, J., 2015. Molecular Epidemiology of Amoebiasis: A Cross-Sectional Study among North East Indian Population. *PLOS Neglected Tropical Diseases*, 9(12), p.e0004225.

Nayak, S. and Ghosh, S.K., 2019a. Nucleotide sugar transporters of *Entamoeba histolytica* and *Entamoeba invadens* involved in chitin synthesis. *Molecular and Biochemical Parasitology*, 234(9), p.111224.

de Oliveira Pedro, R., Ribeiro Pereira, A., Oliveira, O.N. and Barbeitas Miranda, P., 2020. Interaction of chitosan derivatives with cell membrane models in a biologically relevant medium. *Colloids and Surfaces B: Biointerfaces*,192(4), p.111048.

Oyeleye, A. and Normi, Y.M., 2018. Chitinase: diversity, limitations, and trends in engineering for suitable applications. *Bioscience Reports*, 38, p.2018032300.

Pavinatto, A., Delezuk, J.A.M., Souza, A.L., Pavinatto, F.J., Volpati, D., Miranda,

P.B., Campana-Filho, S.P. and Oliveira, O.N., 2016. Experimental evidence for the mode of action based on electrostatic and hydrophobic forces to explain interaction between chitosans and phospholipid Langmuir monolayers. *Colloids and Surfaces B: Biointerfaces*, 145, pp.201–207.

Pavinatto, A., Pavinatto, F.J., Barros-Timmons, A. and Oliveira, O.N., 2010. Electrostatic interactions are not sufficient to account for chitosan bioactivity. *ACS Applied Materials and Interfaces*, 2(1), pp.246–251.

Pavinatto, F.J., Santos Jr., D.S. dos and Oliveira Jr., O.N., 2005. Interaction between cholesterol and chitosan in Langmuir monolayers. *Polímeros*, 15(2), pp.91–94.

Pinto, O.A. and Disalvo, E.A., 2019. A new model for lipid monolayer and bilayers based on thermodynamics of irreversible processes. *PLoS ONE*, 4;14(4): e0212269

Pritt, B.S. and Clark, A.C.G., 2008. Amebiasis CONCISE REVIEW FOR CLINICIANS. *Mayo Clinic Proceedings*, 83(1010), pp.1154–1160.

Pritt, S.B. and Clark, C.G., 2011. *Entamoeba* and *Entamoeba histolytica*. *eLS. John Wiley & Sons Ltd*.

Quintanilla-Licea, R., Mata-Cárdenas, B.D., Vargas-Villarreal, J., Bazaldúa-Rodríguez, A.F., Ángeles-Hernández, I.K., Garza-González, J.N. and Hernández-García, M.E., 2014. Antiprotozoal activity against *Entamoeba histolytica* of plants used in northeast mexican traditional medicine. bioactive compounds from lippia graveolens and ruta chalepensis. *Molecules*, 19(12), pp.21044–21065.

Ralston, K.S., 2015. Chew on this: Amoebic trogocytosis and host cell killing by *Entamoeba histolytica*. *Trends in Parasitology*, 31(9):442-452.

Rengpien, S. and Bailey, G.B., 1975. Differentiation of *Entamoeba*: A New Medium and Optimal Conditions for Axenic Encystation of *E. invadens*. *The Journal of Parasitology*, 61(1), pp.24–30.

Rinaudo, M., 2006. Chitin and chitosan: Properties and applications. *Progress in Polymer Science (Oxford)*, 31(7), pp.603–632.

Robertson, J.D., 1981. Membrane-Structure. *Journal of Cell Biology*, 91(3), pp.S189–S204.

Rodgers, W. and Glaser, M., 1991. Characterization of lipid domains in erythrocyte membranes. *Proceedings of the National Academy of Sciences of the United States of America*], 88(4), pp.1364–1368.

Sackmann, E., 1995. *Biological membranes architecture and function*. R. Lipowsky and E. Sackmann, eds. New York, USA: Elsevier Science Publishing Co.

Samanta, S.K. and Ghosh, S.K., 2012. The chitin biosynthesis pathway in *Entamoeba* and the role of glucosamine-6-P isomerase by RNA interference. *Molecular and Biochemical Parasitology*, 186(1), pp.60–68.

Samanta, S.K., Varghese, S.S., Krishnan, D., Baidya, M., Nayak, D., Mukherjee, S. and Ghosh, S.K., 2018. A novel encystation specific protein kinase regulates chitin synthesis in *Entamoeba invadens. Molecular and Biochemical Parasitology*, 220(April 2017), pp.19–27.

Samuelson, J., Bushkin, G.G., Chatterjee, A. and Robbins, P.W., 2013. Strategies to

discover the structural components of cyst and oocyst walls. *Eukaryotic Cell*, 12(12), pp.1578–87.

Samuelson, J. and Robbins, P., 2011. A simple fibril and lectin model for cyst walls of *Entamoeba* and perhaps Giardia. *Trends in Parasitology*, 27(1), pp.17–22.

Sanchez, L., Enea, V. and Eichinger, D., 1994. Identification of a developmentally regulated transcript expressed during encystation of *Entamoeba invadens. Molecular and Biochemical Parasitology*, 67(1), pp.125–135.

Schmitz, Auza, Koberidze, Rasche, Fischer and Bortesi, 2019. Conversion of Chitin to Defined Chitosan Oligomers: Current Status and Future Prospects. *Marine Drugs* [Online], 17(8), p.452.

Schneider, C.A., Rasband, W.S. and Eliceiri, K.W., 2012. NIH Image to ImageJ: 25 years of image analysis. *Nature Methods*, 9(7), pp.671–675.

Segovia-Gamboa, N.C., Chávez-Munguía, B., Medina-Flores, Y., Cázares-Raga, F.E., Hernández-Ramírez, V.I., Martínez-Palomo, A. and Talamás-Rohana, P., 2010. *Entamoeba invadens*, encystation process and enolase. *Experimental Parasitology*], 125(2), pp.63–69.

Shahabuddin, M. and Vinetz, J.M., 1999. Chitinases of human parasites and their implications as antiparasitic targets. *Experientia Supplementum*, 87, pp.223–234.

Shahi, P., Moreau, F. and Chadee, K., 2019. *Entamoeba histolytica* cyclooxygenase-like protein regulates cysteine protease expression and virulence. *Frontiers in Cellular and Infection Microbiology*, 9(JAN), pp.1–16.

Singh, M., Sharma, S., Bhattacharya, A. and Tatu, U., 2015. Heat Shock Protein 90

regulates encystation in *Entamoeba*. *Frontiers in Microbiology*, 6, 1125.

Spadafora, L.J., Kearney, M.R., Siddique, A., Ali, I.K., Gilchrist, C.A., Arju, T., Hoffstrom, B., Nguyen, F.K., Petri, W.A., Haque, R. and Cangelosi, G.A., 2016. Species-Specific Immunodetection of an *Entamoeba histolytica* Cyst Wall Protein. *PLoS Neglected Tropical Diseases*, 10(5), e0004697.

Spindler, K.D., Spindler-Barth, M. and Londershausen, M., 1990. Chitin metabolism: a target for drugs against parasites. *Parasitology Research*, 76(4), pp.283–288.

Studier, F.W., 2005. Protein production by auto-induction in high density shaking cultures. *Protein expression and purification*, 41(1), pp.207–234.

Vazquezdelara-Cisneros, L.G. and Arroyo-Begovich, A., 1984. Induction of Encystation of *Entamoeba invadens* by Removal of Glucose from the Culture Medium. *The Journal of Parasitology*, 70(5), p.629.

Van Vliet, H.H.D.M., Spies, F., Linnemans, W.A.M., Klepke, A., Op Den Kamp, J.A.F. and Var~ Deenen, L.L.M., 1976. Isolation and characterization of subcellular membranes of *Entamoeba invadens*. *Journal of Cell Bioogyl*,71(2):357-369.

Wang, Z., Samuelson, J., Clark, C.G., Eichinger, D., Paul, J., Van Dellen, K., Hall, N., Anderson, I. and Loftus, B., 2003. Gene discovery in the *Entamoeba invadens* genome. *Molecular and Biochemical Parasitology*, 129(1), pp.23–31.

Weinke, T., Friedrich-Jänlcke, B., Hopp, P. and Janitschke, K., 1990. Prevalence and clinical importance of *Entamoeba histolytica* in two high-risk groups: Travelers returning from the tropics and male homosexuals. *Journal of Infectious Diseases*, 161(5), pp.1029–1031.

Wydro, P., Krajewska, B. and Hąc-Wydro, K., 2007. Chitosan as a lipid binder: A langmuir monolayer study of chitosan-lipid interactions. *Biomacromolecules*, 8(8), pp.2611–2617.

Ximénez, C., Morán, P., Rojas, L., Valadez, A. and Gómez, A., 2009. Reassessment of the epidemiology of amebiasis: State of the art. *Infection, Genetics and Evolution*, 9(6), pp.1023–1032.

Yang, J. and Zhang, K.Q., 2019. *Chitin synthesis and degradation in fungi: Biology and enzymes*. Springer Singapore.

Zermeño, V., Ximénez, C., Morán, P., Valadez, A., Valenzuela, O., Rascón, E., Diaz, D. and Cerritos, R., 2013. Worldwide genealogy of *Entamoeba histolytica*: An overview to understand haplotype distribution and infection outcome. *Infection, Genetics and Evolution*, 17, pp.243–252.

Zuo, X. and Coombs, G.H., 1995. Amino acid consumption by the parasitic, amoeboid protists *Entamoeba histolytica* and *E. invadens*. *FEMS Microbiology Letters*, 130(2–3), pp.253–258.